Role of temperature and soil properties on the thermal interaction between energy piles

Aria Moradshahi

A thesis submitted for the degree of Doctor of Philosophy at Monash University

in 2021

Department of Civil Engineering

Monash University

Australia

Copyright notice

Abstract

Considering the high energy prices and environmental issues, renewable geothermal energy usage is becoming increasingly popular in many applications. The heating and cooling requirements of built structures is a major contributing factor to energy consumptions and greenhouse gas emissions. Reinforced concrete geostructures, coupled with ground source heat pumps, such as energy piles, are promising technologies that can drastically reduce fossil energy consumption and carbon emissions to maintain thermal comfort in built structures. Energy piles incorporate the pile foundation and ground source heat exchanger to generate environmental and economic benefits. Together with the energy design, these piles' geotechnical designs are also critical. Depending on the built structure's energy demand, energy piles can be subjected to various magnitudes of monotonic and cyclic temperature changes. Different sites may also have different soil properties that could influence these piles' thermal response. Installation of energy piles can also include group installation or closely spaced piles. In this case, it could result in thermal interaction between closely spaced energy piles, which will influence the piles' thermo-mechanical response. Although the thermal response of solitary energy piles has been widely studied in recent years, there remains a need to evaluate the effect of thermal interaction between multiple energy piles on the thermal response of energy piles, for typical temperatures and soil properties encountered in energy piles operations.

This thesis addresses this knowledge gap by investigating the thermal response of an energy pile that is part of a pair of cast-in-place concrete bored energy piles below a residential building. The energy piles have a diameter of 0.6 m and length of 10 m and their centre-to-centre spacing is 3.5 m. Field tests involving monotonic and cyclic temperature changes were performed to assess the thermal responses of one of the energy piles when operated alone and when operated simultaneously with the other energy pile in the pair. A numerical model, validated with the field results, was then used to analyze the effects of balanced and imbalanced

cyclic temperatures, different magnitudes of monotonic temperatures, and the consequences of varying soil thermal conductivity, thermal expansion coefficient, and elastic modulus on the thermal response of the considered energy pile. Due to the spacing considered, the operation of the second energy pile had a negligible effect on the thermal response of the considered energy pile for all fluid temperatures and soil properties, even though the soil experienced higher temperature changes than the operation of only the considered energy pile. However, cyclic temperature variations induced lower ground temperature changes and pile thermal stresses than monotonic temperatures during single and dual pile operations. Hence, cyclic temperatures from the ground source heat pump's intermittent operations could be more beneficial than their continuous long-term operations. Among the considered soil parameters, the impact of elastic modulus of the soil was more significant on the thermal stresses of the energy pile than the effects of soil thermal conductivity and thermal expansion coefficient. Furthermore, temperatures and stresses across the planar cross-section of energy piles vary between the centre and the pile's edge. Therefore, they should be accounted for in the design of energy piles.

Declaration

This thesis contains no material which has been accepted for the award of any other degree or diploma at any university or equivalent institution. To the best of my knowledge, this thesis contains no material previously published or written by another person, except where due reference is made in the text of the thesis.

Aria Moradshahi

February 2021

Publications during enrolment

The following is a list of publications arising during enrolment:

Journal papers:

Moradshahi, A., Faizal, M., Bouazza, A., and McCartney, J. S. 2020. Effect of nearby piles and soil properties on the thermal behaviour of a field-scale energy pile. Canadian Geotechnical Journal. **0**(ja): -. https://doi.org/10.1139/cgj-2020-0353.

Moradshahi, A., Faizal, M., Bouazza, A., and McCartney, J. S. (2021). Effects of monotonic and cyclic temperature variations on the thermal interaction between two energy piles under a residential building, International Journal of Geomechanics, Under Review.

Moradshahi, A., Faizal, M., Bouazza, A., and McCartney, J. S. (2021). Cross-sectional thermo-mechanical responses of energy piles. Computers and Geotechnics, 138, 104320.

Faizal, M., Moradshahi, A., M., Bouazza, A., and McCartney, J. S., Soil thermal response to temperature cycles and thermal boundary conditions of field-scale energy piles, Journal of Geotechnical and Geoenvironmental Engineering. Under Review.

Conferences:

Moradshahi, A., A., Faizal, M., Bouazza, A., 2021. Effect of soil elastic modulus on the thermal responses of a field-scale energy pile, Proceedings 20th International Conference on Soil Mechanics and Geotechnical Engineering, Sydney, Australia.

Faizal, M., Moradshahi, A., M., Bouazza, A., and McCartney, J. S., 2020. Soil thermal responses around a field-scale energy pile, Proceedings 2nd International Conference on Energy Geotechnics, La Jolla, California, USA.

Acknowledgements

I want to express my heartfelt appreciation for my supervisor, Professor Abdelmalek Bouazza, and thank him for his continuous and invaluable support throughout the course of my degree. Without his guidance and support, reaching this milestone would not have been possible. I also thank Dr Mohammed Faizal for helping at all stages of my degree with his knowledge on energy piles. Special acknowledgements to Professor John McCartney (University of California- San Diego, USA) for his challenging and pertinent reviews of my technical reports.

I thank Monash University for awarding me the Monash Departmental Scholarship to conduct my research. The support of all the project sponsors, Geotechnical Engineering Pty Ltd, Golder Associates Pty Ltd., Geoexchange Australia Pty. Ltd and Brookfield-Multiplex, is gratefully acknowledged.

I would also like to thank the Department of Civil Engineering's administrative staff (Fatin, Sohail, Min and Noi) and technical staff (Long, Richard, Andres, Zoltan and Michael) for assisting me at different stages of my degree. I also thank my friends (Vahid, Ashkan, Ali Amin, Sarah, Hassam, Mayu and Gonzalo) who provided me with generous support and a productive work environment.

Finally, I would like to thank my father and mother whose support played a vital role in pursuing and successfully completing this degree. Their help will always be cherished.

Table of contents

List of figures

List of tables

1 Introduction

1.1 Motivation and background

Climate change, carbon emissions, global warming, and their consequent adverse effects on the environment are growing international concerns resulting from rapid growth in world energy consumption. Building constructions and operations account for a significant amount (almost 40%) of carbon emissions related to energy consumption globally (GlobalABC, 2018).

According to the Australian Sustainable Built Environment Council (ASBEC, 2018), building operations consume almost 50% of total electricity and contributes approximately 25% to national greenhouse gas emissions. The main areas of energy consumption in buildings globally are heating, ventilation and air conditioning (HVAC) (IEA, 2013). A considerable amount of 40% of all energy consumptions in Australian buildings is due to heating and cooling (DEWHA, 2008). To transit to an environmentally friendly future, Australia has dedicated efforts to reduce carbon emissions and reach zero net emissions by 2050 (Climateworks, 2014). As heating and cooling is necessary for most buildings, it is important to design systems that enhance their energy efficiency. In this respect, Engineers Australia further emphasised the importance of using renewable energy technologies to provide the best comfort and energy-efficient performance of buildings in Australia (Engineers Australia, 2017).

Ground source heat pumps (GSHPs) coupled with structural elements of buildings, known as energy geostructures (such as energy piles, energy diaphragm and retaining walls), are promising renewable energy technologies that are becoming increasingly popular due to their economic and environmental benefits. For new buildings that require foundation piles, the piles can be converted to underground heat exchangers, known as energy piles, to provide low-emission and energy-efficient heating/cooling to the building by using a GSHP. Compared to conventional air conditioning systems, energy piles have shown environmental benefits by

reducing carbon emissions with energy savings up to two-thirds of traditional systems (Brandl, 2006; Pahud and Hubuch, 2007; Amis and Loveridge, 2014; Khan and Wang, 2014). Considering these benefits, energy piles have experienced rapid growth in several countries (Amis and Loveridge, 2014; Brandl, 2013).

As the pile foundations are increasingly used as energy piles, investigations into their temperature-induced geotechnical behaviour are crucial for their safe design. The number of piles in a building footprint constructed as energy piles depends on the built structure's heating/cooling requirements. Hence, multiple pile foundations can be constructed as energy piles to meet the built structure's energy demand. The temperature variations of energy piles and the surrounding soil also depend on the heating/cooling requirements of the built structure and are subjected to different magnitudes of monotonic and cyclic temperature variations (Brandl 2006; Murphy and McCartney 2015; McCartney and Murphy 2017, Faizal et al. 2016, 2018, 2019a, 2019b). The ground temperature variations of multiple energy piles can result in thermal interaction among closely spaced energy piles and influence their thermo-mechanical behaviour. There is currently limited knowledge of the thermal interaction among nearby energy piles experiencing different magnitudes of monotonic and cyclic temperatures.

Moreover, different sites will have different soil properties. Although several studies have been conducted on energy pile groups using field testing and numerical simulations (Mimoumi and Laloui 2015; Rotta Loria and Laloui 2016, 2017a, 2018; Wu et al. 2020), the roles of soil properties (such as soil thermal conductivity, soil thermal expansion coefficient, and soil elastic modulus) and cyclic temperatures on the thermal interaction between energy piles are yet to be investigated. Further studies on the influence of varying soil thermal properties will provide new insight into the thermal response of multiple energy piles.

Furthermore, the operation of the GSHP induces complex temperature and stress distribution across the planar cross-section of the energy piles. Recent numerical studies

conducted for given inlet fluid temperatures and set of soil properties have shown that the temperature measured at a single location in a pile, as is the common current practice in energy pile research, does not fully represent the temperatures across the cross-section of an energy pile and can lead to errors in estimating thermal stresses (Abdelaziz and Ozudogru 2016a, 2016b; Caulk et al. 2016, Han and Yu 2020; Liu et al. 2020). Therefore, further investigation on the cross-sectional thermal response of energy piles for different temperatures and soil properties, particularly for multiple closely spaced energy piles, is warranted to provide new insights into the thermal response of energy piles.

1.2 Problem statement

For the safe and efficient thermal and geotechnical design of energy piles, it is essential to understand the thermal response of energy piles for different magnitudes of inlet fluid temperatures typically used in energy pile operations and the effect of various soil properties commonly encountered at various installation sites. The current knowledge base on the influence of various temperature magnitudes and soil properties on the piles' thermal stresses and ground temperature variations was developed from research conducted on solitary energy piles. However, to support the load of the built structure, piles are often used in groups or are closely spaced, and depending on the energy demands of the structure, all or a certain number of the piles might be used as energy piles. For cases where energy piles operate in groups or are closely spaced, thermal interaction could occur between the piles through the soil volume, which in turn could affect the geotechnical performance of the individual piles. Therefore, the current research findings from solitary energy piles cannot be directly applied to designing closely spaced energy piles. Further field and numerical investigations on the influence of inlet fluid temperature and soil properties on closely spaced energy piles' thermal responses are required to understand better the thermal interaction mechanisms between these piles. These

investigations will enable engineers to make reliable decisions when designing and installing energy piles at different sites and ground source heat pumps' operating requirements.

1.3 Thesis objectives

This thesis investigates the role of inlet fluid temperature and soil properties on the thermal interaction between energy piles. The specific aims of this thesis are:

1. To explore the influence of monotonic and cyclic inlet fluid temperatures and nearby energy pile on an energy pile's thermal responses.
2. To examine the role of soil properties and nearby energy pile on an energy pile's thermal responses.
3. To evaluate the impact of soil properties, inlet fluid temperature and nearby energy pile on the cross-sectional thermal response of an energy pile.

1.4 Research hypotheses

The cyclic temperature variations of the ground source heat pump are hypothesised to induce lower thermal interaction between the energy piles and lower thermal stresses in the piles, compared to monotonic temperature changes. Studies conducted on solitary energy piles have shown that cyclic temperatures induce lower pile stress and ground temperature variations. Furthermore, it is hypothesised that the ground temperature changes between multiple piles would be more significant than that of solitary piles for higher inlet fluid temperatures due to thermal interaction between multiple energy piles.

The variations of soil properties such as soil thermal conductivity, soil thermal expansion coefficient and soil elastic modulus are hypothesised to influence the thermal interaction between energy piles through the soil volume. The variation of soil thermal conductivity would affect the heat transfer between the pile, which in turn would affect the soil temperature variations and thermal interaction between the energy piles. Furthermore, studies on solitary piles have shown that soil thermal expansion and elastic modulus affect the restriction imposed

by surrounding soil to the energy pile, which affects the thermo-mechanical responses of the energy pile.

The temperature and thermal stresses in the energy pile's cross-section are hypothesised to be influenced by variations in inlet fluid temperatures, soil thermal properties, and the presence of a nearby energy pile. Studies on solitary piles have shown evidence that the distribution of temperatures and thermal stresses over the cross-section of an energy pile is not uniform. Since variations in inlet fluid temperatures and soil properties are expected to influence the thermo-mechanical response of piles and the thermal interaction between the piles, it is hypothesised that the uniformity of temperatures and thermal stresses over the cross-section of energy piles would also be influenced by variations in fluid temperatures and soil properties during the operation of multiple energy piles.

1.5 Scope of the thesis

This thesis's objectives were achieved by conducting experimental and numerical studies on one of the two field-scale energy piles spaced at a centre-to-centre distance of 3.5 m. The energy piles were installed at Clayton Campus, Monash University, Melbourne, Australia, under a six-storey residential building. The soil profile at the test site, consisted mostly of dense sands, part of the Brighton Group of materials. One of the two energy piles was instrumented to investigate the temperature, thermal strains/stresses along the length and over the planar cross-section of the energy pile. The ground temperatures between the two energy piles were also monitored. A three-dimensional finite element model was developed and validated with the field test results. A combination of field and numerical tests was used to address the specific aims of the thesis.

The first objective was investigated by conducting field and numerical simulations on the influence of monotonic and cyclic inlet fluid temperatures and nearby energy pile on the instrumented energy pile's thermal responses. The second objective was achieved by

examining the role of soil properties and nearby energy pile on the thermal responses of the instrumented energy pile, experimentally and numerically. The third objective was addressed by conducting field and numerical simulations to evaluate the role of soil properties, inlet fluid temperature and nearby energy pile on the cross-sectional thermal response of the instrumented energy pile.

1.6 Thesis outline

Chapter 1 presents the motivation and background, introduction, the problem statement, research aims and hypotheses, the scope and the outline of the thesis.

A comprehensive literature review on energy piles followed by presenting the knowledge gaps gained from this review is given in Chapter 2.

In Chapter 3, the research methods, including the details of instrumentation of the energy piles and the governing equations for the numerical modelling used to investigate this thesis's objectives, are presented.

In Chapter 4, the influence of monotonic and cyclic inlet fluid temperatures and nearby energy pile on the instrumented energy pile's thermal responses are investigated.

The role of soil properties and nearby energy pile on the thermal responses of the instrumented energy pile is presented in Chapter 5.

In Chapter 6, the role of soil properties, inlet fluid temperature and nearby energy pile on the cross-sectional thermal response of the instrumented energy pile is investigated.

Finally, Chapter 7 summarises the thesis's conclusions and provides recommendations for future work.

2 Literature review

Energy geostructures (such as energy piles, energy tunnels, and energy retaining walls) are used as underground heat exchangers when coupled with ground source heat pumps (GSHPs) to extract shallow geothermal energy to supplement heating and cooling of built structures (Brandl, 2006). Energy geostructures have been successfully operating for over 40 years in different countries. This thesis focuses on expanding the current knowledge on the thermo-mechanical response of energy piles by filling critical knowledge gaps.

Energy piles are dual-purpose geostructures that can support structural loads of a building and access the ground's relatively constant temperature within the building footprint to operate a GSHP. Depending on the buildings' heating and cooling demand, the energy can be extracted from the ground and delivered to the building for heating in winter or stored into the ground during summer to cool the building (Bouazza et al., 2011). There are two primary circuits of an energy pile system which are connected via the GSHP: (*i*) primary circuit below the ground which contains the foundation system; and (*ii*) secondary circuit in the overlying building containing the heat pump and ducting system. A schematic of the primary and secondary circuits of an energy pile system is shown in Figure 2.1. The process of exchanging heat between the energy pile and the ground occurs via heat carrier pipes attached to the reinforcement cage of energy piles during construction, without any further modifications of the foundation structure (Bouazza et al., 2011; De Moel 2010; Laloui and Di Donna 2011; Lu et al., 2017; Lu and Narsilio, 2019). These heat carrier pipes are formed mostly from high-density polyethylene (HDPE) pipes. The temperature changes of energy piles induce thermal stresses in the piles and ground temperature changes typically not accounted for in traditional geotechnical designs of energy piles. Therefore, an understanding of these additional thermal loads is required for safe design practices of these piles.

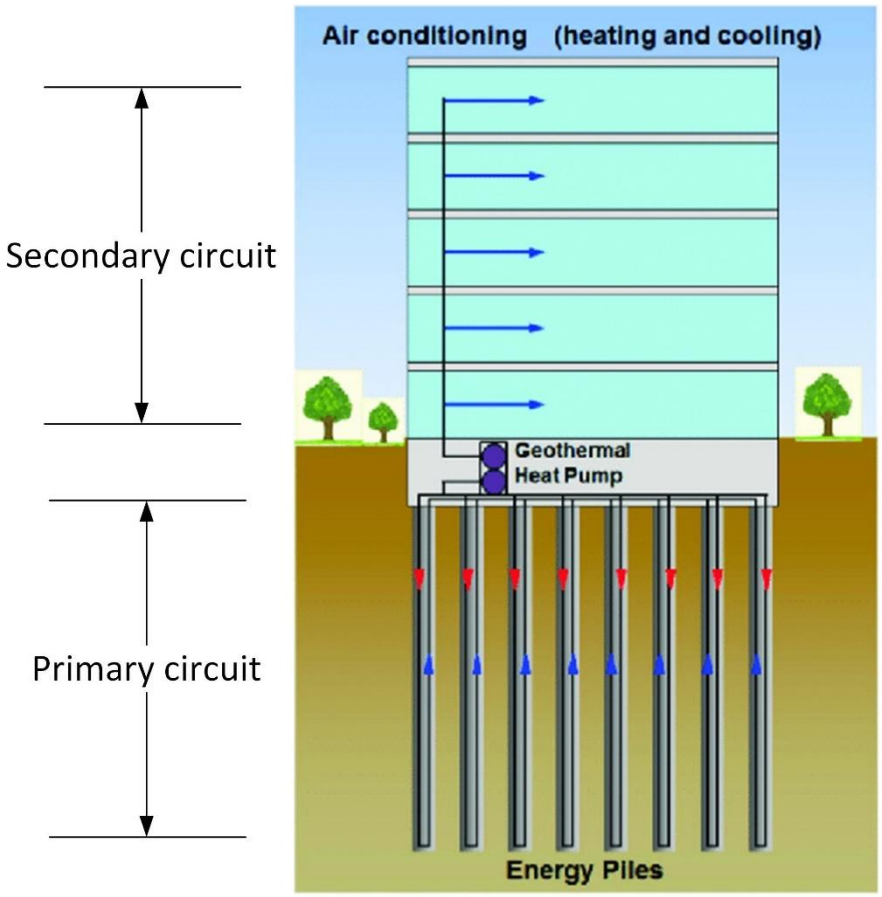

Figure 2.1. Schematic of an energy pile system under a built structure (modified from Olgun 2013).

Heavy buildings are typically supported by pile foundations depending on the site conditions. If an energy pile system is adopted to lower the energy costs, some of the piles can be constructed as energy piles based on the building's energy demand. However, many unknowns remain on how the energy piles might interact with each other under different heating and cooling cycles with various inlet fluid temperatures. There is also limited knowledge of soil properties' effect, representing different site conditions, on energy piles' thermal responses. Furthermore, the influence of varying fluid temperatures and soil properties on the cross-sectional thermal responses of energy piles have also received limited attention.

This chapter summarises the current literature available on the thermal responses of energy piles. Based on the literature reviewed, knowledge gaps were identified and used to determine this thesis's scope.

2.1 Effect of monotonic and cyclic temperature variations on the thermal interaction between energy piles

Energy piles and surrounding soils are subjected to different magnitudes of monotonic and cyclic temperatures depending on the built structure's heating/cooling requirements (Brandl 2006; Murphy and McCartney 2015; McCartney and Murphy 2017, Faizal et al. 2016, 2018, 2019a, 2019b). Moreover, energy piles may interact thermally with other nearby energy piles through the soil due to soil temperature changes, which could influence the piles' thermal responses.

Current studies have mostly focused on the thermal responses of a single energy pile subjected to monotonic temperatures (e.g. Laloui et al. 2006; Bourne-Webb et al. 2009; Akrouch et al. 2014; Mimouni 2014; Murphy and McCartney 2015; Wang et al. 2015; Murphy et al. 2015; Sutman et al. 2015; Khosravi et al. 2016; Adinolfi et al. 2018; Anongphouthet al. 2018; Rui and Soga 2018; Sung et al. 2018; Faizal et al. 2019a; Liu et al. 2019; Moradshahi et al. 2020) and cyclic temperatures (Abdelaziz and Ozudogru 2016; Faizal et al. 2016; Ng and Gunawan 2016; Suryatriyastuti et al. 2016; Faizal et al. 2018, 2019b; Sung et al. 2018; Huang et al. 2018; Sarma and Saggu 2020; Yang et al. 2020). Compared to monotonic temperatures, cyclic temperatures tend to induce lower ground temperatures and different thermal stresses in single energy piles (Faizal et al. 2016) as shown in Figure 2.2. Cyclic temperatures can also lead to the development of lower axial and radial thermal stresses in solitary energy piles, as shown in Figure 2.3. Since cyclic temperature variations have been shown to reduce ground temperature changes and thermal stresses in solitary energy piles (e.g. Faizal et al. 2016, 2018, 2019b), the same can be expected for the operation of more than one energy pile. However, these studies (e.g. Faizal et al. 2016, 2018, 2019b) did not evaluate the impact of different temperature magnitudes on the thermal response of energy piles. Increasing and decreasing inlet fluid temperatures during heating and cooling operations results in pile temperature

changes which can affect the thermal stresses and axial loads in the piles (Han and Yu 2020) (Figure 2.4) as well as the pile head displacements (Yang et al., 2020) (Figure 2.5).

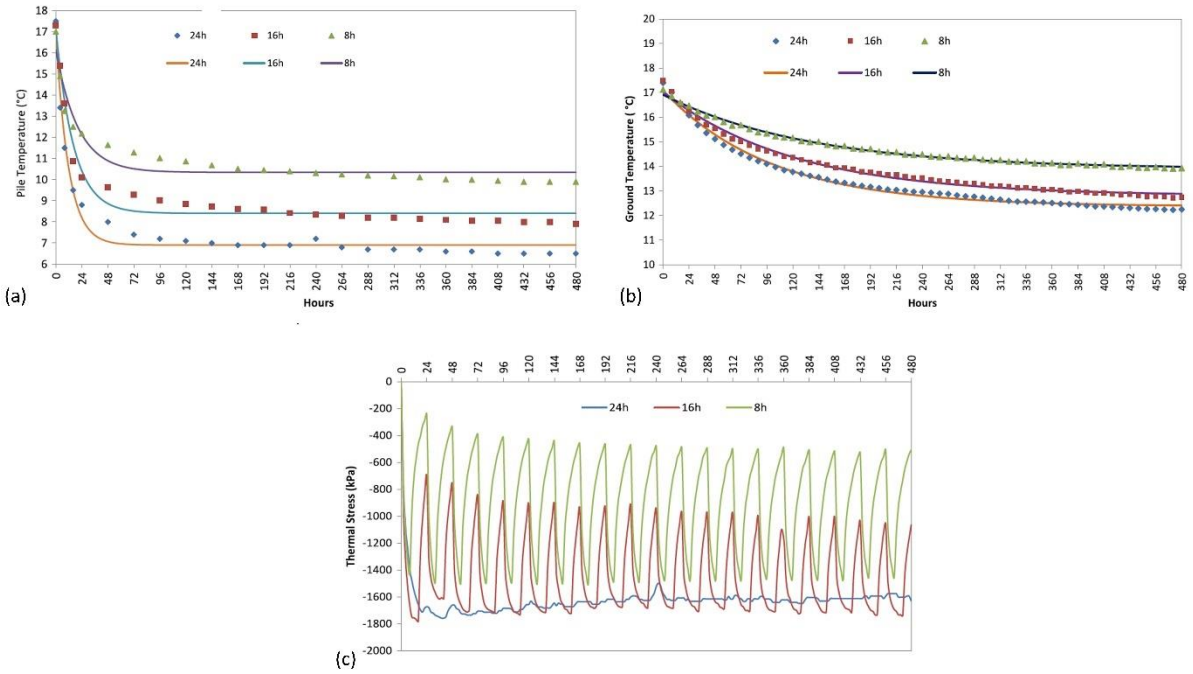

Figure 2.2. The variations of: (a) pile temperatures; (b) ground temperatures; and (c) axial thermal stress for different types of operation for a depth of 5.4 m (from Faizal et al., 2016).

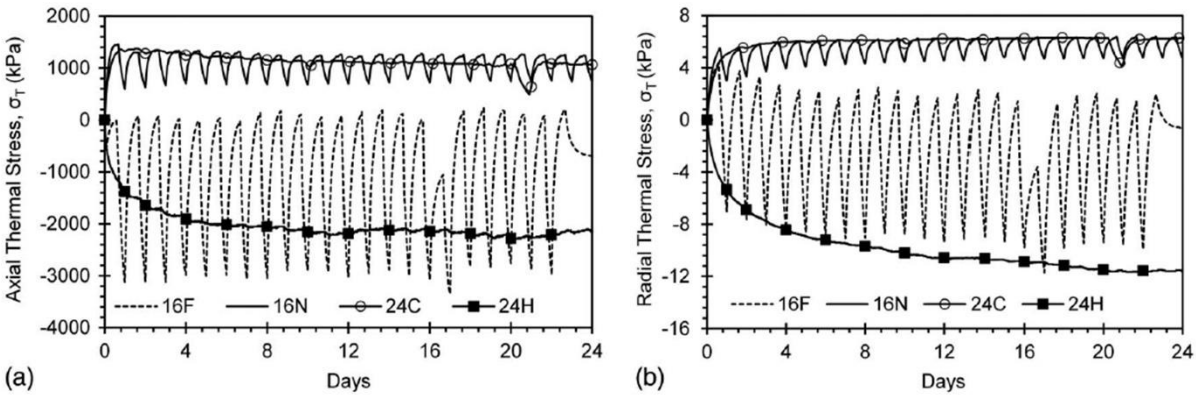

Figure 2.3. Effect of monotonic and cyclic temperature variations on: (a) thermal axial stress; and (b) radial thermal stress of a single energy pile (The cyclic operations: 16h of operation followed by 8h of forced (16F) and natural (16N) ground recovery. The monotonic operations: 24h of continuous heating (24H) and continuous cooling (24C) of the energy pile) (from Faizal et al., 2018).

Higher ground temperatures resulting from higher inlet fluid temperatures might increase the thermal interaction between energy piles via increased heat transfer through the ground, influencing the thermal stresses and pile displacements of individual energy piles.

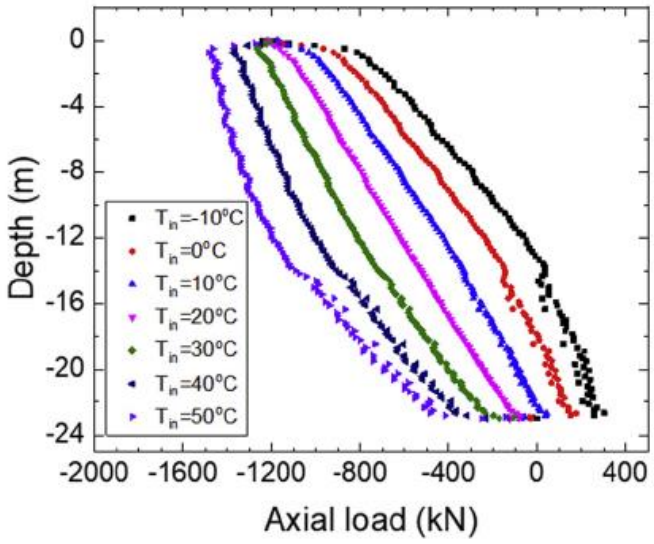

Figure 2.4. Influence of inlet fluid temperature on axial thermal loads in a single energy pile (from Han and Yu, 2020).

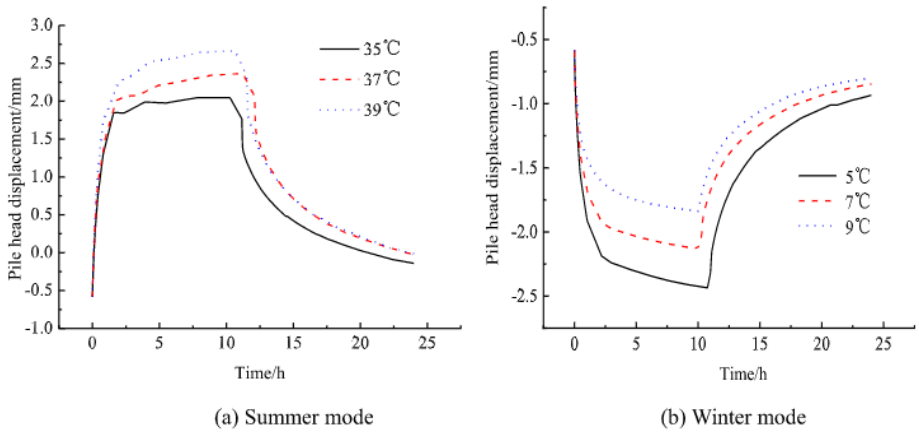

Figure 2.5. Pile head displacement variation of a single energy pile with inlet temperature (from Yang et al., 2020).

Moreover, the influence of different magnitudes of monotonic and balanced and imbalanced cyclic temperatures on/between dual piles or group of piles has received very little attention. Depending on the daily operating to rest time ratios of the ground source heat pump, the piles and the ground could experience daily balanced (e.g., 12 hours of operation followed by 12 hours of rest)or imbalanced (e.g., 16 hours of operation followed by 8 hours of rest) cyclic thermal loads (Olgun et al. 2015). Figure 2.6 shows the effect of the operation of one energy pile (Pile #1) on the nearby energy piles connected with a pile cap (Mimouni and Laloui

2015). A similar observation was reported by Jeong et al. (2014), where different axial thermal loads were observed for a group of energy piles located beneath a raft foundation (Figure 2.7).

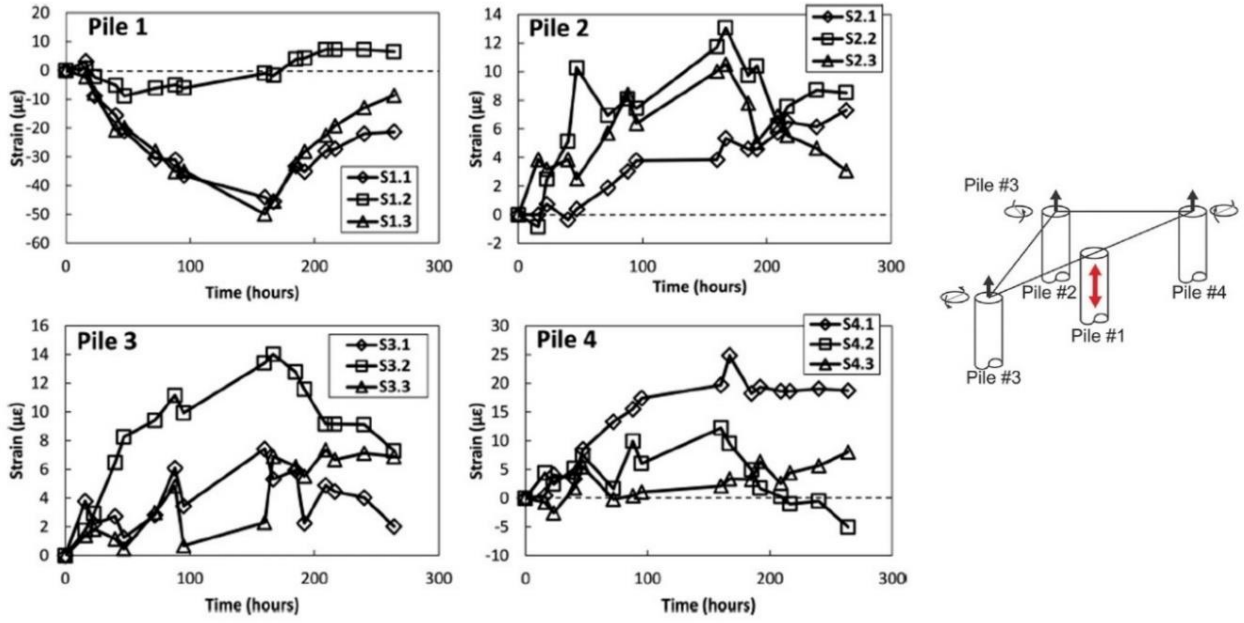

Figure 2.6. Pile head axial strains evolution in nearby energy piles due to Pile #1 operation (modified from Mimouni and Laloui 2015).

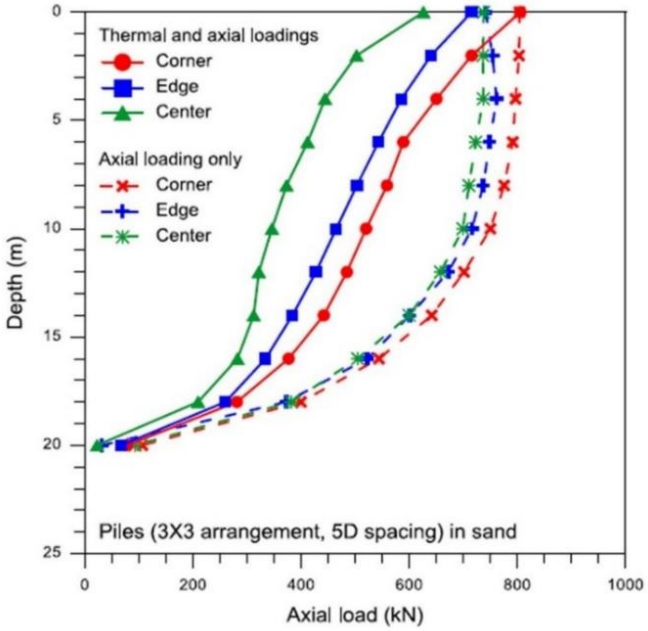

Figure 2.7. Load redistribution between energy piles in a group (from Jeong et al. 2014).

These studies showed that solitary energy piles' behaviour is different from a group of energy piles due to thermal interaction between the piles, especially if a pile-cap connects the

piles. Wu et al. (2020) and Fang et al. (2020), also provided evidence of thermal interaction among nearby energy piles connected with a slab (Figure 2.8 and 2.9, respectively).

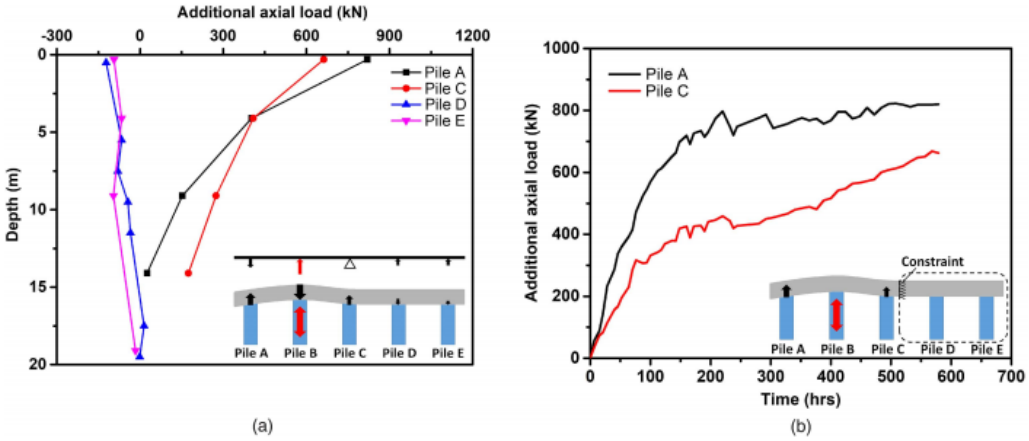

Figure 2.8. Thermally induced axial loads in piles: (a) in the four traditional piles; and (b) at the top of Piles A and C (From Wu et al., 2020).

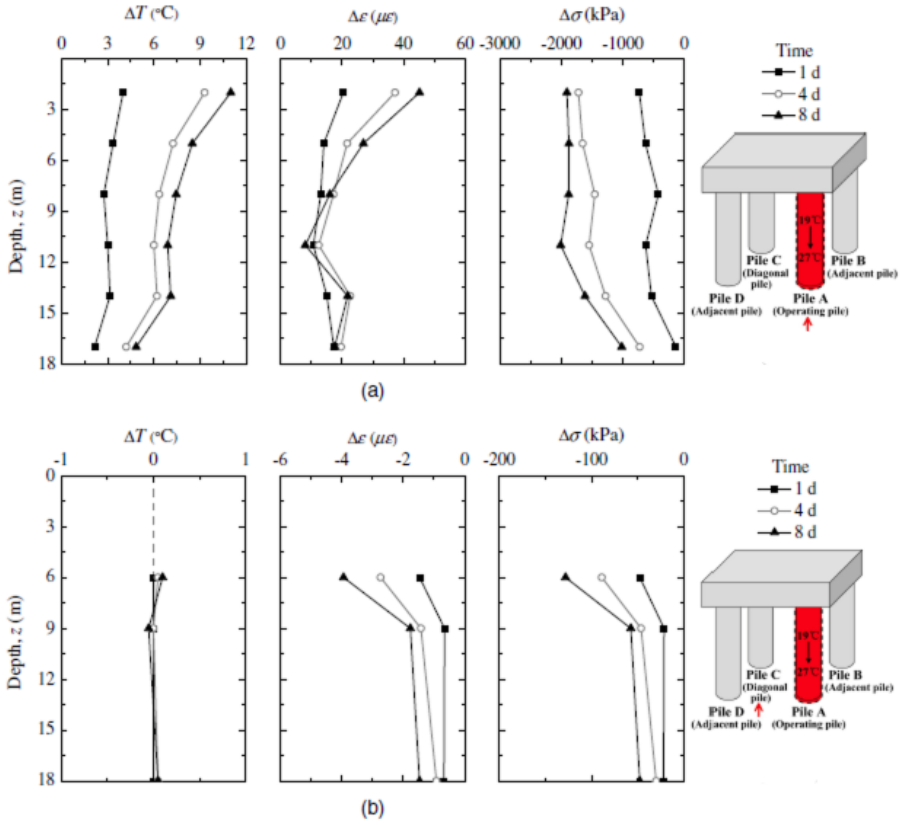

Figure 2.9. Distributions of temperature, strain, and stress along the pile depth: (a) operating pile (Pile A); and (b) diagonal, non-operating pile (Pile C) (modified from Fang et al., 2020).

The work of Jeong et al. (2014); Mimouni and Laloui (2015); Fang et al. (2020); Han and Yu (2020); Wu et al. (2020); and Yang et al. (2020) indicate that closely spaced energy

piles could interact thermally with each other. However, there remains limited knowledge of the influence of various monotonic and cyclic inlet fluid temperatures on the thermal interaction between energy piles and the influence of a nearby energy pile on the thermal stresses in an energy pile.

2.2 Effect of nearby piles and soil properties on the thermal responses of an energy pile

Energy piles may interact with other energy piles or nearby standard piles through a coupled heat transfer and volume change in the surrounding soil. Although there have been several studies on energy pile groups using field testing and numerical simulations, soil properties' role on this interaction is not well understood. For example, field studies conducted by Mimouni and Laloui (2015) showed that thermal interactions between thermal and non-thermal piles, for spacing ranging from 3D to 5D (where D is the pile's diameter), could lead to the development of differential thermal loads in the piles. Field studies on a group of 6 energy piles conducted by You et al. (2014) indicated that ground temperatures overlapped between closely spaced (5D) energy piles. However, the effect of this overlap on the thermal response of the piles was not investigated. Field tests on the axial thermal responses of a group of eight energy piles spaced between 9 m and 12 m (15 D and 20 D) were conducted by Murphy and McCartney (2014) and Murphy et al. (2015). The recorded ground temperatures indicated that the energy piles likely did not interact thermally during the duration of the thermal response tests. Rotta Loria and Laloui (2018) reported the results from field tests on thermal interaction between a triangular-spaced energy pile group with the same spacing as Mimouni and Laloui (2015) that included both operational and non-operational energy piles. They found that higher displacements and lower stresses occurred when all of the energy piles were heated. These observations were confirmed in full-scale tests on a row of energy piles, with 5D spacing, performed by Wu et al. (2020).

A crucial gap in the current literature is that the previous studies did not assess the impact of the variation of some of the soil properties on the piles' thermal responses. Some of these properties that could affect the thermal stresses in energy piles are the thermal conductivity, λ_{soil}, the thermal expansion coefficient, α_{soil}, and the elastic modulus, E_{soil}, of the soil. Studies reported in current literature have investigated the effect of the above soil parameters for single energy piles; however, there is a lack of knowledge of how these soil parameters can affect the energy pile thermal responses if more than one energy pile is operating.

The soil thermal conductivity, λ_{soil}, determines the magnitude of conductive heat transfer between the energy pile and the surrounding soils. Guo et al. (2018) and Salciarini et al. (2017) showed that soils with higher λ_{soil} tend to affect the temperature of a larger volume of soil surrounding an energy pile (Figure 2.10). Therefore, an increase in λ_{soil} could increase the thermal interaction between closely spaced energy piles. Previous numerical studies (Jeong et al. 2014; Salciarini et al. 2017; Guoet al.018) have indicated that soils with lower λ_{soil} tend to reduce the soil temperature changes due to more moderate heat transfer between the energy pile and the soil, leading to an increase in the energy pile temperature (Sani et al. 2019). Numerical studies also reported variations in axial thermal stresses (axial thermal loads) of energy piles (Jeong et al. 2014; Salciarini et al. 2017) when λ_{soil} varied, as shown in Figure 2.11. These studies indicate that λ_{soil} is a key parameter that could affect the thermal responses of thermally interacting piles. The soil thermal expansion coefficient, α_{soil}, provides the magnitude of thermal deformations of the soil when subjected to temperature changes. The soil temperatures between thermally interacting energy piles are anticipated to be higher compared to isolated energy piles; thus, higher soil thermal deformations are also expected (You et al. 2014). The differences in the pile concrete's thermal expansion coefficients and the soil could affect the magnitudes of thermal stresses developed in the energy pile.

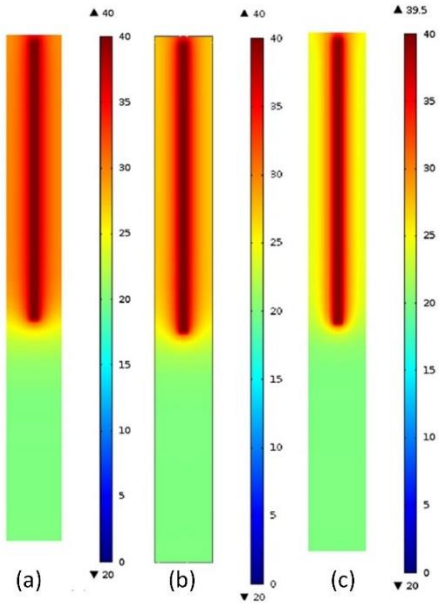

Figure 2.10. Contours of the temperature along the vertical plane for different thermal conductivities: (a) λ_{soil} = 2.5; (b) λ_{soil} = 1.7; and (c) λ_{soil} = 0.9 (from Salciarini et al. 2017).

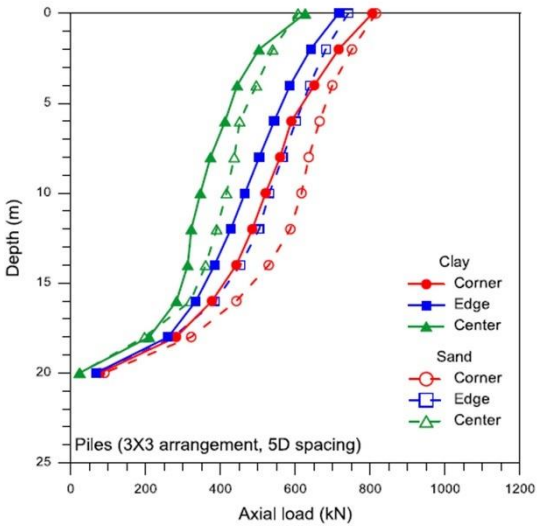

Figure 2.11. Effect of soil thermal conductivity on axial load distribution in a single energy pile, sand with higher λ_{soil} and clay with lower λ_{soil}, (from Jeong et al. 2014).

This aspect has been highlighted by Rotta Loria and Laloui (2017b) in an experimental and numerical study on an energy pile surrounded by non-thermal piles. They indicated that the axial thermal strains developed in the pile varied by the variation of the ratio of soil thermal expansion coefficient, to that of the pile concrete (i.e. $\alpha_{soil}/\alpha_{pile}$) as shown in Figure 2.12.

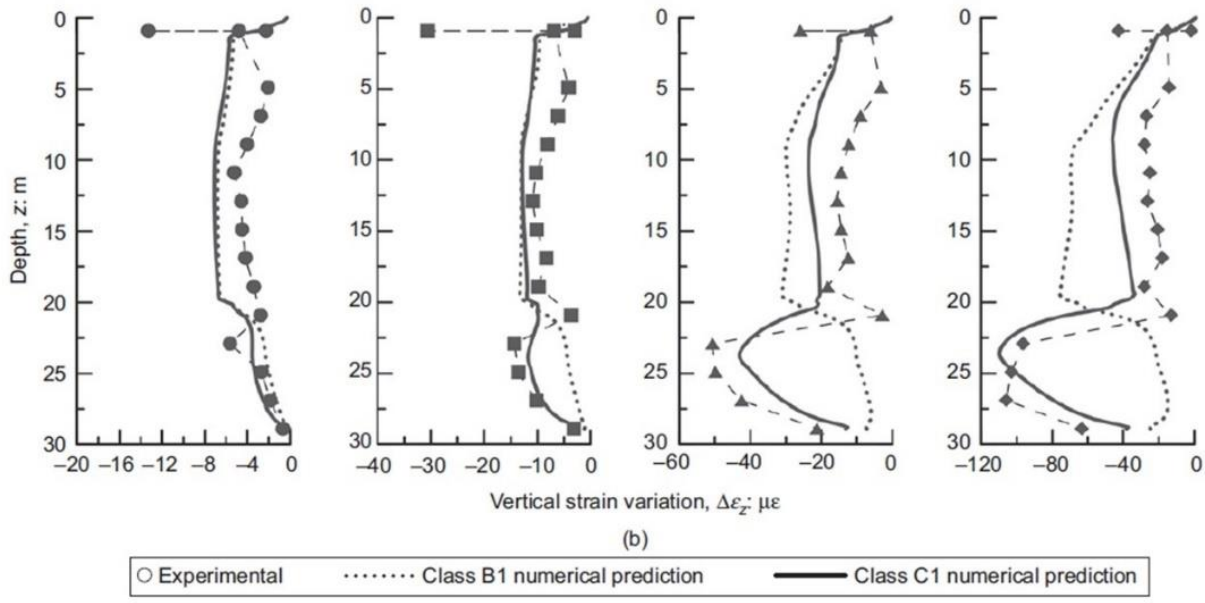

Figure 2.12. Variations in thermal axial strains for Class B1 ($\alpha_{soil}/\alpha_{pile}$>1 for depths above 20m and $\alpha_{soil}/\alpha_{pile}$<1 for depth below 20 m) and Class C1 ($\alpha_{soil}/\alpha_{pile}$<1 for depths above 20m and $\alpha_{soil}/\alpha_{pile}$>1 for depth below 20 m) after 2, 8, 35, and 156 days of testing (from Rotta Loria and Laloui 2017b).

Similar observations were reported by Salciarini et al. (2017) for a single energy pile in a group of energy piles (Figure 2.13) and by Bodas Freitas et al. (2013) and Bourne-Webb et al. (2016) on isolated energy piles (Figure 2.14). Therefore, further investigations on the impact of α_{soil} will provide more insight into the thermal responses of thermally interacting piles.

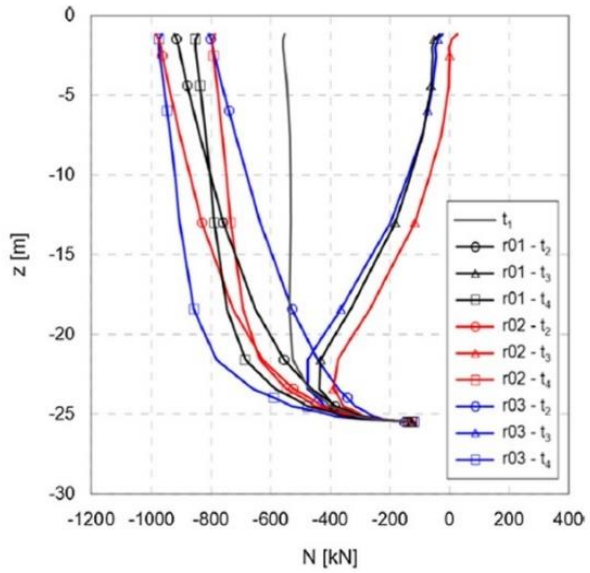

Time station	t (months)	T (°C)	Note
t_1	0	20	Initial equilibrium state
t_2	3	40	Maximum temperature, first cycle
t_3	9	0	Minimum temperature, first cycle
t_4	12	20	End of first cycle
t_5	15	40	Maximum temperature, second cycle
t_6	21	0	Minimum temperature, second cycle
t_7	24	20	End of second cycle

Column 3 provides the temperature of the thermo-active piles

Figure 2.13. Effect of soil thermal expansion coefficient on axial thermal load distribution in an energy pile, r01: $\alpha_{soil}=1\times10^{-4}$, r02: $\alpha_{soil}=9\times10^{-5}$, and r01: $\alpha_{soil}=1.3\times10^{-4}$ (from Salciarini et al. 2017).

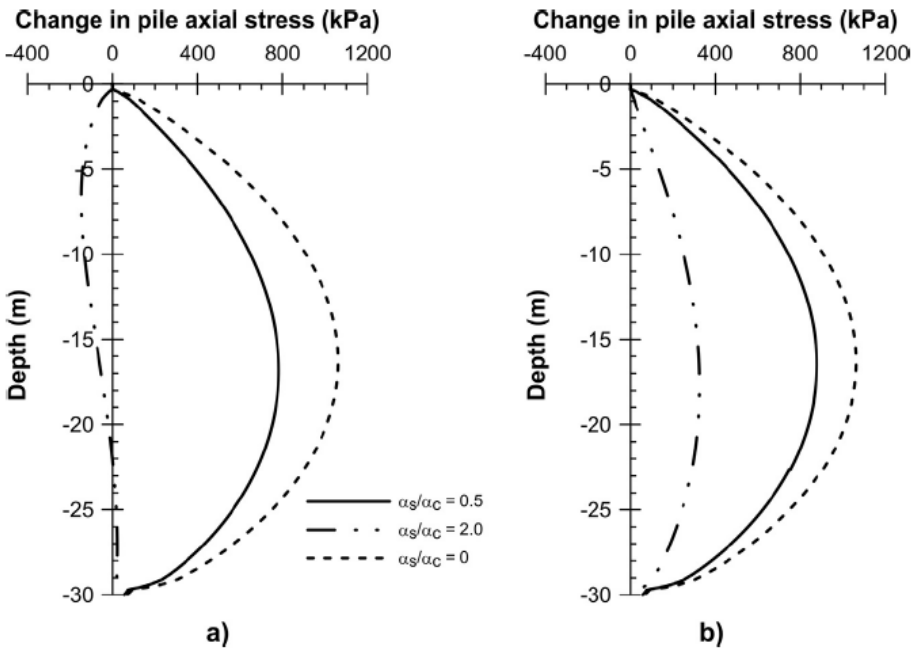

Figure 2.14. Effect of α_{soil} on pile axial thermal stress for: (a) adiabatic ground surface; and (b) constant temperature ground surface (from Bourne-Webb et al., 2016).

The elastic modulus of the soil, E_{soil}, may also affect the thermal responses of energy piles since the restraints to the pile thermal expansion/contraction can be affected. A numerical study conducted by Khosravi et al. (2016) showed that an increase in E_{soil} led to the development of higher magnitudes of axial thermal stresses in an energy pile (Figure 2.15). Moreover, Olgun et al. (2014) observed that increasing E_{soil} resulted in higher magnitudes of radial contact stresses at the pile-soil interface (Figure 2.16).

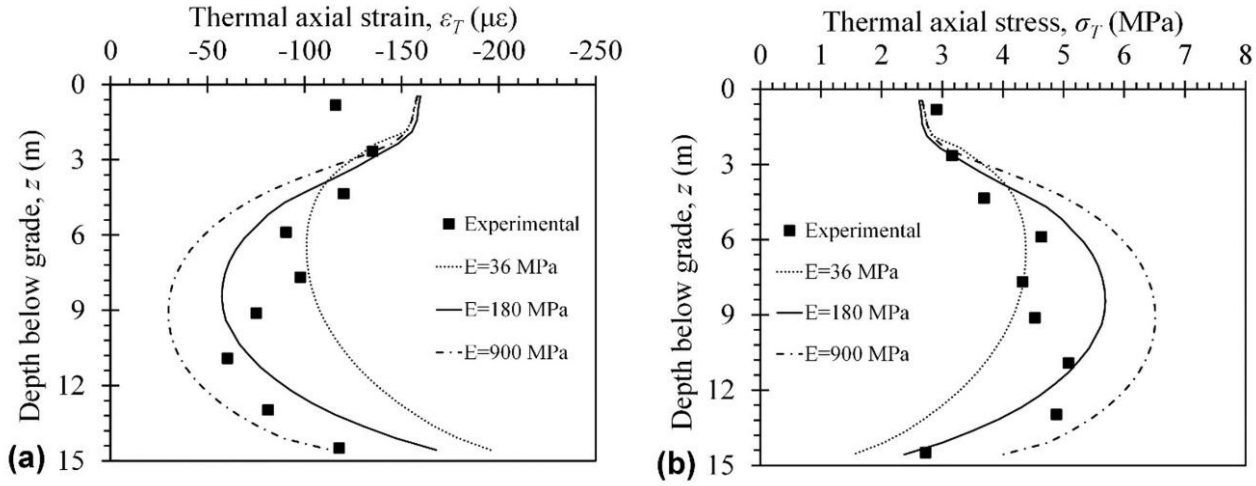

Figure 2.15. Effect of elastic modulus on: (a) thermal axial strain; and (b) thermal axial stress (from Khosravi et al., 2016).

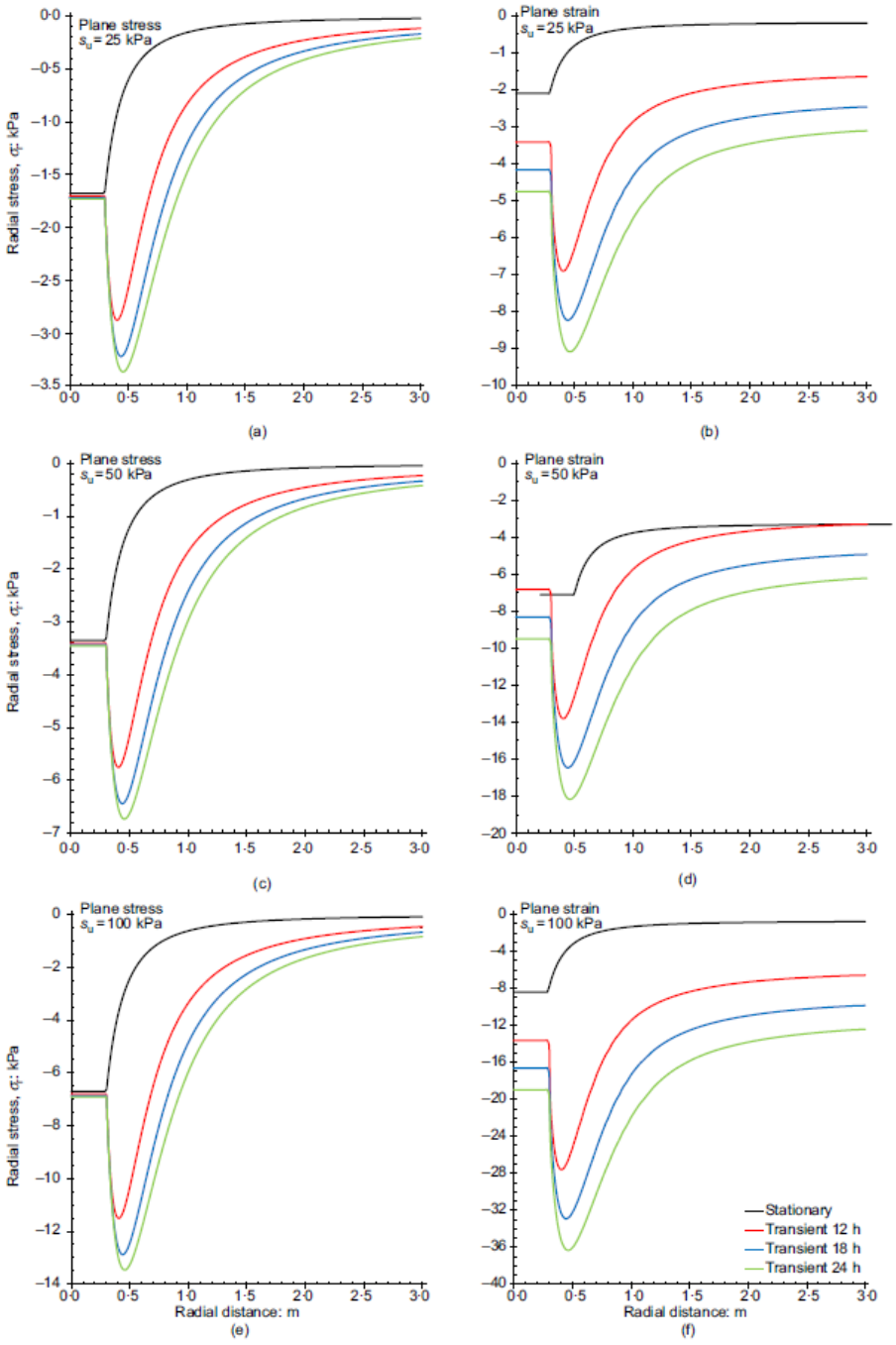

Figure 2.16. Effect of soil elastic modulus ($1000s_u$ in this study) on radial contact stress of an energy pile for (a), (c), and (e) plane-stress model; (b), (d), and (f) plane-strain model (from Olgun et al., 2014).

These limited studies indicate that variation of E_{soil} could affect the axial and radial thermal responses of energy piles and should be, therefore, a subject of further investigation for thermally interacting piles. The current literature indicates that further studies are required on the role of soil properties and nearby energy piles on an energy pile's thermal responses.

2.3 Cross-sectional thermal responses of an energy pile

Due to the transient changes in the temperature of the heat pump circulating fluid, the temperature across an energy pile's cross-section will also vary (Abdelaziz and Ozudogru 2016a, 2016b; Caulk et al. 2016; Han and Yu 2020; Liu et al. 2020). However, the majority of field-scale studies on energy piles only measured the thermal response of the energy pile at a single location in the cross-section of the pile (e.g. Laloui et al. 2006; Bourne-Webb et al. 2009; Akrouch et al. 2014; Murphy et al. 2015; Murphy and McCartney 2015; Sutman et al. 2015; Faizal et al. 2016, 2018; Mimouni and Laloui 2015; Rotta Loria and Laloui 2017a, 2017b, 2018; Fang et al. 2020; Moradshahi et al., 2020; Wu et al. 2020). Assuming that the temperature measured at the single location is representative of the temperature across the cross-section of an energy pile has been shown to lead to errors in estimating thermal strains and stresses, mostly when heating and cooling occurs (McCartney et al. 2015; Murphy and McCartney 2015; Abdelaziz and Ozudogru 2016a, 2016b; Caulk et al. 2016).

Numerical studies showed that non-uniform temperature and stress variations occurred between the centre and edge of the energy pile (Abdelaziz and Ozudogru 2016a, 2016b; Caulk et al. 2016; Han and Yu 2020; Liu et al. 2020), as shown in 2.17, 2.18, 2.19, and 2.20, but very few field studies have been performed to validate these numerical observations (e.g. Faizal et al. 2019a; 2019b).

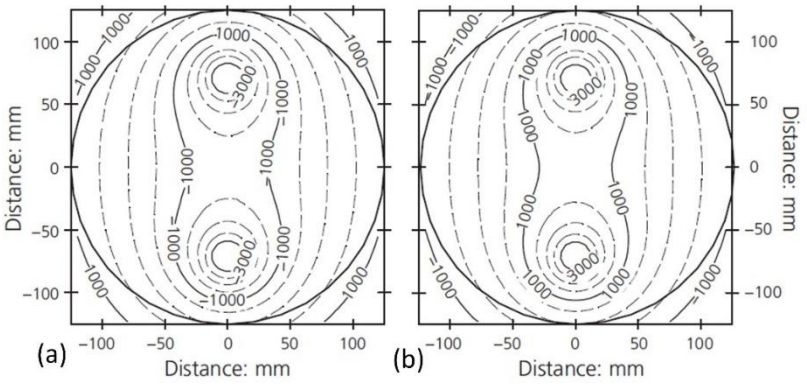

Figure 2.17. Cross-sectional distribution of axial thermal stresses (kPa) for: (a) mid-heating; and (b) mid-cooling (from Abdelaziz and Ozudogru 2016a).

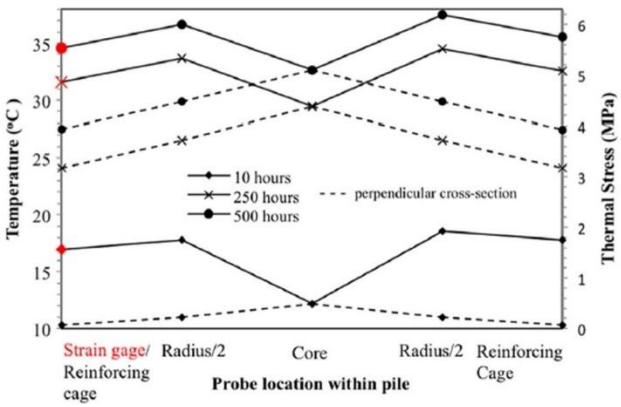

Figure 2.18. Distribution of temperature and thermal axial stress across the pile cross section at 7.6m depth (from Caulk et al. 2016).

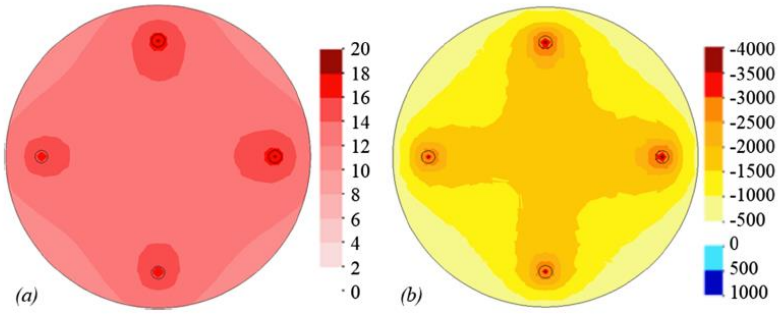

Figure 2.19. Distribution of (a) temperature and (b) thermal axial stress (kPa) across the pile cross section at 17m depth (from Liu et al. 2020).

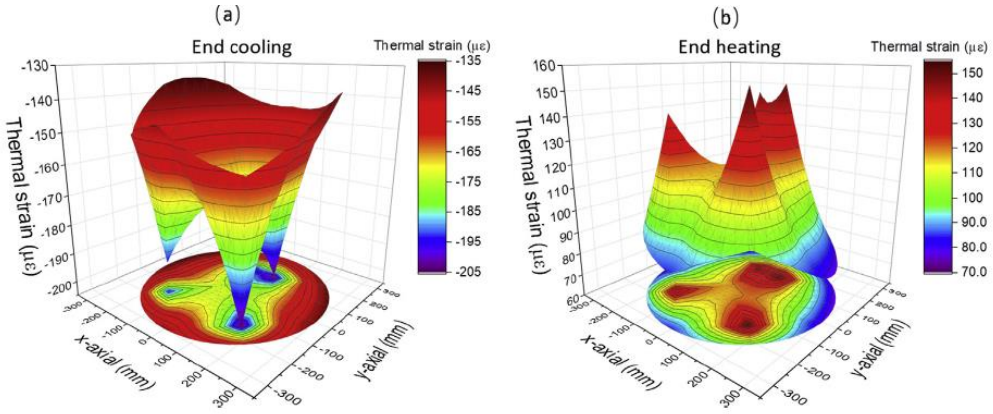

Figure 2.20. Contours of thermal strain inside the energy pile at 11.5 m depth at the (a) end of cooling; (b) end of heating (from Han and Yu 2020).

Although Faizal et al. (2019a, 2019b) found that temperature and stress calculated using vibrating wire strain gauges (VWSGs) at similar radial distances, they did not measure the temperature or thermal axial stresses near the pile-soil interface (Figure 2.21). The pile

temperature at the edge of the pile would be expected to be similar to the soil temperature, hence leading potentially to temperature and stress gradients across the pile's diameter.

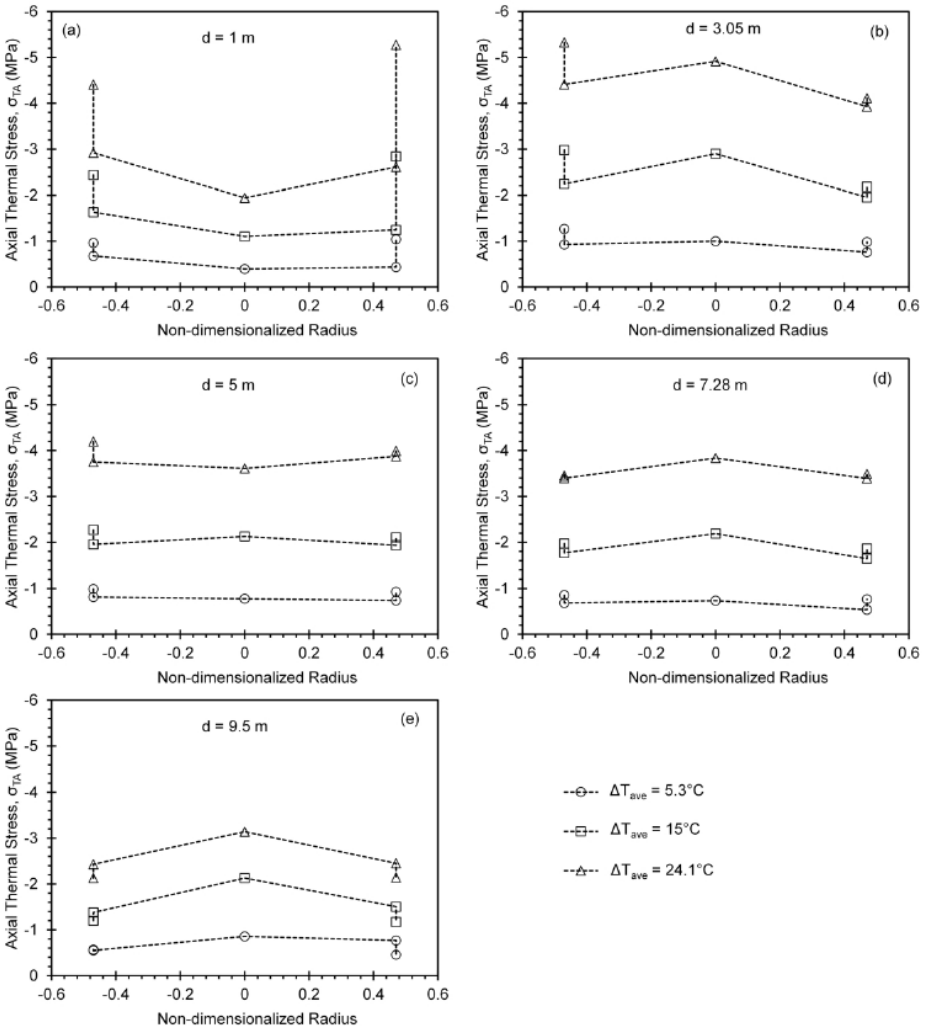

Figure 2.21. Axial thermal stress distribution over the planar cross-section of the pile at different depths, d: (a) d = 1 m; (b) d = 3.05 m; (c) d = 5 m; (d) d = 7.28 m; (e) d = 9.5 m (from Faizal et al. 2019a).

The numerical studies reported by Abdelaziz and Ozudogru (2016a, 2016b); Caulk et al. (2016); Han and Yu (2020); Liu et al. (2020) were conducted for single energy piles with given inlet fluid temperatures and one set of soil properties, so the factors governing the distribution in temperature and stress across the cross-section of an energy pile are not fully understood. Accordingly, there is currently a knowledge gap on the effects of inlet fluid temperatures, soil properties, and the presence of a nearby energy pile on the distribution of

temperatures and stresses in the cross-section of energy piles. The magnitudes of thermal stresses in energy piles depend on the magnitudes of inlet fluid temperatures (e.g. You et al. 2014; Mimouni and Laloui 2015; Murphy and McCartney 2015; Faizal et al. 2016; Han and Yu 2020). Variations of λ_{soil} affect the heat transfer between the pile and the soil (Jeong et al. 2014; Salciarini et al. 2015, 2017; Guo et al. 2018; Sani et al. 2019; Moradshahi et al. 2020) which can affect the pile-soil interface temperatures and hence the temperature and stress distribution in the cross-section.

Variations in α_{soil} and E_{soil} affect the restrictions imposed by the soil on the thermal expansion and contraction of energy piles (Bodas Freitas et al. 2013; Bourne-Webb et al. 2015; Salciarini et al. 2015; Khosravi et al. 2016; Rotta Loria and Laloui 2017b; Salciarini et al. 2017; Moradshahi et al. 2020), which in turn could influence the magnitudes of stresses developed in the cross-section of the energy pile. Moreover, the presence of a nearby energy pile can also influence the cross-sectional temperature and stress distributions of an energy pile due to possible thermal interaction between the piles through the soil and is also a subject for further study. Further studies are required to investigate the influence of inlet fluid temperatures, soil properties (soil thermal conductivity, λ_{soil}, thermal expansion coefficient, α_{soil}, and elastic modulus, E_{soil}) and the presence of a nearby energy pile on the temperature and stress distribution in the cross-section of an energy pile.

2.4 Conclusions from the literature review

Studies conducted on single field-scale energy piles showed that the ground temperature changes and the piles' thermal response during continuous operation of GSHP are different from intermittent operations. A single energy pile's thermal response can be significantly affected by different magnitudes of inlet fluid temperature. However, in practice, multiple pile foundations are constructed as energy piles to meet the built structure's energy demands and hence could interact thermally with each other. Studies on closely spaced energy piles showed

evidence of higher ground temperature changes due to thermal interaction among the energy piles. Since intermittent operations of single energy piles have shown to induce lower ground temperature changes, it is expected that intermittent operations of energy piles would reduce the thermal interaction among closely spaced energy piles due to lower ground temperature changes.

Past studies also showed that the variations in soil properties such as soil thermal expansion coefficient, soil thermal conductivity, and soil elastic modulus, affect the thermal response of single energy piles. It is expected that the operation of multiple energy piles for various soil properties would affect the thermal interaction between the energy piles through the soil volume, hence influencing the thermal stresses developed in the energy piles. Furthermore, studies on single energy piles have also shown that the temperature and stresses in the planar cross-section of the pile vary between the centre and edge of the pile. The cross-sectional thermal responses of an energy pile could also be influenced by nearby energy piles and varying inlet fluid temperatures and soil properties.

2.5 Knowledge gaps

Most of the studies reported in the current literature have focused on a single energy pile's thermal response. Limited field and numerical studies have focused on the thermal interaction between closely spaced energy piles. There is a lack of knowledge on the effect of fluid temperature on the thermal interaction between closely-spaced energy piles. Hence, the thermal stresses developed in the piles due to thermal interaction, for varying magnitudes of monotonic and cyclic inlet fluid temperatures. There is also a lack of knowledge of soil properties, such as soil thermal conductivity, soil thermal expansion coefficient, and soil elastic modulus, on the thermal interaction among energy piles when more than one energy pile is operating. There is also a lack of knowledge on the distribution of temperature and thermal stresses in the cross-section of energy piles for closely spaced energy piles, for varying inlet

fluid temperatures and soil properties. This thesis aims to address these knowledge gaps to improve the geotechnical design of energy piles for a wide range of parameters encountered in practice.

3 Research methods: field-scale energy piles and numerical simulation

3.1 Introduction

This thesis's research objectives were investigated using field-scale energy piles and finite element (FEM) analysis. Two instrumented energy piles were installed beneath a student residential building in 2015 as part of an extensive research program on energy piles. The energy piles site was located at Monash University, Clayton Campus, Melbourne, Australia. The building was erected on sedimentary deposits which are part of the Brighton Group of Sediments (BGS) and consisted of dense to very dense sands. A detailed description of the installation and instrumentation of the energy piles are given in Faizal (2018) and Faizal et al. (2018). A three-dimensional numerical model was developed based on the field data to conduct a parametric evaluation. This chapter summarises the field scale energy piles and provides a detailed description of the numerical model adopted to investigate this thesis's specific aims.

3.2 Field-scale energy piles

3.2.1 Site description

The test site's soil formation comprises tertiary age sedimentary deposits forming part of the Brighton Group (Barry-Macaulay et al., 2013; Singh et al., 2015). The lithology at the site consists of fill material, up to a depth of 0.4 m, moist with medium density, and comprised of crushed rock and/or silty sands. Moist natural silty and sandy clay with stiff to a very stiff consistency with interbedded thin sandy lenses is present up to a depth of approximately 3.5 m. This is underlain to 12.5 m depth by moist dense sand with interbedded layers of clayey sand and silty sand and cemented lenses. No groundwater was encountered within the depth of the pile during drilling, and the soil was inferred to be unsaturated. The ground conditions are summarised in Table 3.1.

Table 3.1. Summary of ground conditions under the student residential building (modified from Faizal et al. 2019a).

Soil type	Depth (m)	Soil description
Fill material	0-0.4	Moist medium dense sand, silt, crushed rocks
Sandy clay	0.4-3.5	Stiff to very stiff, consists of silt, sand traces
Sand	3.5-12.5	Moist dense sand, traces of clay and cemented lenses

3.2.2 Energy piles

Two foundation piles below a new 6-storey student residential building at Monash University, Clayton Campus, Melbourne, Australia, were constructed as energy piles. The building construction began in September 2014 and was completed in December 2015 (Figure 3.1).

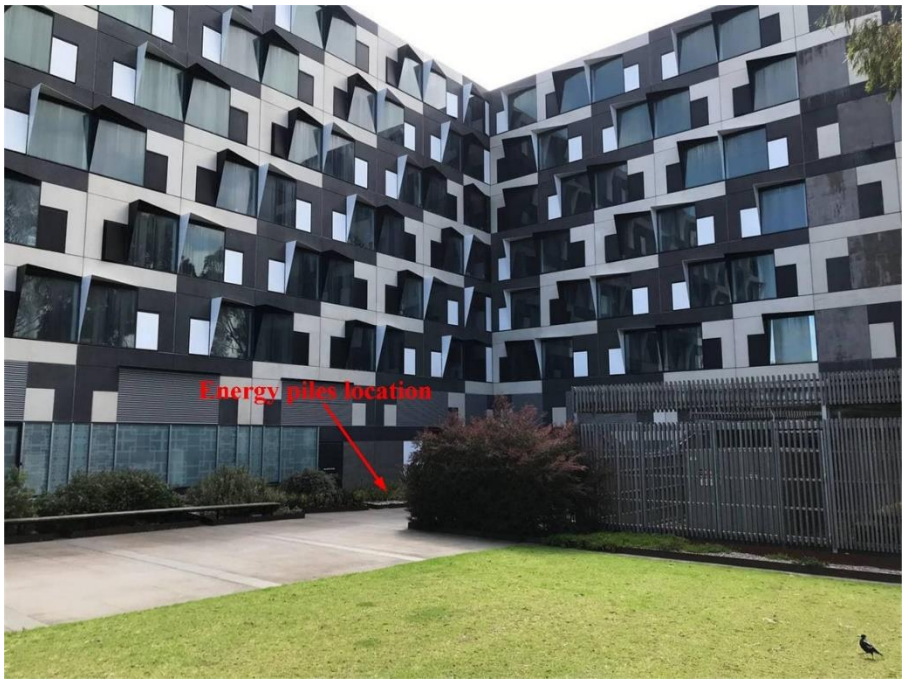

Figure 3.1. The student residential building beneath which the new energy piles were installed (Logan Hall, Monash University, 2021).

The piles had a diameter of 0.6 m and were installed to a depth of 10 m. The pile reinforcement cages had a mass of approximately 150 kg each, a length of roughly 10 m and contained ten vertical reinforcement bars of 30 mm diameter. The cage's outer rings had a

diameter of 445 mm and were made of 16 mm diameter rods spread spirally across the length of the pile cage at a spacing of 150 mm. A schematic of the field setup with the instruments' locations is shown in Figure 3.2. The energy piles were not linked with a slab and were located at a centre-to-centre distance of 3.5 m. To monitor ground temperature between the two energy piles, two boreholes, BH1 and BH2, of 0.1 m diameter were installed at radial distances of 0.63 m and 1.95 m from the edge of EP1. Each borehole was instrumented with six thermocouples at 2 m depth intervals; a cementitious grout was used in each borehole. A schematic of two energy piles and boreholes are described in Figure 3.2. The instrumentation and the two boreholes' location are shown in Figure 3.3a and 3.3b, respectively.

The energy piles had four U-shaped heat exchangers formed from high-density polyethylene (HDPE) pipes attached to the inside of the reinforcement cage prior to lowering it into the ground (Figure 3.4). These pipes carried the heat transfer fluid. They were connected to U-connectors at the base of piles. The inner and outer diameters of the HDPE pipes are 20 mm and 25 mm respectively with a horizontal spacing of 200 mm between the pipes in a U-loop. All the U-loops were pressure tested to check for potential leakages once they were connected with U-connections. Removable tremies were used to prevent damage to the sensors due to pouring wet concrete.

One of the energy piles (referred to as EP1) was instrumented with vibrating wire strain gauges (VWSGs) and thermocouples while another one (referred to as EP2) was only instrumented with thermocouples. As shown in Figure 3.2, the VWSGs in EP1 were oriented vertically and radially at 5 depths to capture axial and radial thermal responses. This pile contained 30 VWSGs (model Geokon 4200) installed in the concrete (which measured temperatures as well), 14 type T thermocouples installed on the external pipe wall of the U-loops, and three thermocouples at the pile-soil interface at depths of 1.1 m, 3.6 m, and 6.6 m. The second pile (EP2) was only instrumented with two thermocouples installed on the external

wall of the first U-loop at depths of 1 m and 9.8 m, respectively. The concrete cover to the edge of the HDPE pipes was approximately 95 mm.

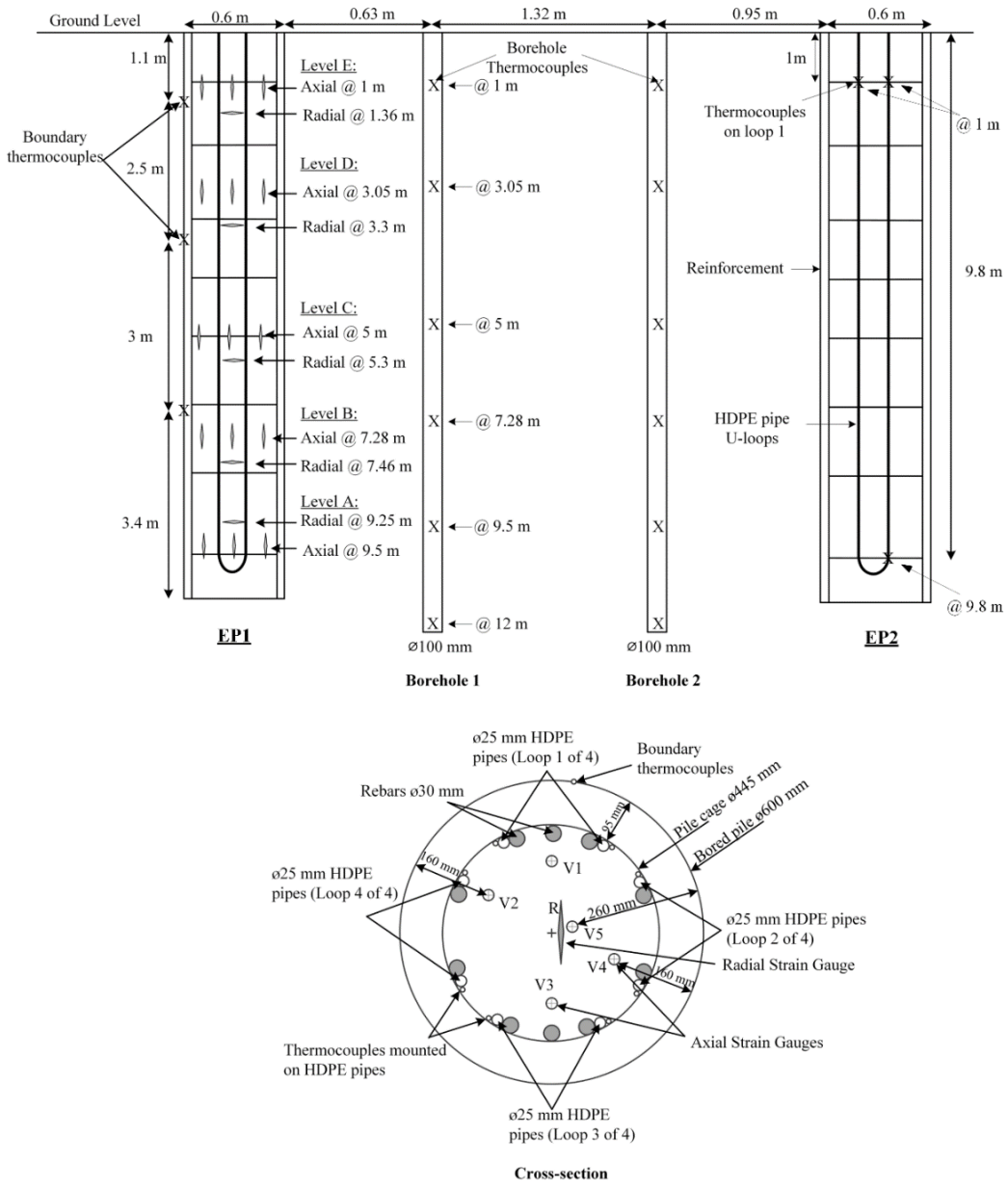

Figure 3.2. Schematic of the instrumented energy pile and location of the sensors over the cross section at each depth (after Faizal 2018).

The axial VWSGs were installed at depths of 1 m (Level E), 3.05 m (Level D), 5 m (Level C), 7.28 m (Level B), and 9.5 m (Level A) with reference to the ground surface. The radial VWSGs were positioned at depths of 1.36 m (Level E), 3.3 m (Level D), 5.3 m (Level C), 7.46 m (Level B), and 9.25 m (Level A). The axial strain gauges at each level are labelled as V1, V2, V3, V4, and V5, while the radial gauges are labelled as R. For instance, AV1 and

AR mean vertical strain gauge and radial strain gauge at depth of 9.5 m and 9.25 m respectively. At each of these five levels, four axial VWSGs (V1, V2, V3, and V4) at average concrete cover of about 160 mm together with an axial and radial VWSG (V5 and R respectively) near the centre of energy pile were installed. The presence of the axial VWSGs at different locations over the cross-section of EP1 at different depths was used to study the thermal responses across the planar cross-section of the pile (Chapter 6).

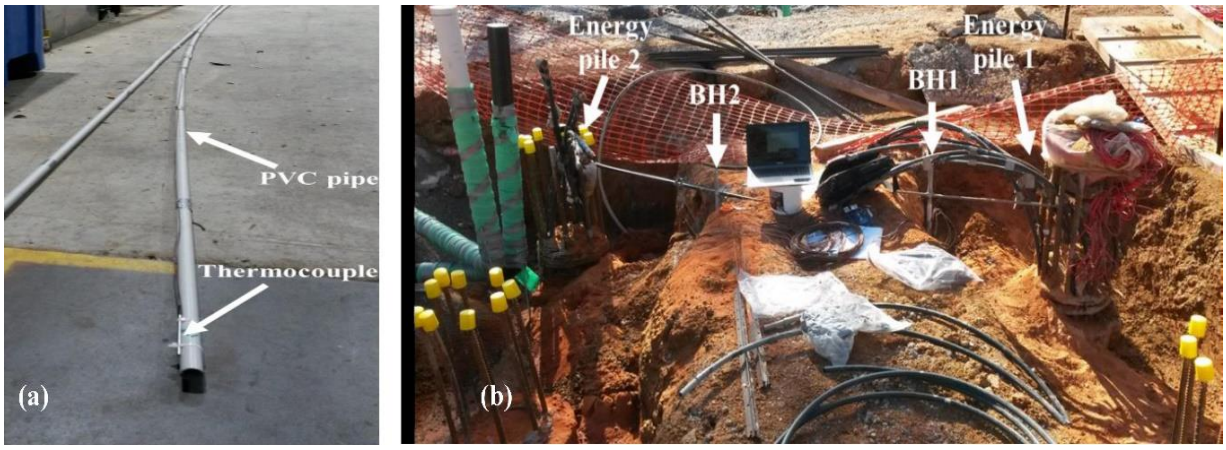

Figure 3.3. Boreholes installation details: (a) PVC pipes and attached thermocouples; and (b) energy piles and borehole locations.

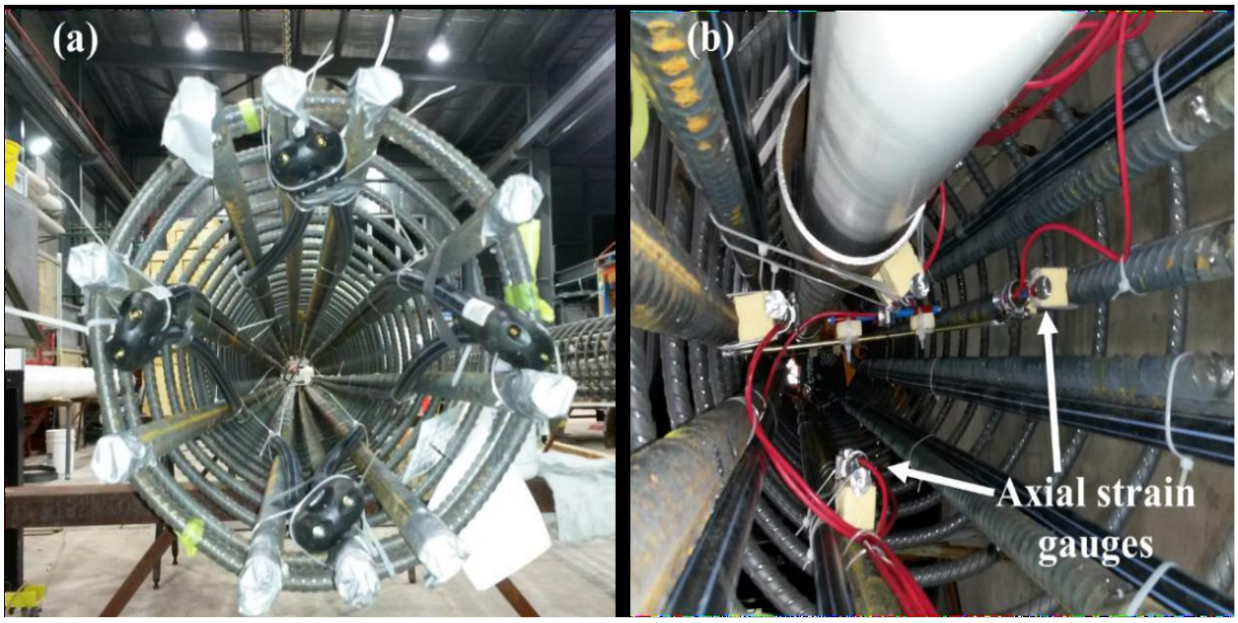

Figure 3.4. HDPE heat exchanger pipes and details of the instrumentation of pile cage: (a) heat-exchangers attached to the reinforcement cage; and (b) axial strain gauges (modified from Faizal et al., 2019b).

3.2.3 Heating and cooling systems

Seven field tests were conducted to investigate single and dual-energy piles' thermal responses under monotonic heating, monotonic cooling, and cyclic temperatures, as shown in Table 3.2. The monotonic heating and cooling of the considered energy pile (EP1) and dual-energy piles (EP1+EP2) included 24 hours of continuous heating (24H) and continuous cooling (24C) operations. The cyclic experiments were conducted as daily intermittent operation with 16 hours of cooling followed by 8 hours of heating (16C8H) for both single (EP1) and dual pile (EP1+EP2) operations. Additionally, a 24-hour continuous heating experiment in which only EP2 was operating (i.e. single pile heating (EP2)) was conducted to investigate the effect of the operation of EP2 on the thermal response of the non-operating EP1.

Table 3.2. Description of the field experiments.

Experiment #	Operation mode	Description	Inlet water temperature (°C)	Inlet water flow rates (L/min)	Experiment duration (Days)	Chapter
1	Single heating	24 hours of heating of EP1(Faizal et al. 2019a)	48	11	18	4, 5 and 6
2	Single heating	24 hours of heating of EP2	46	40	11	5
3	Dual heating	24 hours of heating of EP1 and EP2	42	10	42	4, 5 and 6
4	Single cooling	24 hours of cooling of EP1	1	12	21	4 and 6
5	Dual cooling	24 hours of cooling of EP1 and EP2	5	10	14	4 and 6
6	Single cyclic	Daily intermittent operation of EP1 (Faizal et al. 2019b)	8-26	16	16	4
7	Dual cyclic	Daily intermittent operation of EP1 and EP2	4-25	14	15	4

A commercial 2-5 kW Envision geothermal/water source heat pump and a 0.37 kW Grundfos CRI 1-3 vertical centrifugal water pump were used for cooling and cyclic operations as shown in Figure 3.5a. The water temperature entering the energy pile was manually adjusted by the thermostat control valve used to control the air temperature exiting the heat pump. To avoid the possibility of freezing water that could block the pipes and damage the pump during the cooling cycles, a Fernox Alphi-11 antifreeze protector was added to the buffer tank's water at approximately 25% of the total volume of water in the system.

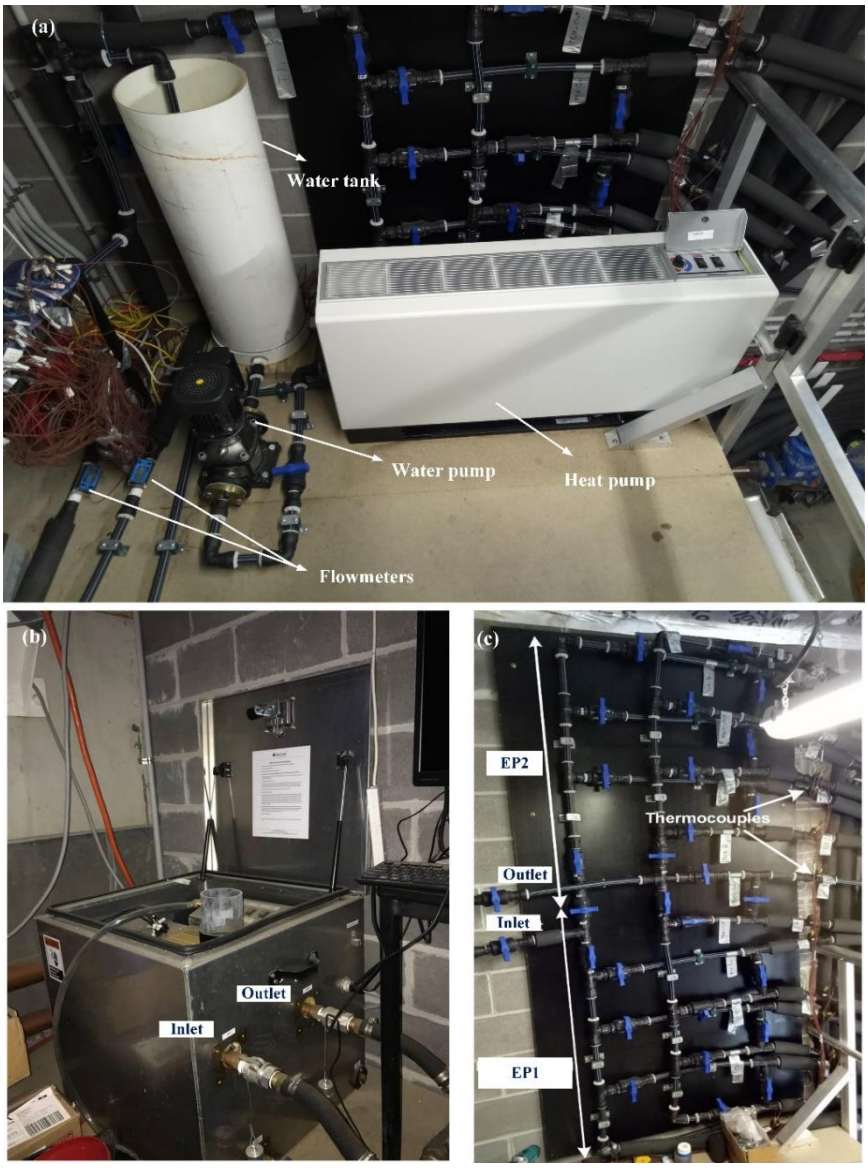

Figure 3.5. The heating and cooling system setup in the plant room 15 m away from the energy piles: (a) heat pump for cooling and cyclic operations; (b) TRT unit for heating operations; and (c) the plumbing manifold.

The heat pump was specifically used for cooling and cyclic heating/cooling. A GeoCube TRT unit with approximately 4 litres of tank volume (Figure 3.5b) was used as a heating unit to circulate the hot water in the energy piles for single and dual pile heating operations. Figure 3.5c shows the HDPE pipe connections running through both energy piles into the plumbing manifold mounted on the wall. The inlet and outlet of the U-loops installed in both energy piles were connected to the heating and cooling units' inlet and outlet. T-type thermocouples were used to record the fluid temperature for each loop.

3.2.4 Data derivation and analysis

Pico Technology's USB-TC08 data loggers were used to record data from all the thermocouples in the piles and the ground. For recording data from VWSGs, Campbell scientific CR1000 data loggers were used (Figure 3.6). GPI TM075 flowmeters installed at the inlet and outlet pipelines of the plumbing manifold were used to record the flow rate of fluid circulating in the energy pile system.

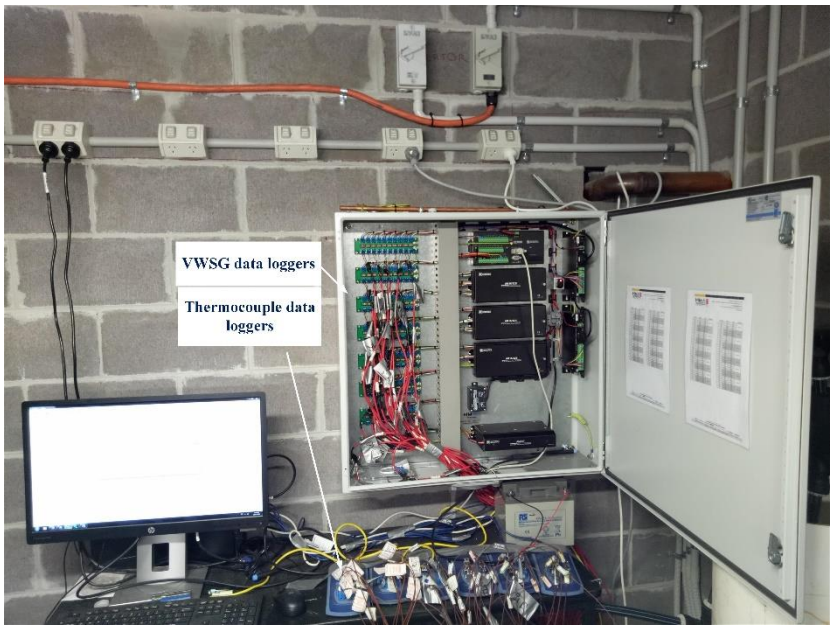

Figure 3.6. Data logging systems for VWGSs and thermocouples.

The thermal strains, ε_T, were obtained by correcting for the temperature effects using the following equation:

$$\varepsilon_T = (\varepsilon_i - \varepsilon_0)B + (T_i - T_0)\alpha_s \quad (3.1)$$

where ε_i is strain at time i, ε_o is the initial reference strain, B is the batch calibration factor of the strain gauges with a value of 0.975, T_i is the temperature of the strain gauges at time i, T_o is the reference temperature of the strain gauges, α_s is the coefficient of linear thermal expansion of steel wire in the strain gauges (12.2 με/°C). As the value of ε_o was selected at the beginning of each experiment, the mechanical strains imposed by the superstructure and the pile weight were neglected in thermal strain calculations. As a result, all of calculated axial and radial thermal strains and stresses were only due to temperature changes. The strains in Equation 3.1 was calculated with the following equation:

$$\varepsilon = G(f^2 \times 10^{-3}) \quad (3.2)$$

where f is the resonant frequency of the strain gauges at the reference or at time i, and G is the gauge factor with a magnitude of 3.304.

3.3 Numerical simulation

3.3.1 Numerical model description

A three-dimensional finite element model was developed using COMSOL Multiphysics software and validated with field data. The 40×15×30 m^3 3D finite element model, shown in Figure 3.7, consisted of 344821 tetrahedral, triangular, prismatic, linear and vertex elements. The model geometry was developed based on the dimensions of the field piles. A preliminary numerical analysis was conducted to determine the ground domain range to avoid boundary effects. The roller boundary conditions were applied to the numerical model's sides to allow vertical movements. The bottom boundary was fully mechanically restricted, whereas the top boundary was considered a free boundary. No interface element was assumed for the soil-pile interface. The energy piles and the soil were assumed to be perfectly bonded to each other at the pile-soil interface; hence, the possibility of yielding at the interface was not considered. Similar assumptions were made in recent numerical studies reported in the

literature (e.g. Batini et al. 2015; Gawecka et al. 2017; Rotta Loria and Laloui 2017b, 2018; Salciarini 2017; Adinolfi et al. 2018; Liu et al. 2020).

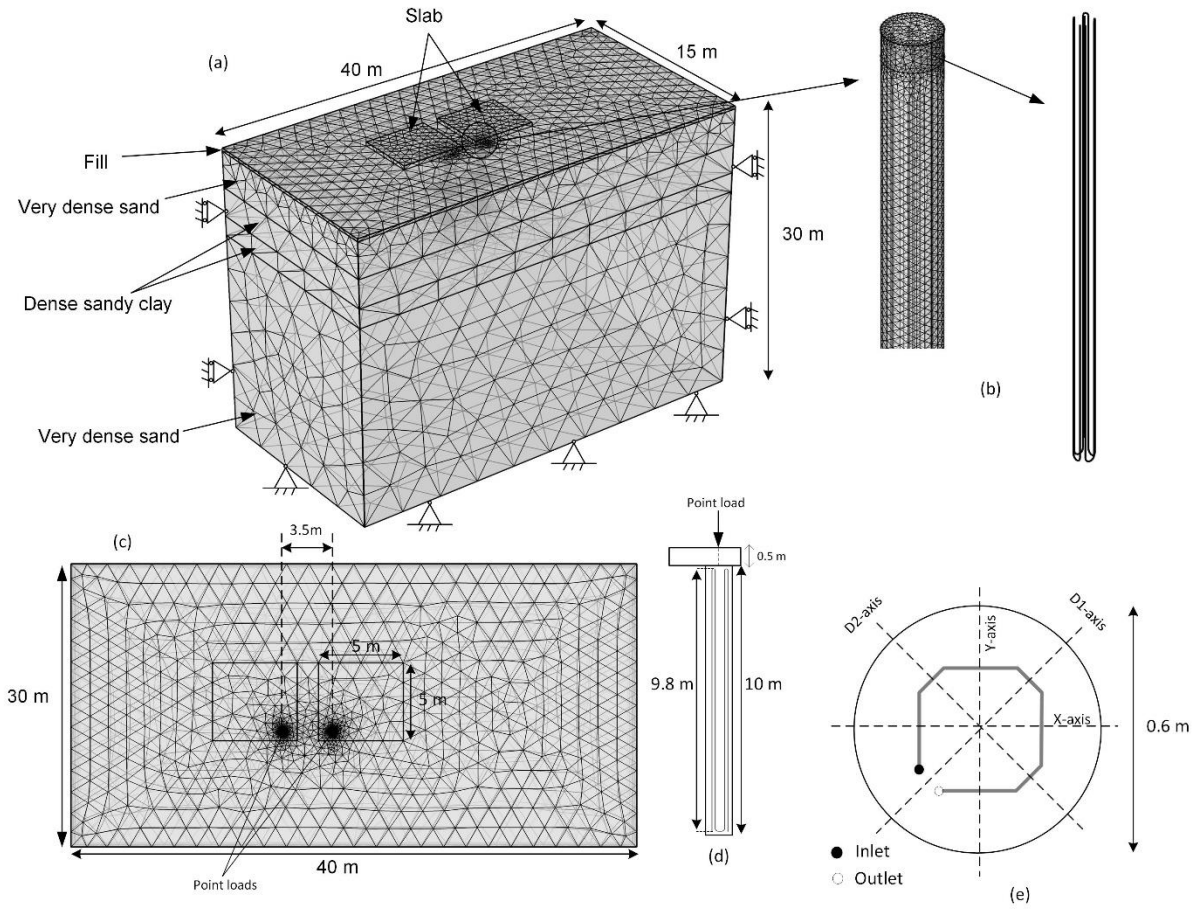

Figure 3.7. Finite element mesh of the numerical model (a) 3D view; (b) pile mesh and heat exchanger; (c) plan view; (d) side view of energy pile and heat exchanger loops; (e) plan view of energy pile, heat exchanger loops, and cross-sectional axes

Each energy pile was connected to a separate slab with a dimension of 5.0×5.0×0.5 m (length × width × height). There was no groundwater encountered within the depth of the pile, and the soil at the site was considered to be dry.

In the first step of the calculation, the geostatic stress was analysed, then the working load of 1400 kN (Faizal et al. 2019) was applied at the surface of the slabs above the two piles heads to simulate the building loads. The soil, energy piles, slab and HDPE pipe thermal and mechanical properties used in the numerical model were selected based on previous studies conducted on the same field test site (Barry-Macaulay et al. 2013; Singh et al. 2015; Faizal et

al. 2018, 2019) and from common properties reported in the literature (Bowles 1968; Peck et al. 1974; Mitchell and Soga 2005; Bourne-Webb et al. 2009; Amatya et al. 2012, Singh and Bouazza 2013) and are presented in Table 3.1.

Table 3.3. Material properties for numerical simulations calibrated against field test measurements.

Soil properties	**Fill**	**Dense sand**	**Sandy clay**	**Sand**	**Pile**	**Slab**	**HDPE pipes**
Depth, z (m)	0.0-0.5	0.5-3.5	3.5-6.0	6.0-12.5	1750	800	—
Elastic modulus, E (MPa)	15	600	75	120	35000	35000	—
Poisson's ratio, ν (—)	0.30	0.28	0.30	0.30	0.22	0.22	—
Total density, ρ (kg/m^3)	1750	1800	1950	2200	2200	850	—
Specific heat capacity, C_p (J/kg°C)	800	840	810	850	810	850	—
Thermal conductivity, λ (W/(m°C))	1.1	1.7	2.0	2.3	1.5	1.5	0.4
Linear coefficient of thermal expansion, α (με/°C)	10	10	10	10	13	13	—
Friction angle (degrees)*	30	38	32	35	—	—	—
Apparent cohesion (kPa)*	1	0.1	0.2	0.1	—	—	—

* These two parameters are for the Mohr-Coulomb model and were used in Chapter 4 and 6 only.

The numerical analysis of the thermo-mechanical response of the energy piles is based on the following assumptions: (a) the energy piles and slabs were considered to be isotropic, elastic materials; (b) the solid (piles and slabs) is considered to be incompressible under isothermal conditions; (c) the inertial effects of the solid skeleton are negligible, and the simulations represent quasi-static conditions; (d) a linear elastic behaviour (in Chapter 4 due to monotonic heating) and a Mohr-Coulomb model governed by non-associated flow rules (in Chapters 5 and 6 due to cyclic heating/cooling) assuming a dry condition was used for the ground surrounding the energy pile; and (e) heat transfer was considered to be purely conductive. The linear elastic behaviour of the soil material, which was used in Chapter 4, can

be considered acceptable for the cohesionless soil profiles studied in this thesis according to most of the numerical studies (Salciarini et al. 2015; Batini et al., 2015; Di Donna et al. 2016; Rotta Loria and Laloui 2017; Salciarini et al. 2017; Han and Yu 2020). However, to consider the possible plastic deformations, resulting from cyclic operations (Chapter 4), a Mohr-Coulomb model was used to represent the soil behaviour and also was used in Chapter 6.

3.3.2 Numerical model formulation

The piles and the soil were considered isotropic and porous materials filled with air and assumed to be purely conductive. The solid and liquid phases are considered to be incompressible under isothermal conditions. Thus, the governing equations of the coupled thermo-mechanical problem commonly used in energy pile analysis (Caulk et al. 2014; Batini et al. 2015; Di Donna et al. 2016; Rotta Loria 2017b) are presented below.

The mechanical equilibrium equation can be written as follows:

$$\mathbf{F}_v = -\nabla.\boldsymbol{\sigma} \tag{3.3}$$

where F_v is the volume force factor; $\nabla.$ Indicates divergence, and $\boldsymbol{\sigma}$ is stress tensor. The heat conduction equation can be written as follows:

$$(\rho C)_{eff}\frac{\partial T}{\partial t} = -\nabla.\lambda_{eff}\nabla T \tag{3.4}$$

where T is temperature and $(\rho C)_{eff}$ and λ_{eff} are the effective volumetric heat capacity at constant pressure and effective thermal conductivity, respectively, defined as follows:

$$(\rho C)_{eff} = \theta_p\rho_p C_{p,p} + (1-\theta_p)\rho_s C_{p,s} \tag{3.5}$$

$$\lambda_{eff} = \theta_p\lambda_p + (1-\theta_p)\lambda_s \tag{3.6}$$

where ρ_p and ρ_s are pore fluid (air in this study) and soil densities, λ_p and λ_s and $C_{p,p}$ and $C_{p,s}$ are representing thermal conductivities and specific heat capacity of these two materials respectively. θ_p is the volume fraction of solid material (the ratio of the area occupied by the pore fluid to the entire cross-section of the soil).

The fluid and solid materials' thermal properties were assumed to be temperature-dependent and temperature-independent, respectively. The effect of a temperature gradient, which leads to thermal expansion and contraction of the energy pile and soil is considered in the stress tensor equation, written as follows:

$$\sigma - \sigma_0 = \mathbf{E}(\boldsymbol{\varepsilon} - \boldsymbol{\varepsilon_0} - \frac{\beta}{3}(T - T_0)\mathbf{I}) \tag{3.7}$$

Where **I** is the unit matrix; $\boldsymbol{\varepsilon}$ is strain tensor, and β is the linear thermal expansion coefficient of the material.

The heat transfer between the circulating fluid and HDPE pipe can be described by non-isothermal pipe flow model which includes convection heat transfer between circulating fluid and pipe wall (Eq. 3.8a), momentum equation (Eq. 3.8b), and energy conservation equation (Eq. 1.8c) as follows:

$$\frac{\partial A\rho_f}{\partial t} = -\nabla.(A\rho_f u_f) \tag{3.8a}$$

$$\rho_f \frac{\partial u_f}{\partial t} = -\nabla p - \frac{1}{2} f_D \frac{\rho_f}{d_h} |u_f| u_f \tag{3.8b}$$

$$\rho_f A C_f \frac{\partial T_f}{\partial t} + \rho_f A C_f u_f.\nabla T_f = \nabla.\left(A\lambda_f \nabla T_f\right) + \frac{1}{2} f_D \frac{\rho_f A}{d_h} |u_f| {u_f}^2 + Q_{wall} \tag{3.8c}$$

where ρ_f, C_f, u_f, λ_f and T_f are density, specific heat, velocity vector, thermal conductivity, and temperature of the circulating fluid, respectively. f_D is Darcy fraction factor, d_h is the hydraulic pipe diameter. A represents a cross-section of the pipe in which fluid is flowing and Q_{wall} indicates the heat flux per unit length of the pipe and is written as follows:

$$Q_{wall} = h_{eff}(T_{ext} - T_f) \tag{3.9}$$

where h_{eff} is an effective pipe heat transfer coefficient considering the wetted perimeter of the pipe cross-section; and T_{ext} is external temperature surrounding the pipe. The effective heat transfer coefficient for circular pipe shapes used in this study can be determined as follows:

$$h_{eff} = \frac{2\pi r_{int}}{\frac{1}{h_{int}} + \frac{r_{int}}{k_p} ln\,(\frac{r_{ext}}{r_{int}})} \tag{3.10}$$

where r_{int} and r_{ext} are internal and external pipe radius, respectively; k_p is pipe thermal conductivity; and h_{int} is convective heat transfer coefficient inside the pipe which can be obtained by:

$$h_{int} = \frac{Nuk_f}{d_h} \tag{3.11}$$

$$d_h = \frac{4A}{2\pi r_{int}} \tag{3.12}$$

where d_h is the hydraulic diameter, and Nu is Nusselt number which for round pipes can be defined as a function of Reynolds, R_e and Prandtl, Pr numbers as follows:

$$Nu = max\,(3.66; Nu_{turb}) \tag{3.13}$$

$$Nu_{turb} = \frac{\left(\frac{f_D}{8}\right)(Re - 1000)Pr}{1 + 12.7\sqrt{\frac{f_D}{8}}(Pr^{\frac{2}{3}} - 1)} \tag{3.14}$$

$$f_D = [-1.8\,log\left(\frac{6.9}{Re}\right)]^{-1} \tag{3.15}$$

where f_D is the Darcy fraction factor; $Re = \rho VD/\mu$, $Pr = \mu C_f/\lambda_f$, ρ is the fluid density, V is the velocity of the fluid, μ is the dynamic viscosity of the fluid, D is pipe diameter, C_f and λ_f are the specific heat, and the thermal conductivity of the fluid, respectively.

The numerical model was validated against field data, followed by a parametric evaluation of varying soil properties and fluid temperatures on the thermal responses of the instrumented energy pile (EP1). The validation results, together with the parametric evaluation results, are presented in Chapters 4, 5, and 6.

3.4 Chapter summary

This chapter presented the research methods adopted to study this thesis's specific aims. A description of the field setup, experimental equipment and procedure, and the different heating, cooling, and cyclic/heating cooling experiments were provided. A description of the numerical model geometry, boundary conditions, and the methodology adopted to analyse the energy piles' thermal responses were also presented. The experimental results from the two energy piles were used to validate the three-dimensional finite element method developed in COMSOL Multiphysics software, which was used to perform parametric studies to investigate this thesis's specific research aims. The parametric analyses results are presented in Chapters 4, 5, and 6

4 Effect of monotonic and cyclic temperature variations on the thermal interaction between two energy piles

4.1 Introduction

Energy piles and the surrounding soil are subjected to different magnitudes of monotonic and intermittent temperature variations, depending on the heating/cooling demands of the built structure (Brandl 2006; Murphy and McCartney 2015; McCartney and Murphy 2017, Faizal et al. 2016, 2018, 2019a, 2019b). Moreover, energy piles may interact thermally with other nearby energy piles through the soil due to soil temperature changes, which could influence the piles' thermal responses. Studies conducted on solitary energy piles have shown that ground temperature changes and pile thermal stresses vary for different magnitudes of intermittent and monotonic temperature changes of the pile. Intermittent operations induce lower thermal effects in the piles and the soil (Faizal et al. 2016, 2018, 2019b). It can therefore be expected that different magnitudes of pile temperature changes will also influence the thermal responses and thermal interaction between closely spaced multiple

This chapter investigates the influence of monotonic and cyclic temperatures on the thermal responses of the instrumented energy pile, EP1 (i.e. address the first specific aim of this thesis). After validating the numerical model against field results, different magnitudes of monotonic heating and cooling temperatures, and balanced and imbalanced cyclic thermal temperatures are investigated numerically for single and dual pile operations. Analyses are conducted for different inlet fluid inlet temperatures using the numerical model described in Chapter 3.

4.2 Validation of numerical model with experimental results

In this chapter, the piles were subjected to monotonic heating, monotonic cooling, and daily cyclic heating/cooling temperatures. Six field tests were conducted in total (the details of the experiments are given in Table 3.2 in Chapter 3), where the instrumented pile (EP1) was tested alone and simultaneously with the second pile (EP1 + EP2). The inlet water temperatures for each experiment is shown Figure 4.1. There were some performance issues with the heat pump during dual pile cooling and cyclic operations, which affected the inlet fluid temperature trends.

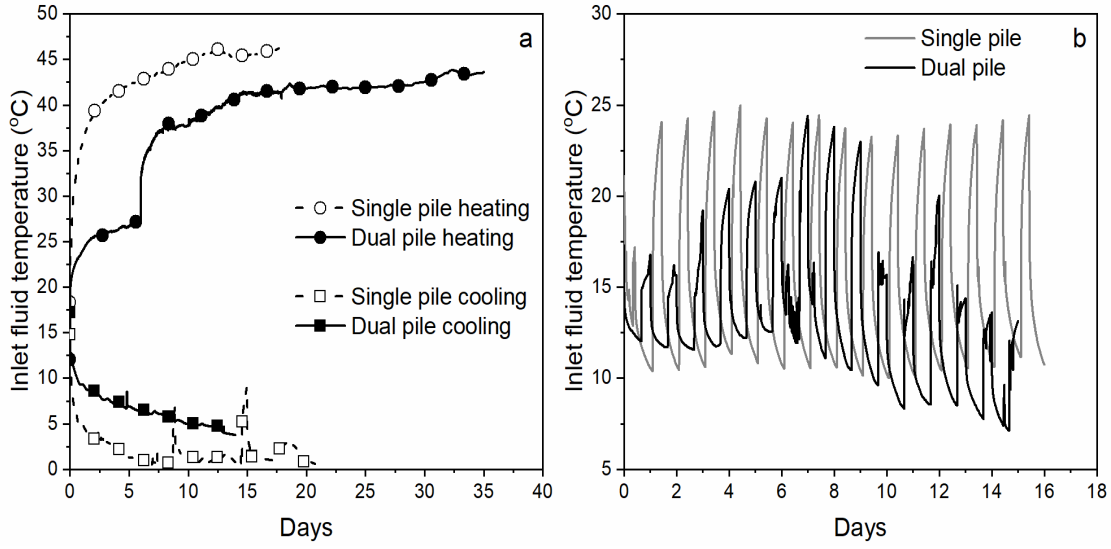

Figure 4.1. Experimental fluid temperatures for (a) monotonic heating and cooling and (b) cyclic operations.

Figure 4.2 shows the field and numerical results for monotonic and cyclic operations, respectively, for single and dual pile operation at the end of each experiment. The numerical axial and radial contact thermal stresses of EP1 were extracted from the finite element analysis at the pile centre and the pile-soil interface, respectively. The experimental axial thermal stresses in EP1 were estimated by the following equation:

$$\sigma_T = E_P(\varepsilon_{obs} - \alpha_{free}\Delta T) \tag{4.1}$$

where E_P is the elastic modulus of the concrete (taken as 34 GPa), ε_{obs} is experimentally observed thermal strains, α_{free} is the free thermal expansion coefficient of the concrete, taken

as 13 με/°C (Faizal et al., 2019a,b), and ΔT is the change in temperature of the pile. The thermal expansion coefficient of concrete selected in the current study is within the range of 9 με/°C to 14.5 με/°C reported by Stewart and McCartney (2014) and Bourne-Webb et al. (2016).

The experimental radial contact stresses of EP1 were estimated using cavity expansion analysis as follows:

$$\sigma_n = \frac{E_s \Delta r}{(1 + v_s) r} \tag{4.2}$$

Where E_s and v_s are the elastic modulus and Poisson's ratio of the surrounding dense sand, respectively, assumed to be 60 MPa and 0.3, respectively, based on typical values for dense sand (Faizal et al., 2019a,b; Elzeiny et al., 2020), r is the radius of EP1, and Δr is the thermally induced radial displacement of EP1.

For cyclic operations, the results are presented at the end of heating and end of cooling for each experiment's last cycle. The changes in temperature of EP1 for single and dual pile operations, as shown in Figure 4.2a and 4.2b, are almost uniform with depth for all operations. Due to differences in inlet fluid temperature, mostly for cyclic operations (Figure 4.2b), the changes in pile temperatures are different for the cyclic experiments as shown in Figure 4.2b. The changes in ground temperature changes with increasing radial distance from the sides of EP1 and EP2 for a depth of 5 m for monotonic and cyclic operations, respectively, are shown in Figure 4.2c and 4.2d. A depth of 5 m was selected because it is at the mid-depth of the pile with negligible thermal effects from the pile ends. Due to the overlap of temperatures resulting from simultaneous operation of energy piles, dual pile operation induced higher ground temperatures between the two energy piles. However, cyclic temperatures caused lower ground temperature changes than monotonic temperatures for both single and dual pile operations due to frequent recovery of the ground temperatures.

The lowest and highest axial thermal strains and stresses were observed at a depth of around 2.5 m for monotonic operations (Figure 4.2e and 4.2i). This depth represents the null

point's location, which indicates that the overlying structure stiffness is dominant compared to the underlying soil stiffness.

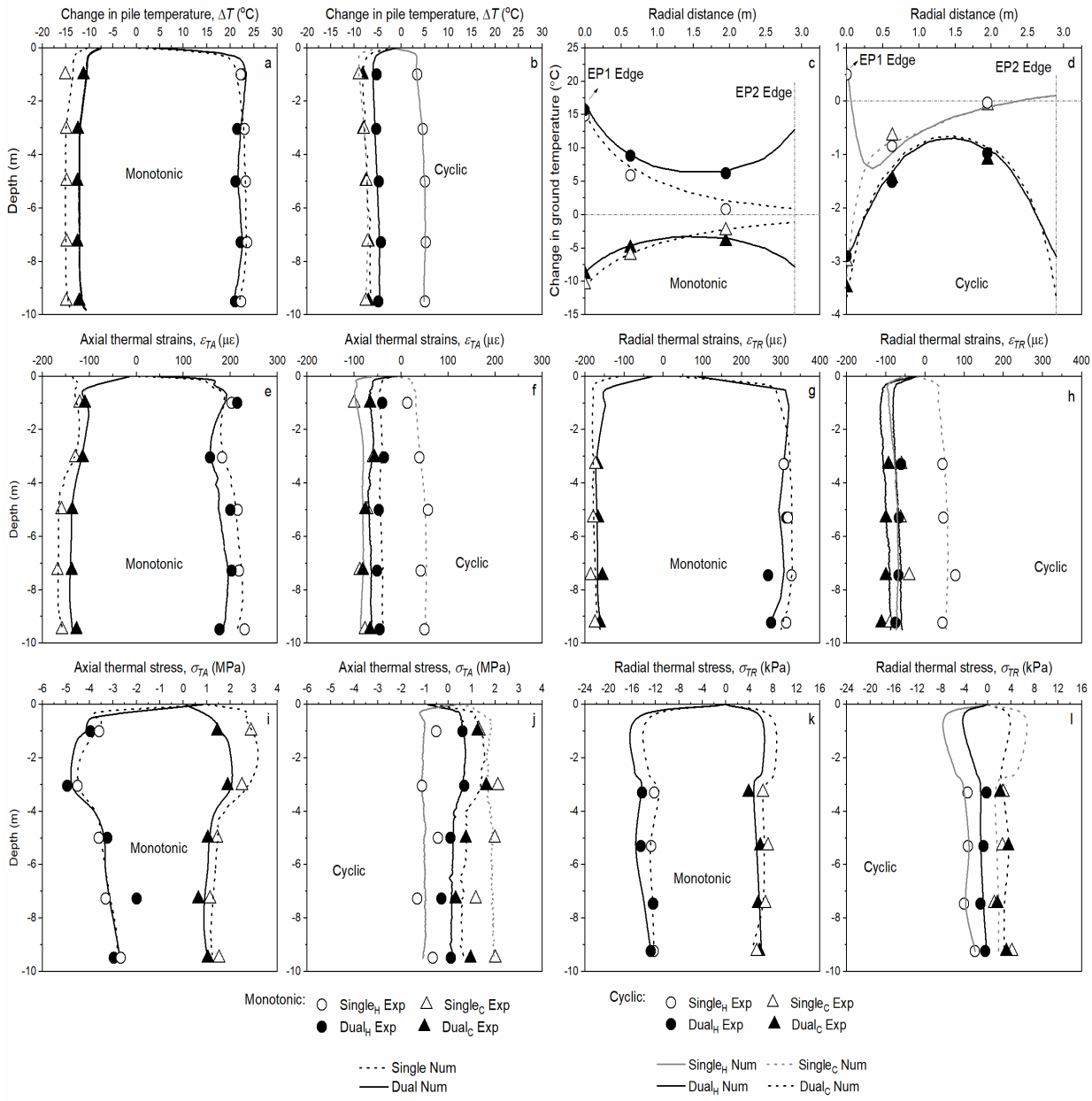

Figure 4.2. Experimental and numerical profiles in EP1 of: (a) and (b): ΔT during monotonic and cyclic temperatures, respectively; (c) and (d): ΔT of ground at depth of 5 m during monotonic and cyclic temperatures, respectively; (e) and (f) ε_{TA} during monotonic and cyclic temperatures, respectively; (g) and (h) ε_{TR} during monotonic and cyclic temperatures, respectively; (i) and (j) σ_{TA} during monotonic and cyclic temperatures, respectively; (k) and (l) σ_{TR} during monotonic temperatures and cyclic temperatures, respectively.

The radial thermal strains in all operations (Figure 4.2g and 4.2h), are generally higher than axial thermal strains, indicating lower restriction to thermal expansion/contraction in the

radial direction. The radial thermal stresses in EP1 were significantly lower than the axial thermal stresses (Figure 4.2k and 4.2l) for all cases.

4.3 Results of parametric evaluation of monotonic and cyclic inlet fluid temperatures

The validated numerical model was used to assess the effect of varying inlet fluid temperatures on the thermal responses of EP1. Four inlet fluid temperatures were studied for each heating and cooling monotonic temperatures and three for cyclic temperatures, as shown in Figure 4.3a. The initial fluid temperature was set to 20°C at the beginning of all tests, close to the average initial ground temperature. The fluid temperatures were varied by ± 5°C intervals for monotonic temperatures (i.e. $|\Delta T_f|$ = 5°C, 10°C, 15°C, 20°C, where ΔT_f is the difference between the inlet fluid temperatures and the initial fluid temperature of 20°C). Three patterns of cyclic temperatures were simulated, shown in Figure 4.3b to 4.3d

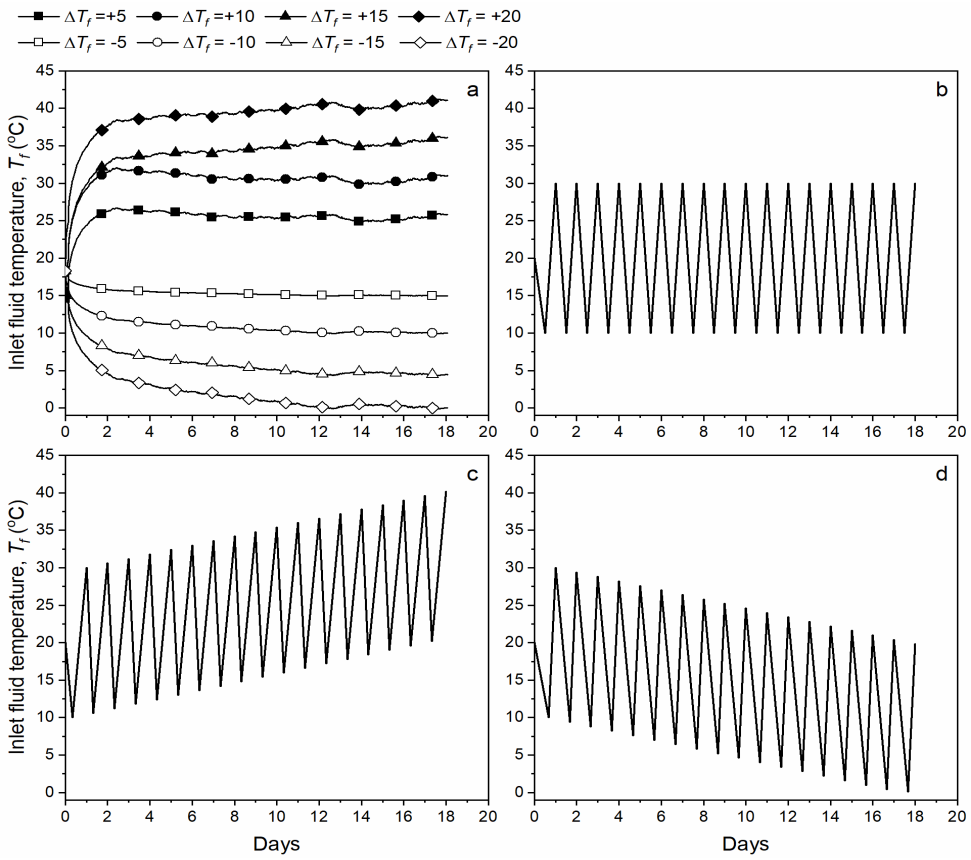

Figure 4.3. Inlet fluid temperatures (a) monotonic heating and cooling; (b) balanced cyclic; (c) heating oriented imbalanced cyclic; and (d) cooling oriented imbalanced cyclic fluid temperature for the parametric study.

First, balanced cyclic temperatures with 12 hours heating and 12 hours cooling between 10°C and 30°C (referred to as balanced cyclic in Figure 4.3). Second, imbalanced cyclic temperatures inclined towards heating, with 16 hours heating and 8 hours cooling. The minimum and maximum temperatures were 10°C and 40°C, respectively. Third, imbalanced cyclic temperatures inclined towards cooling, with 8 hours heating and 16 hours cooling. The maximum and minimum temperatures were 30°C and 0°C, respectively. In the analyses of balanced and imbalanced thermal loads, it was assumed that the two energy piles were working separately (i.e. heat exchanger pipes are not connected in series) with the same inlet fluid temperatures (shown in Figure 4.3) and same fluid flow rate of 11 L/min. In this way, both EP1 and EP2 have the same heating or cooling rate. Also, the initial pile and ground temperatures were assumed to be the same for all simulations for the sake of simplicity. The results in the following section are presented for the last day of operation (Day 18).

4.3.1 Pile temperatures

The effect of fluid temperature variations on temperatures and change in temperatures in EP1 is shown in Figure 4.4 for all simulations. The pile temperatures increased with increasing magnitudes of inlet fluid temperatures, with relatively uniform profiles with depth for all cases. Cyclic fluid temperatures induced lower pile temperatures in EP1. The change in EP1 temperatures varied between -19 ^{o}C to 18 ^{o}C for monotonic temperatures (Figure 4.4b) and between -12.5 ^{o}C to 11 ^{o}C for cyclic temperatures (Figure 4.4c and 4.4d). Also, the balanced cyclic temperatures imposed lower temperatures than the other two imbalanced cyclic temperatures. There were no significant differences in EP1 temperatures for single and dual pile operation for all tests, indicating that the operation of EP2 did not affect the temperatures of EP1 and the effect of thermal interaction through the soil between the piles was negligible on pile temperatures for the spacing investigated in this study.

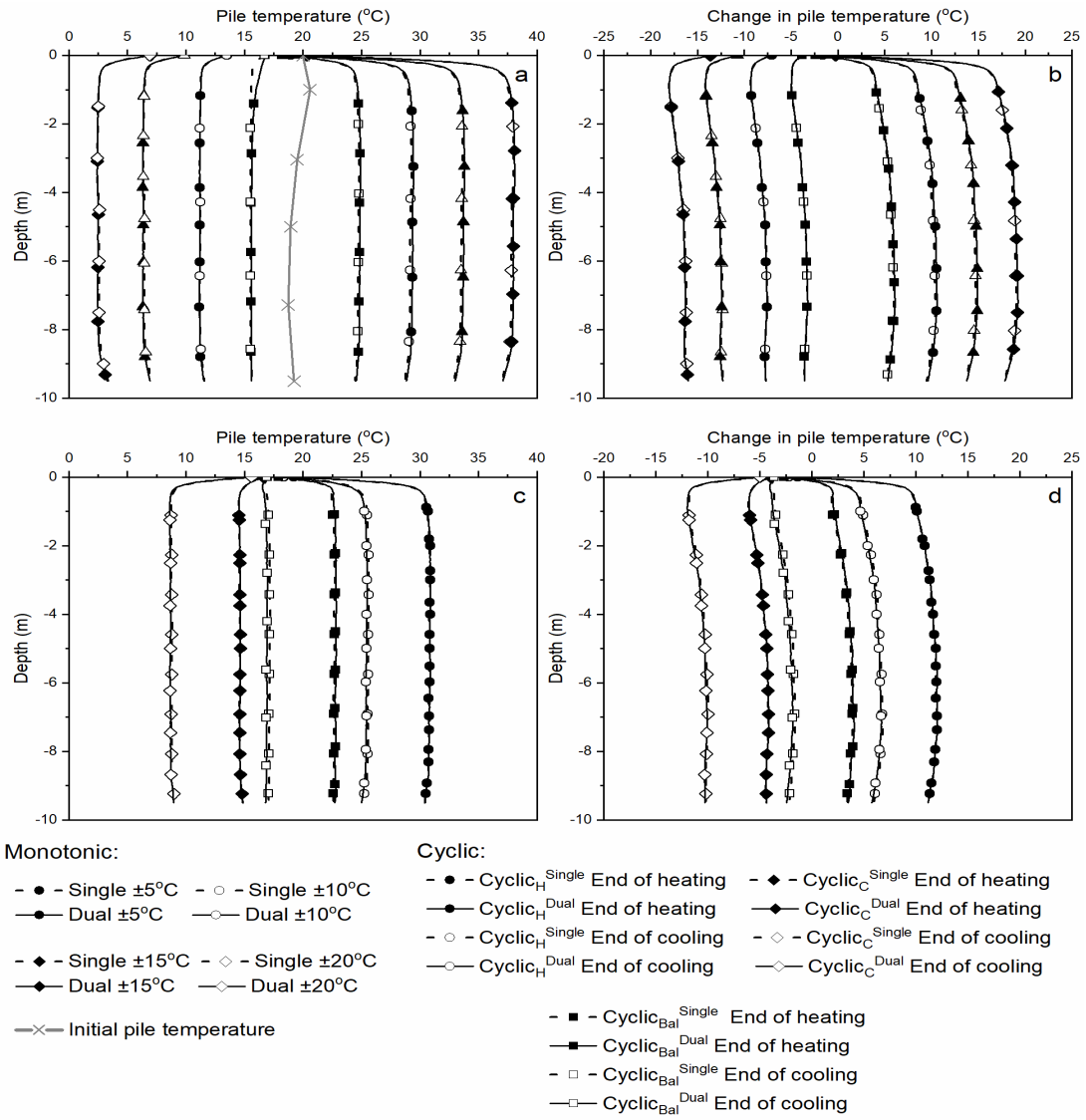

Figure 4.4. Numerical predictions of temperature and change in temperatures in EP1: (a) and (b) temperature and change in pile temperature for monotonic heating and cooling; (c) and (d) temperature and change in pile temperature for cyclic operation.

4.3.2 Ground temperatures

The effect of fluid temperature variations on change in ground temperatures between the two energy piles at a depth of 5 m (mid-depth of the pile where pile ends thermal effects are negligible) is shown in Figure 4.5 for both single and dual pile operation. For any given operation mode, ground temperature changes increased with increasing absolute fluid temperatures for both single and dual pile operation. For the operation of EP1 alone and any given fluid temperature, the changes in ground temperatures were highest near EP1 and

reduced with increasing radial distance from the edge of EP1. For a single energy pile operation, the zone of radial thermal influence in the soil increased with increasing absolute fluid temperatures.

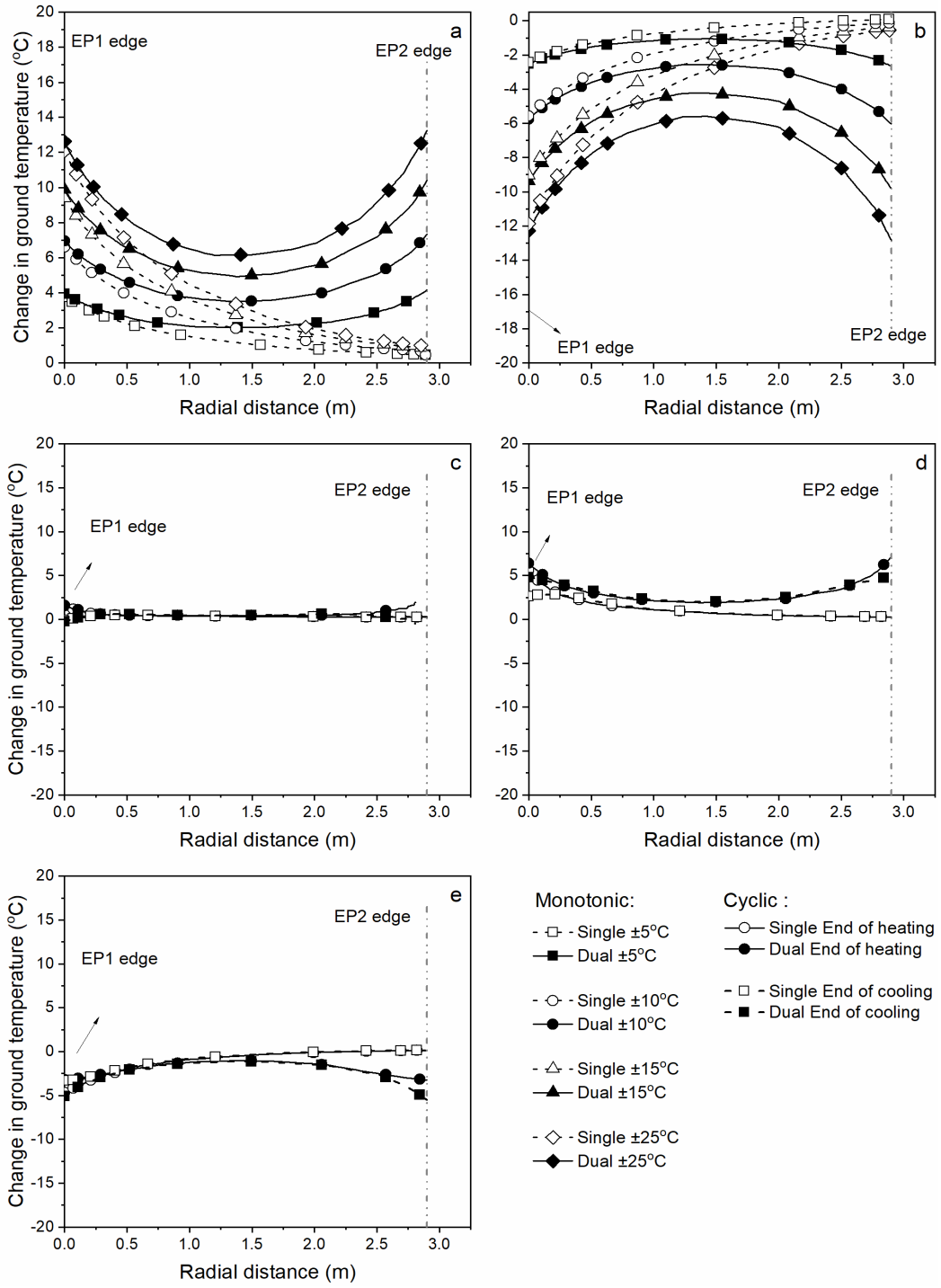

Figure 4.5. Numerical prediction of ground temperature distributions between the piles: (a) monotonic heating; (b) monotonic cooling; (c) balanced cyclic temperatures; (d) heating oriented imbalanced cyclic temperatures; and (e) cooling oriented imbalanced cyclic temperatures.

During dual pile operation, for any given fluid temperature, the ground temperatures initially reduced with increasing radial distance from the edges of the two piles but overlapped between the two piles and induced greater changes in ground temperatures compared to single pile operation. The effect of cyclic temperature variations on ground temperature changes (with the maximum temperature change of 7^{o}C for heating oriented cyclic temperatures) is significantly lower than monotonic temperatures (with the maximum temperature change of 13^{o}C for both monotonic heating and cooling), for both single and dual pile operation. The lowest change in ground temperature of 2.5°C was observed for the balanced cyclic operation (Figure 4.5c). Cyclic temperatures, particularly the balanced cyclic temperatures, would induce lower ground temperatures and thermal interaction between the piles through the soil.

4.3.3 Axial thermal responses

The effect of fluid temperature on the axial thermal strains and stresses of EP1 is shown in Figure 4.6. The thermal strains and stresses increased with the increasing absolute value of inlet fluid temperatures, for both single and dual pile operations. The location of the maximum axial thermal stresses remained at approximately 2.5 m depth for all the cases due to the considerable stiffness of the building on the pile head which indicates the location of the null point is independent of magnitudes of inlet fluid temperature for the current in-situ conditions.

The strains and stresses of EP1 were similar for single and dual pile operation with slight differences in the upper pile section for all fluid temperatures, indicating that the operation of EP2 during dual pile operation did not influence the thermal response of EP1 even though the ground temperature changes were greater during dual pile operation (Figure 4.5).

The maximum axial thermal stresses were -4.2 MPa and 3.5 MPa for monotonic heating and monotonic cooling, respectively (Figure 4.6b and 4.6d). Due to lower temperature changes, cyclic operations induced lower axial thermal strains and stresses in EP1 compared to monotonic temperatures, with the maximum thermal stresses ranging between -3.4 – 3.2 MPa

for imbalanced heating and imbalanced cooling, respectively, at a depth of 2.6 m (Figure 4.6f). However, these magnitudes were as low as 1.2 MPa for balanced cyclic operation.

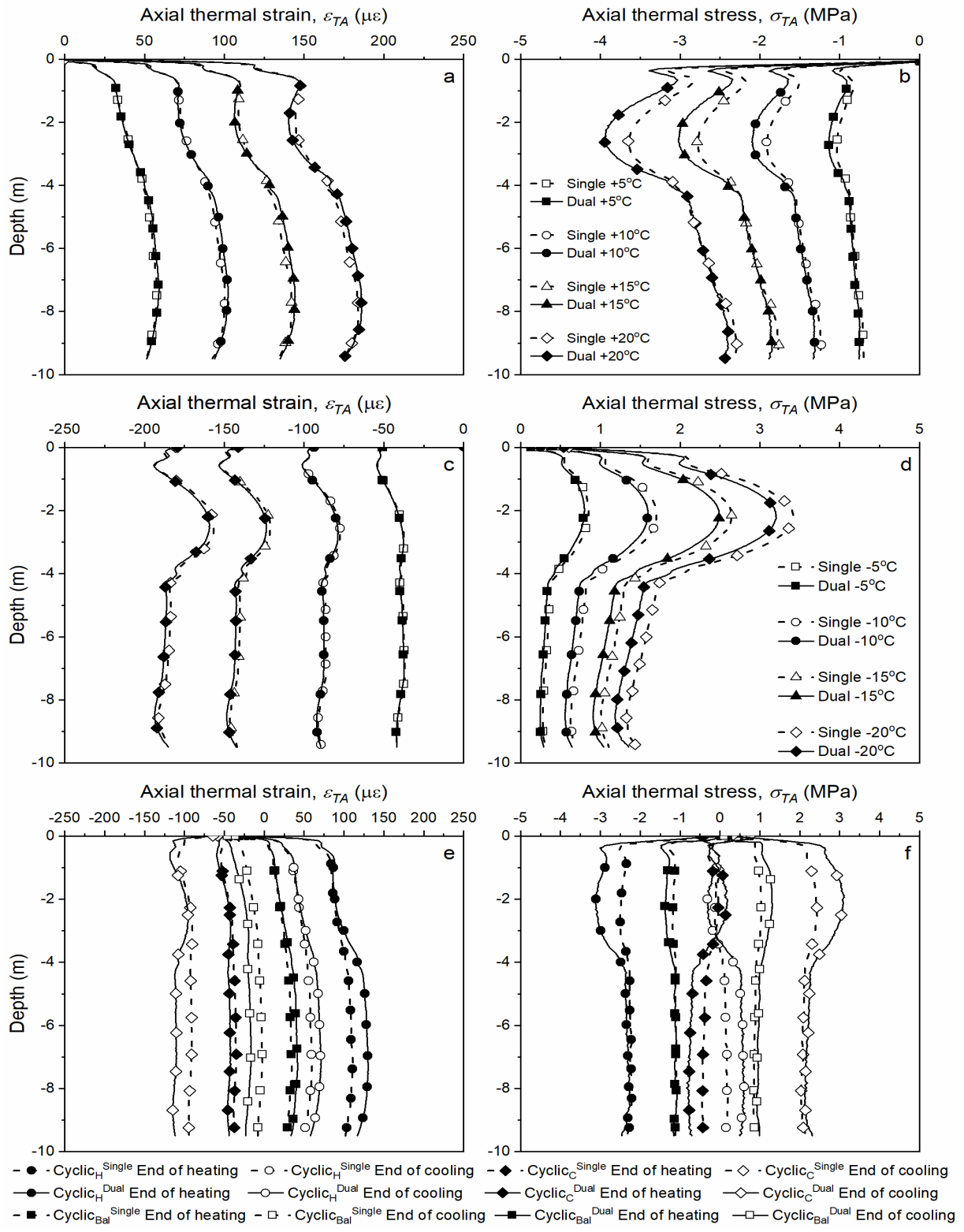

Figure 4.6. Numerical axial thermal responses of EP1: (a) and (b), strains and stresses at the end of monotonic heating; (c) and (d), strains and stresses at the end of monotonic cooling; (e) and (f), strains and stresses for the last cycle of cyclic operations.

4.3.4 Radial thermal responses

The effect of fluid temperature on the radial thermal responses of EP1 is shown in Figure 4.7.

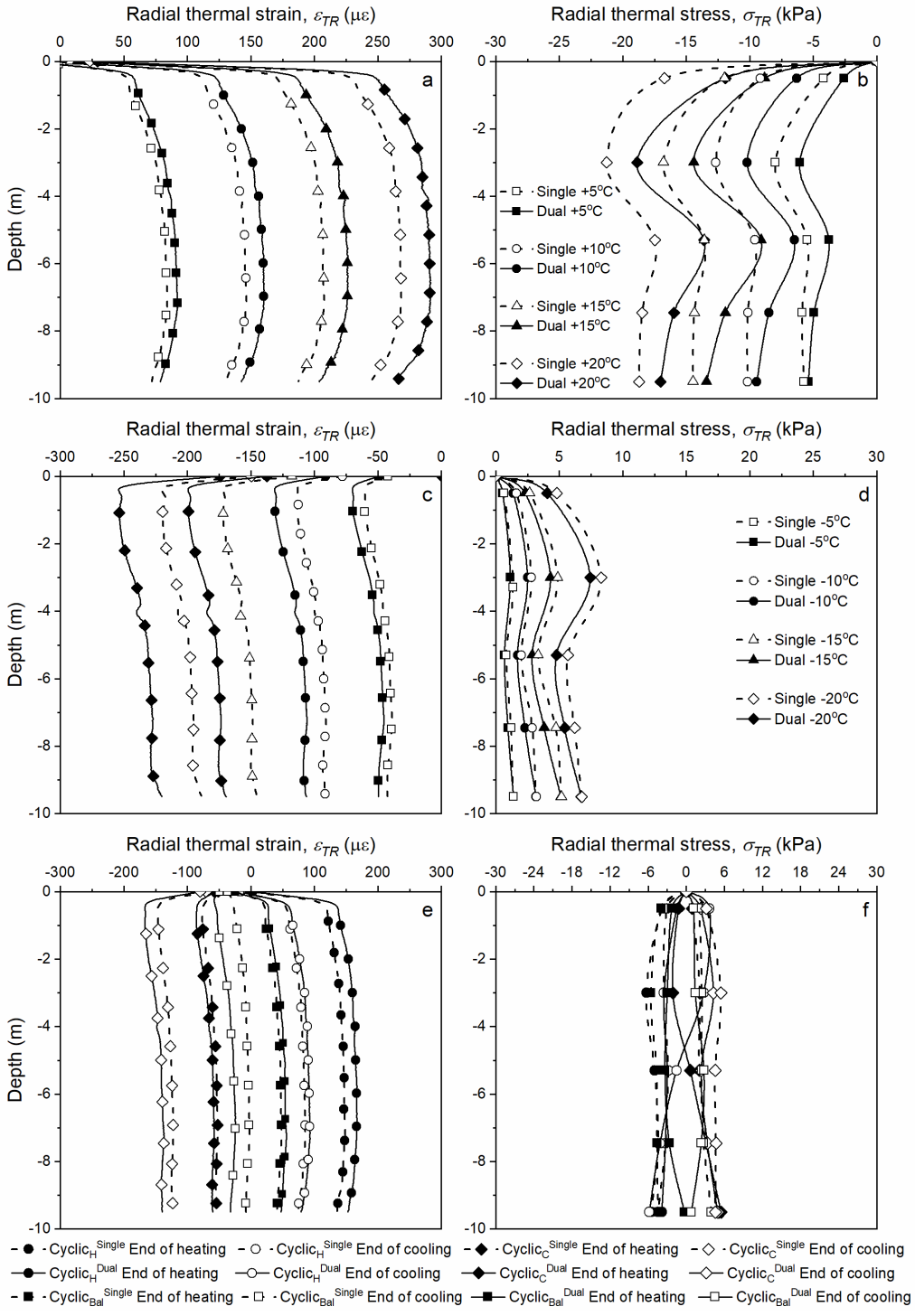

Figure 4.7. Numerical prediction of radial thermal responses in EP1: (a) and (b), strains and stresses at the end of monotonic heating; (c) and (d), strains and stresses at the end of monotonic cooling; (e) and (f), strains and stresses for the last cycle of cyclic operations.

Higher inlet fluid temperatures induced higher radial thermal strains and stresses in EP1, for both single and dual pile operation. However, the radial thermal stresses were significantly lower than the magnitudes of axial thermal stresses for all tests, consistent with the findings from other studies (Ozudogru et al. 2015; Gawecka et al. 2017; Faizal et al. 2018, 2019). Similar to the axial thermal responses, the radial thermal stresses in EP1 was not significantly affected by the operation of EP2 during dual pile operation which further confirms the negligible effects of the operation of one energy pile on the other nearby energy pile for the pile spacing investigated in this study.

The three cyclic temperature modes generated lower thermal radial stresses ranging from -6 kPa to 6 kPa in EP1 for both single and dual pile operations compared to monotonic temperatures with values of -22 kPa and 10 kPa for monotonic heating and monotonic cooling, respectively. Moreover, higher magnitudes of radial thermal stresses were observed for imbalanced cyclic temperature variations compared to balanced cyclic operations.

4.3.5 Thermal displacements

The effect of varying fluid temperature on the axial and radial thermal displacements of EP1, for all monotonic and cyclic operations, is shown in Figure 4.8. Positive and negative displacement values mean upward and downward movements of the pile, respectively. Thermal radial displacements (Figure 4.8b, d, and f) were very low compared to axial thermal displacements (Figure 4.8a, c, and e) and ranged between -0.05 mm to 0.02 mm, for all tests. The axial thermal displacements at the pile head (ranged between -0.6 mm to 0.6 mm) were lower than near the toe (ranged between -1.2 mm to 1.2 mm) due to the higher restriction imposed by the building loads and higher stiffness of soil layers at the upper part of EP1. There were no significant differences between the displacements of EP1 in single and dual pile operations indicating that the second pile's operation in dual pile operation did not affect the

displacements of EP1. Increasing inlet fluid temperature increased the magnitudes of thermal displacements of EP1 for both single and dual pile operations.

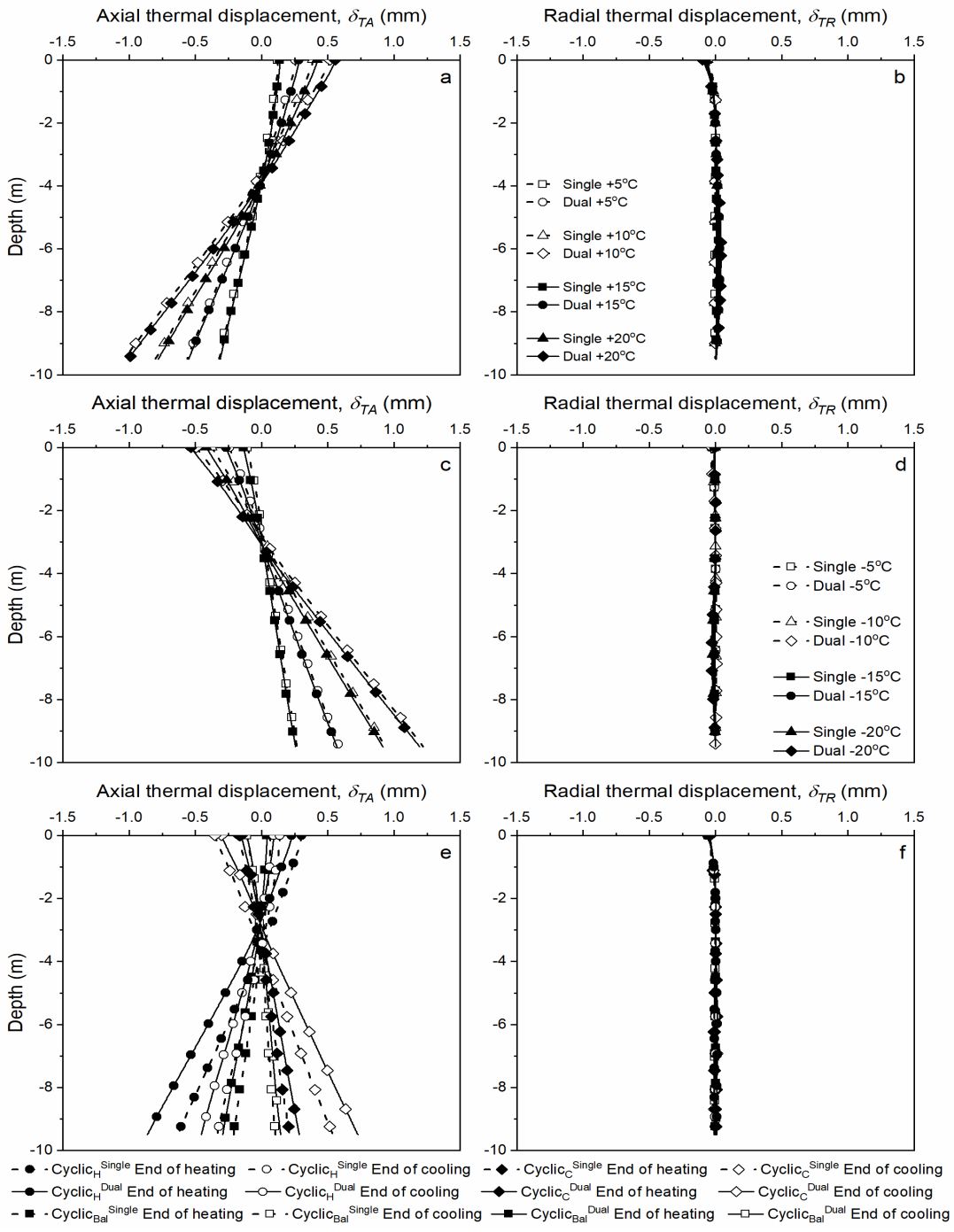

Figure 4.8. Numerical prediction of axial (δ_{TA}) and radial (δ_{TR}) displacements of EP1: (a) and (b) δ_{TA} and δ_{TR} for monotonic heating; (c) and (d) δ_{TA} and δ_{TR} for monotonic cooling; (e) and (f) δ_{TA} and δ_{TR} for the last cycle of cyclic operations.

The maximum thermal axial displacements for monotonic temperatures were between -1.2 mm to 1.2 mm. However, cyclic temperatures had lower axial thermal displacements than

monotonic temperatures, particularly for the balanced cyclic temperatures, the maximum axial thermal displacements were between -0.1 and 0.1 mm. The imbalanced cyclic operations had higher axial displacements than balanced cyclic temperatures (between -0.8 and 0.3 for imbalanced cyclic heating and between -0.3 and 0.8 for imbalanced cyclic cooling).

4.3.6 Thermal strains versus change in pile temperature

The axial and radial thermal strains of EP1 variations against change in pile temperatures of EP1 were plotted (Figure 4.9) for all cases to compare the pile's temperature-dependent responses for different inlet fluid temperatures for both single and dual pile operations. The results are presented for a depth of 2.5 m, which is the null point's location, where the lowest thermal strains and highest thermal stresses were observed.

For any given simulation (i.e. for either monotonic or cyclic temperatures and single or dual pile operations), the change in axial and radial thermal strains against change in pile temperatures was between 6.67 – 7.88 με/°C and 11.6 – 13 με/°C, respectively. This confirms that the axial thermal strains of EP1 had higher restrictions on thermal expansion/contraction compared to radial thermal strains.

For a given test, there were negligible differences in the change in thermal strains (for either axial or radial thermal strains) against change in pile temperatures between the single and dual pile tests, confirming that the operation of EP2 had negligible effects on the thermal responses of EP1. Linear responses for thermal axial and radial thermal strains against changes in pile temperatures were observed for monotonic heating and cooling temperatures (Figure 4.9and 4.9b).

The thermal strains showed cyclic changes with respect to cyclic changes in pile temperatures (Figure 4.9c to 4.9f). However, the trends were linear with similar slopes to the monotonic temperature tests. The similarity in slopes between monotonic and cyclic temperature tests indicate that the cyclic temperature variations did not lead to unexpected

plastic deformations for the range of temperatures, types of piles and soil conditions investigated in the current study.

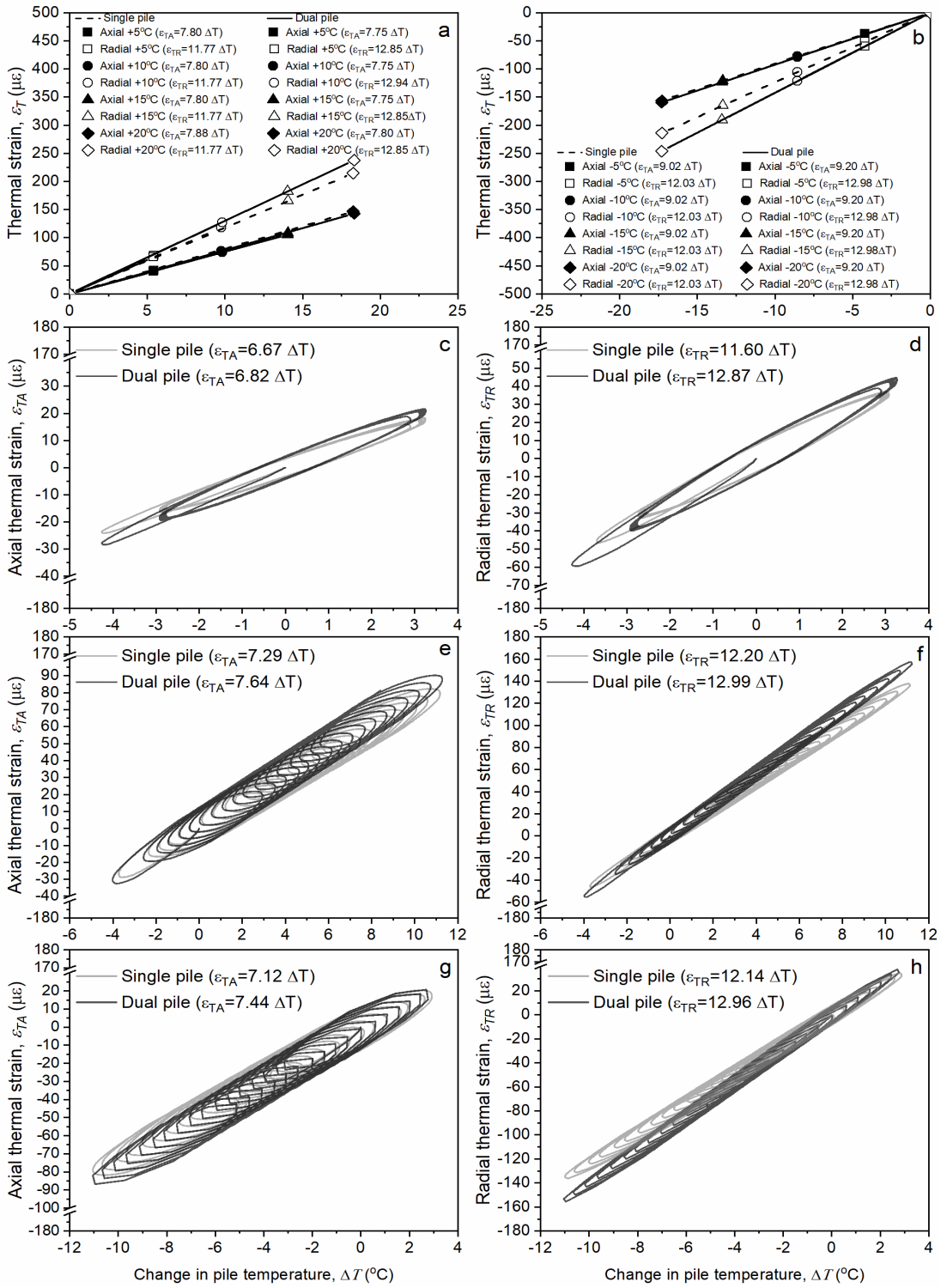

Figure 4.9. Numerical prediction of axial (ε_{TA}) and radial (ε_{TR}) thermal strains against change in pile temperatures at a depth of 2.6 m near the null point: (a) monotonic heating; (b) monotonic cooling; (c) and (d) ε_{TA} and ε_{TR} for balanced cyclic, respectively; (e) and (f) ε_{TA} and ε_{TR} for heating oriented imbalanced cyclic, respectively; and (g) and (h) ε_{TA} and ε_{TR} for cooling oriented imbalanced cyclic.

The axial and radial thermal strains followed a reversible cyclic path between a constant range of change in pile temperature of -4 to 4 ^{o}C in the balanced cyclic temperature tests for both single and dual pile tests (Figure 4.9c and 4.9d). There was a slight ratcheting behaviour for the first few cycles in the balanced cyclic temperature tests which can be related to unstable pile temperatures at the beginning of the simulation (Figure 4.9c and 4.9d). For the imbalanced heating and cooling modes (Figure 4.9e to 4.9h), the range of change in pile temperatures variation led to irreversible responses of the thermal strains; the responses of thermal strains can therefore be inferred as being temperature-dependent and were not due to plastic deformations of the pile and the soil.

4.4 Chapter summary

This chapter assessed the effect of monotonic and cyclic temperature changes on the thermal responses of one of the energy piles when operated alone and when operated simultaneously with the other energy pile in the pair. Different magnitudes of monotonic heating/cooling temperatures and balanced and imbalanced cyclic temperature variations were investigated numerically. The second energy pile operation in dual pile simulations resulted in higher ground temperature changes between the energy piles, which was more significant for monotonic temperatures with higher inlet fluid temperatures. However, the influence of the second energy pile's operation on the magnitudes of temperature, and axial and radial thermal stresses of the considered energy pile was negligible for the pile spacing considered in this thesis. The gradients of thermal strains with changes in the temperature of the considered energy pile were similar for both single and dual pile operations for any given fluid temperature, indicating negligible effects of thermal interaction between the piles on the pile thermal responses for the setting investigated in this thesis.

The monotonic heating and monotonic cooling operations resulted in higher magnitudes of pile temperatures and thermal stresses in the considered energy pile, compared

to cyclic operations for both single and dual pile tests. Lower head and toe thermal displacements of the considered pile were observed during cyclic operations compared to monotonic operations. Cyclic intermittent operations of the GSHP will therefore be beneficial in reducing thermal stresses in the piles and ground temperature variations due to thermal interaction between multiple energy piles for long-term operations of energy piles.

5 Effect of nearby piles and soil properties on the thermal response of an energy pile

5.1 Introduction

Thermal interaction between energy piles with other nearby energy piles or nearby conventional piles might occur through a coupled heat transfer and volume change in the surrounding soil. In this respect, the variations in soil properties can influence the thermal interaction between the piles and the magnitudes of thermal stresses developed in the piles. Although there have been several studies on energy pile groups and thermal interaction (Mimoumi and Laloui 2015; Rotta Loria and Laloui 2016, 2017a, 2018; Wu et al. 2020), considering the role of soil properties such as soil thermal conductivity, soil thermal expansion ceofficient, and soil elastic modulus on this interaction is still not well understood.

This chapter investigates the role of soil properties and nearby piles on the thermal behaviour of an instrumented energy pile (i.e. EP1). Specifically, this chapter addresses the second objective of this thesis which is assessing the effect of soil properties on the thermal response of energy piles operating solo and together with a nearby energy pile. Thus, three scenarios were investigated: (1) heating of the energy pile (EP1) alone next to a non-operating energy pile (EP2); (2) heating of both energy piles simultaneously, and (3) heating of the energy pile EP2 while the considered energy pile (EP1) was not heated (i.e., a non-operating energy pile). After comparing the results from the experiments and field simulations for the three cases, a parametric evaluation was conducted to explore the effects of varying soil properties (i.e., thermal conductivity, λ_{soil}, thermal expansion coefficient, α_{soil}, and the elastic modulus, E_{soil}) on the thermo-mechanical responses of one of the two energy piles.

5.2 Validation of numerical model with experimental results

Three tests were conducted to investigate the objective of this chapter: (i) heating EP1 only, referred to herein as $EP1_{active}$, to establish the axial and radial thermal responses of EP1 (ii) heating EP1 and EP2 simultaneously, referred to herein as $(EP1 + EP2)_{active,}$ to examine the effect of EP2 on the thermal response of EP1 (i.e., to investigate the impact of one operating energy pile on the other operating energy pile), and (iii) heating EP2 only, referred to herein as $EP2_{active}$ to examine the effect of EP2 as an operating energy pile on the thermal response of EP1 as a nearby non-operating pile. The axial and radial thermal responses of EP1 were monitored in all the experiments due to its substantial instrumentation.

The ambient, inlet water and initial pile and ground temperatures for the three experiments are shown in Figure 5.1. The atmospheric temperatures used for all the parametric studies were obtained from a weather station located approximately 13 km from the experimental site (Figure 5.1a). The initial ground temperatures were measured by thermocouples located 0.63 m away from the edge of EP1. The heating test on EP1 ($EP1_{active}$) lasted for 18 days. Water at 48°C was circulated at a flow rate of 11 l/min in all the four loops. The experimental data for this experiment was reported in Faizal et al. (2019).

The heating test on the two piles together, $(EP1 + EP2)_{active}$, lasted for 35 days. The piles were connected in series with a water flow rate of 11 l/min and temperature of 44°C. The heating test on EP2 ($EP2_{active}$) lasted for 40 days with a flow rate of 11 l/min and water temperature of about 46°C. The cases presented herein are for continuous operation of ground source heat pumps that would be applicable to commercial buildings such as hospitals and any other application that require long term heating/cooling. The field and numerical results are shown for average temperature changes of EP1, ΔT_{ave} of 10°C and 20°C for both $EP1_{active}$ and $(EP1 + EP2)_{active}$ tests (Figure 5.2). For $EP1_{active}$, these temperature intervals correspond to 0.67, and 6 days of operation, respectively, and for $(EP1 + EP2)_{active}$, these intervals correspond to

6.2, and 13.9 days of operation, respectively. For $EP2_{active,}$ the results are shown for the maximum temperature change of 2.2°C of EP1 as a result of EP2 operation, corresponding to 40 days of operation.

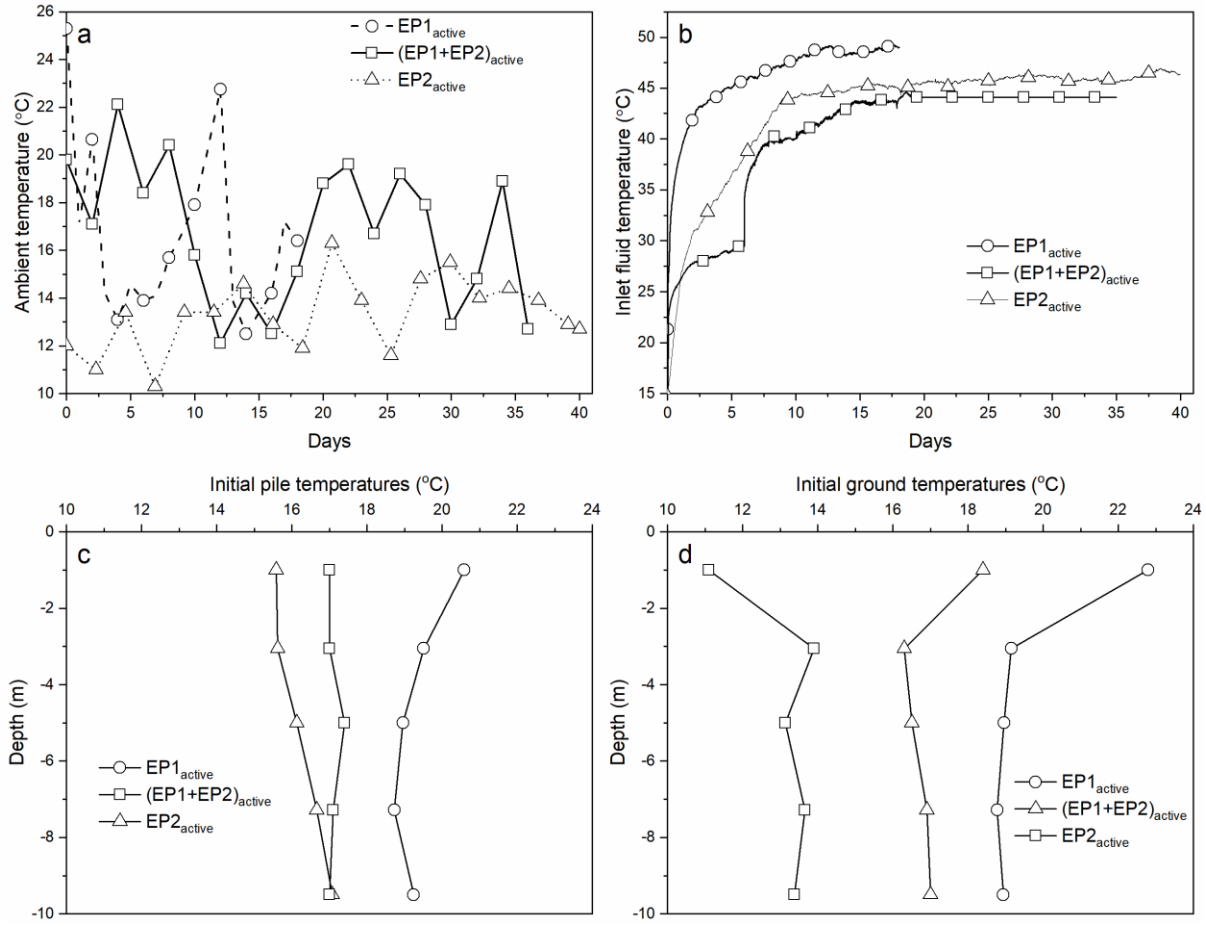

Figure 5.1. Ambient, inlet fluid temperature, and initial pile and ground during three experiments: (a) ambient atmospheric temperature; (b) inlet fluid temperature; (c) initial pile temperatures, and (d) initial ground temperatures.

The field and numerical results of temperatures, and axial and radial thermal strains/stresses of EP1 plotted against depth, for all experiments, are shown in Figure 5.2. Positive thermal strains indicate expansion and negative thermal stresses indicate compression. The numerical simulation results matched well with the in-situ results. The temperatures of EP1 for $EP1_{active}$ and $(EP1 + EP2)_{active}$ tests (shown in Figure 5.2a and 5.2b, respectively) were uniform with depth and reached a magnitude of approximately 38°C for both cases. There were negligible differences in the temperatures for EP1 for all tests, indicating that the operation of

EP2 has insignificant effects on temperature of EP1 for the given spacing of 3.5 m. The temperature change of EP1 is not significant in the $EP2_{active}$ test compared to the $EP1_{active}$ and $(EP1 + EP2)_{active}$ tests and is also slightly non-uniform with depth. The radial and axial thermal strains (Figure 5.2c and 5.2d, respectively) and thermal stresses (Figure 5.2e and 5.2f) of EP1 increased when ΔT_{ave} increased from 10°C to 20°C for both $EP1_{active}$ and $(EP1 + EP2)_{active}$ tests. Due to the slight increase in temperature of EP1 in the $EP2_{active}$ test, small variations in axial and radial thermal strains/stresses were also observed in EP1. The lowest magnitude of axial thermal strains (Figure 5.2d), and thus the highest axial thermal stresses (Figure 5.2f), were observed at a depth of around 3 m in EP1 for all three experiments. This depth can be considered as the location of the null point, indicating dominant stiffness of the overlying structure relative to the stiffness imposed by the soil beneath the pile toe. The radial thermal strains of EP1 (Figure 5.2c) were significantly higher than the axial thermal strains of EP1 (Figure 5.2d) during the $EP1_{active}$ and $(EP1 + EP2)_{active}$ tests, indicating the energy pile had less restrain to thermal expansion in the radial direction than in the axial direction. As a result, the radial thermal stresses (Figure 5.2e) were significantly lower than axial thermal stresses (Figure 5.2f) in EP1 for both $EP1_{active}$ and $(EP1 + EP2)_{active}$ tests.

Figure 5.3a shows the experimental and numerical change in ground temperatures with depth for $EP1_{active}$ and $(EP1 + EP2)_{active}$ tests at the two boreholes located at 0.63 m and 1.95 m from the edge of EP1. The ground temperatures at depths of 7.3 m, 9.5 m, and 12 m were not recorded from day 7 of the $EP2_{active}$ experiment due to technical issues; thus, this experiment's temperature data was not shown in Figure 5.3a. The transient ground temperature changes with increasing radial distance from the sides of EP1 and EP2 for a depth of 5 m is shown in Figure 5.3b. These ground temperatures are for ΔT_{ave} = 20°C of EP1 for $EP1_{active}$ and $(EP1 + EP2)_{active}$ tests and ΔT_{ave} = 32°C of EP2 in the $EP2_{active}$ test.

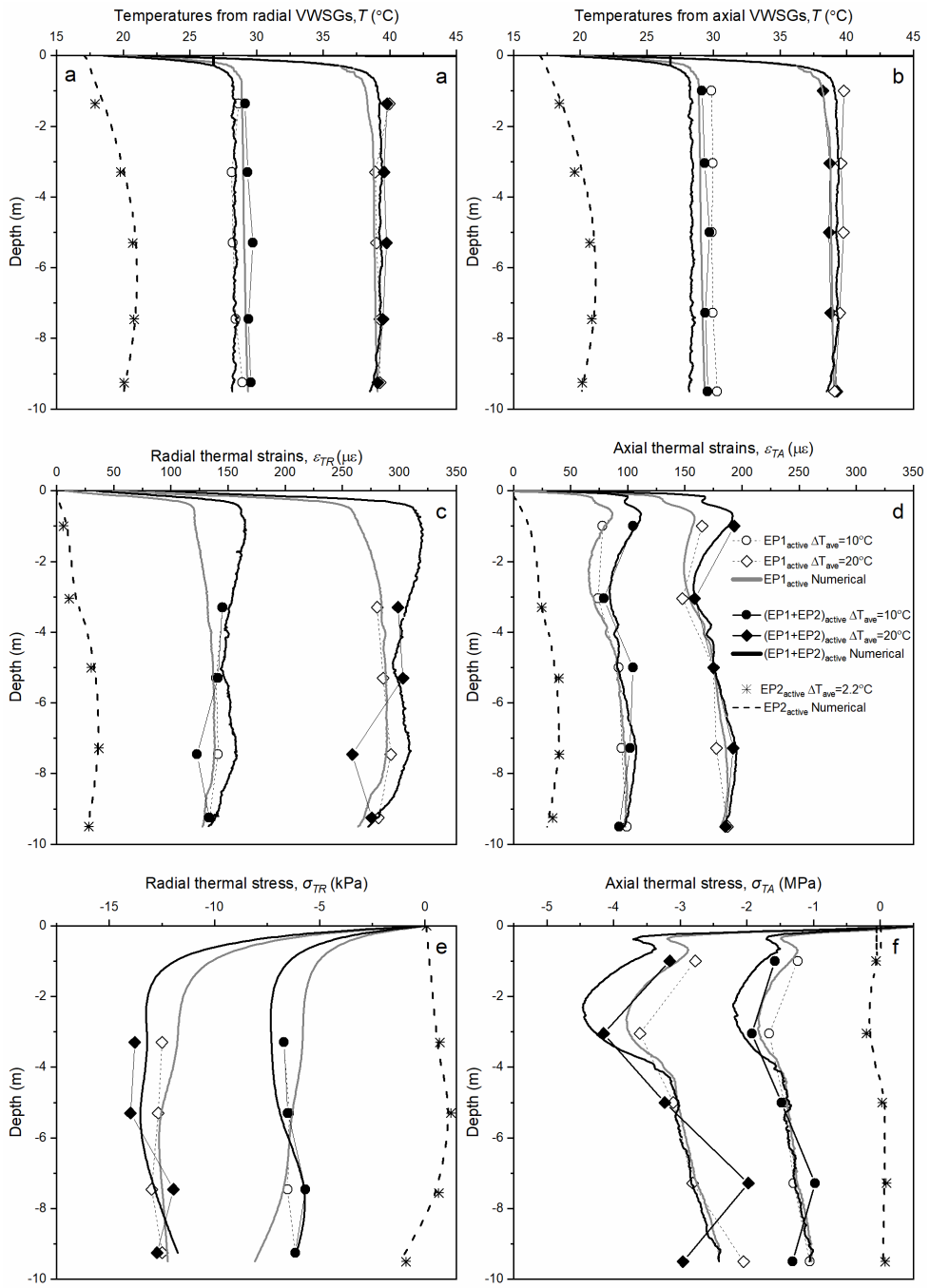

Figure 5.2. Experimental and numerical profiles of EP1 (a) temperatures from radial VWSGs; (b) temperatures from axial VWSGs; (c) radial thermal strains; (d) axial thermal strains; (e) radial thermal stresses; (f) axial thermal stresses.

The ground temperatures at a radial distance of 0 m and 2.9 m from the edge of EP1 are the soil-pile interface temperatures of EP1 and EP2, respectively (Figure 5.3b). The soil temperature changes between the piles are more significant for the $(EP1 + EP2)_{active}$ test, indicating that heating both piles simultaneously increased the thermal interaction between the piles due to overlapping of ground temperatures.

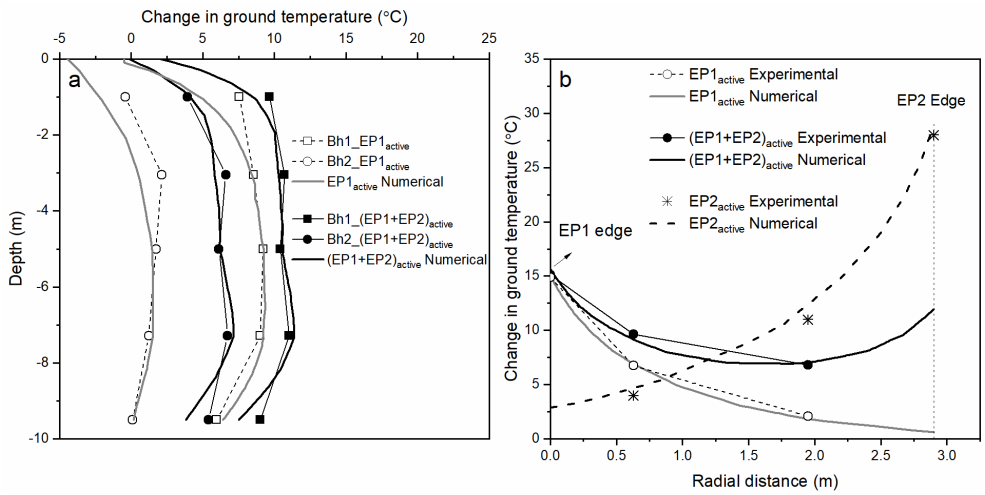

Figure 5.3. Effect of varying soil thermal conductivity on (a) EP1 temperature; (b) ground temperature.

The ground temperature change at the edge of EP2 is lower than at the edge of EP1 in the $(EP1+EP2)_{active}$ test. This is because the two piles' heat exchangers were connected in series. Since EP1 was heated first, the heating rate of EP1 was higher than in EP2, and the temperature of the fluid entering EP2 was lower than that entering EP1. As a result, EP1 had higher temperature changes than EP2, which resulted in lower temperatures at the edge of EP2. The ground temperatures predicted by numerical simulations matched well with the field results.

5.3 Results of parametric evaluation of different soil properties

A parametric evaluation using the validated numerical model was conducted to investigate the effect of soil elastic modulus, E_{soil}, thermal expansion coefficient, α_{soil}, and thermal conductivity, λ_{soil}, on the thermal responses of EP1 for the three field tests described above. Three different values of each soil parameter were considered for all soil layers typical of sandy soil profiles after Bowles (1968) and Mitchel and Soga (2005) (i.e. $0.5E_{soil}$, E_{soil}, $2E_{soil}$; $0.5\lambda_{soil}$, λ_{soil}, $2\lambda_{soil}$; and $0.1\alpha_{soil}$, α_{soil},$10\alpha_{soil}$). The parameters of E_{soil}, λ_{soil}, and α_{soil} have the same magnitudes used for the numerical validation of experimental results. The experimental data for all three field tests had different inlet fluid temperatures, different atmospheric temperatures and different initial pile and ground temperatures (Figure 5.2).

In the parametric study, however, the same test and boundary conditions were applied to all three simulations to assess better the effects of individual soil properties under the same boundary conditions, i.e. same inlet fluid temperatures, fluid velocity (11 l/min), initial pile and ground temperatures, and ambient temperatures. The ambient, inlet fluid, and initial pile and ground temperatures used in the parametric study are obtained from $EP1_{active}$ test and are shown in Figure 5.4. The inlet fluid temperatures represent typical fluid temperatures for energy piles during heating mode of a GSHP. The parametric simulations were conducted for 14 days for all three field tests. The results in the following sections are presented at Day 14 of the tests.

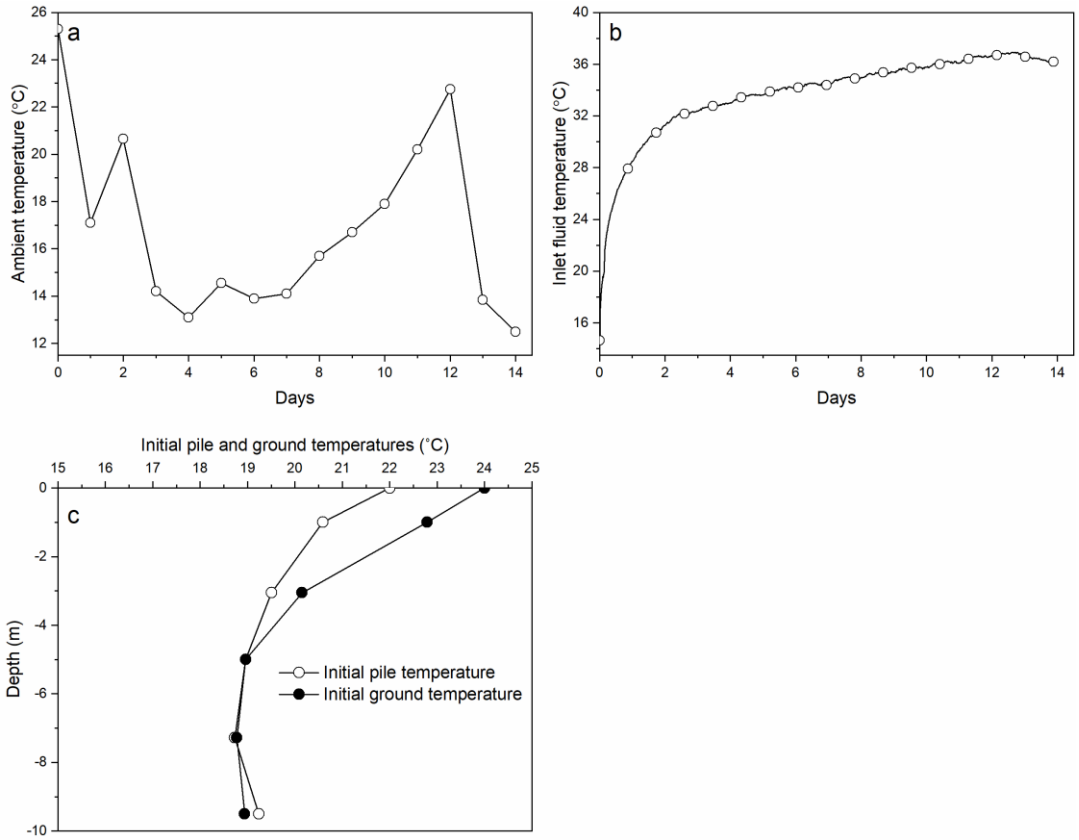

Figure 5.4. Ambient, inlet fluid temperature, and initial pile and ground temperature used in the parametric analyses: (a) ambient atmospheric temperature; (b) inlet fluid temperature; and (c) initial pile and ground temperatures.

The parametric evaluation assumed that the two energy piles were working separately (not connected in series) with the same inlet fluid temperatures, as shown in Figure 5.4b. This was done so that both energy piles had the same inlet fluid temperatures when heated

simultaneously. Heating the two piles together in series would reduce the inlet fluid temperatures to EP2 compared to that of EP1 since EP1 will have a faster heating rate, as was observed in the field test.

5.3.1 Pile and ground temperatures

The effect of varying soil properties on the change in pile temperatures of EP1 and change in ground temperatures between the two piles is shown in Figure 5.5a and 5.5b, respectively. The pile temperatures and ground temperatures were not affected by variations in E_{soil} and α_{soil} for all three tests (not shown here). The temperatures of EP1 reduced by approximately 2.5°C when λ_{soil} increased from $0.5\lambda_{soil}$ to $2\lambda_{soil}$ (Figure 5.5a) for both $EP1_{active}$ and $(EP1+EP2)_{active}$ tests. Higher values of λ_{soil} caused faster heat propagation in the soil, which resulted in lower thermal confinement around EP1, hence lower pile temperatures of EP1 are observed.

For a given λ_{soil}, the temperatures of EP1 were same for both $EP1_{active}$ and $(EP1+EP2)_{active}$ tests since the operation of EP2 did not affect the soil temperature at the edge of EP1, even though higher ground temperature changes occurred between the piles when both piles were heated simultaneously, as shown in Figure 5.5b. No significant differences were observed in temperatures of EP1 for the $EP2_{active}$ test. Negative temperature changes of EP1 near the surface during the $EP2_{active}$ test is due to the very low ambient temperatures at Day 14 (Figure 5.4a). During the $EP1_{active}$ test, the ground temperatures reduced with increasing radial distance from the edge of EP1. The ground temperatures during the $(EP1+EP2)_{active}$ test also initially reduced with increasing radial distance from the edges of EP1 and EP2, but eventually overlapped and developed higher temperatures near the mid-point between the two energy piles. This overlapping of ground temperatures indicates the presence of thermal interaction between the two energy piles when heated simultaneously in the $(EP1+EP2)_{active}$ test. Increasing λ_{soil} reduced the ground temperatures near the energy piles, confirming the findings

of Salciarini et al. (2017). This occurred due to higher heat propagation away from the energy piles when λ_{soil} was increased. As a result of faster heat propagation near the piles, the ground temperatures increased farther away from the piles for both $EP1_{active}$ and $(EP1+EP2)_{active}$ tests.

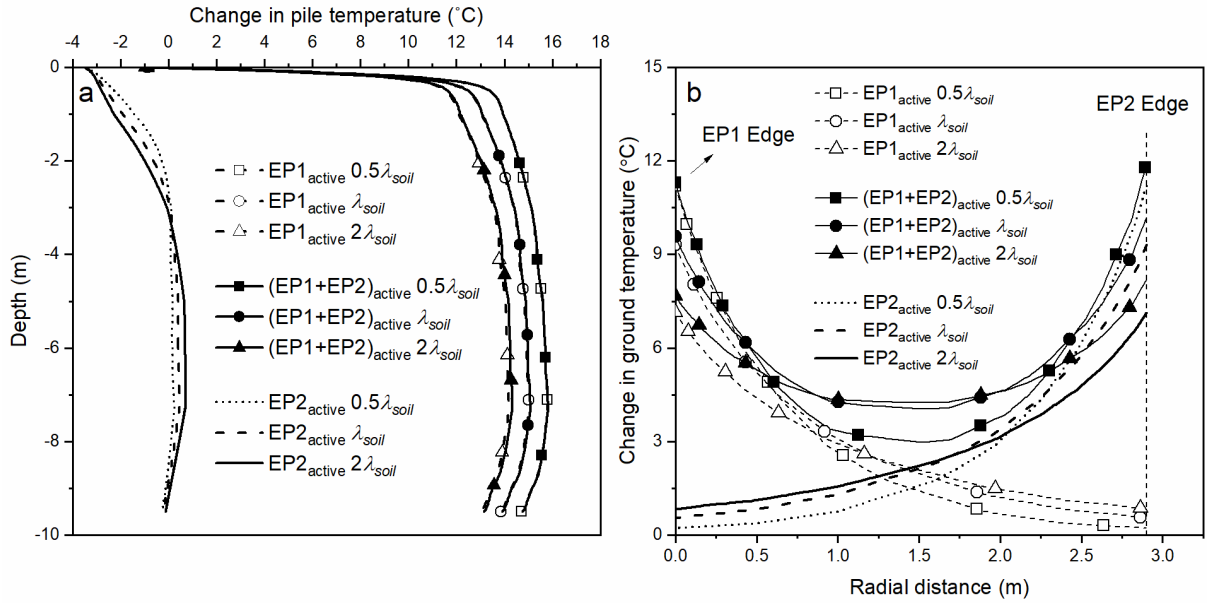

Figure 5.5. Effect of varying soil thermal conductivity on (a) EP1 temperature; (b) ground temperature.

5.3.2 Pile axial thermal strains and stresses

The effect of varying soil properties on the axial thermal strains and stresses of EP1 for all three test conditions are shown in Figure 5.6. The location of the maximum thermal stresses in EP1 remained approximately at the same depth of 3 m for all studied cases. Varying E_{soil} had more effects on the axial thermal strains and stresses of EP1 compared to the impacts of λ_{soil} and α_{soil} for all three field tests. The impacts of E_{soil} on the axial thermal strains and stresses of EP1 are shown in Figure 5.6a and 5.6b, respectively. An increase in E_{soil} significantly increased the axial thermal stresses in EP1 for both $EP1_{active}$ and $(EP1+EP2)_{active}$ tests. Similar observations were noted by Khosravi et al. (2016). The axial thermal stresses in EP1 almost doubled in $EP1_{active}$ and $(EP1+EP2)_{active}$ tests at 3 m depth when E_{soil} increased from $0.5E_{soil}$ to $2E_{soil}$. Higher E_{soil} results in higher rigidity of the soil; hence, a higher restriction is imposed on the axial thermal expansion of the energy pile (Figure 5.6a). For a given E_{soil}, the thermal

stresses developed in EP1 were similar for the $EP1_{active}$ and $(EP1+EP2)_{active}$ tests, with slight differences in the upper section of the pile. This indicates that the operation of one energy pile did not affect the thermal stresses developed in the nearby operating energy pile when both piles were heated simultaneously. Operation of EP2 in the $EP2_{active}$ test induced insignificant thermal axial strains and stresses in EP1, indicating that the heating of an energy pile had negligible effects on the nearby non-operating pile. This can be due to the issue that a pile-cap does not connect EP1 and EP2. The slightly positive (tensile) axial thermal stresses developed in the upper parts of EP1 in the $EP2_{active}$ test (Figure 5.6b) can be attributed to negative temperature changes in EP1 due to atmospheric effect (see Figure 5.5a).

Figure 5.6c and 5.6d show the effects of λ_{soil} on the axial thermal strains and stresses of EP1, respectively. The thermal stresses developed in EP1 were lower than those developed for different E_{soil}. There was a slight increase in axial thermal stresses of EP1 when λ_{soil} was increased from $0.5\lambda_{soil}$ to $2\lambda_{soil}$ in $EP1_{active}$ and $(EP1+EP2)_{active}$ tests (by approximately 0.3 MPa at 3 m depth), even though the pile temperatures had reduced by 2.5°C (Figure 5.5a). This could be attributed to the lower expansion of the soil near the pile-soil interface due to lower ground temperatures for larger thermal conductivity (Figure 5.5) which possibly increased restraint of the axial thermal expansion of the pile. The thermal strains and stresses in EP1 were similar for $EP1_{active}$ and $(EP1+EP2)_{active}$ for any given λ_{soil} with slight differences in the upper pile section, indicating negligible thermal effects of one energy pile on the other when heated simultaneously. The magnitudes of axial thermal stresses and strains in EP1 in the $EP2_{active}$ test were negligible indicating negligible thermal effects on a nearby non-thermal pile due to the operation of an energy pile. The effects of α_{soil} on the axial thermal strains and stresses of EP1 are shown in Figure 5.6e and 5.6f, respectively. The range of thermal stresses was lower than that for E_{soil}. Similar to what was observed for E_{soil} and λ_{soil}, the thermal stresses in EP1 were

similar for both $EP1_{active}$ and $(EP1+EP2)_{active}$ test with slight differences in the upper pile section, for a given α_{soil}.

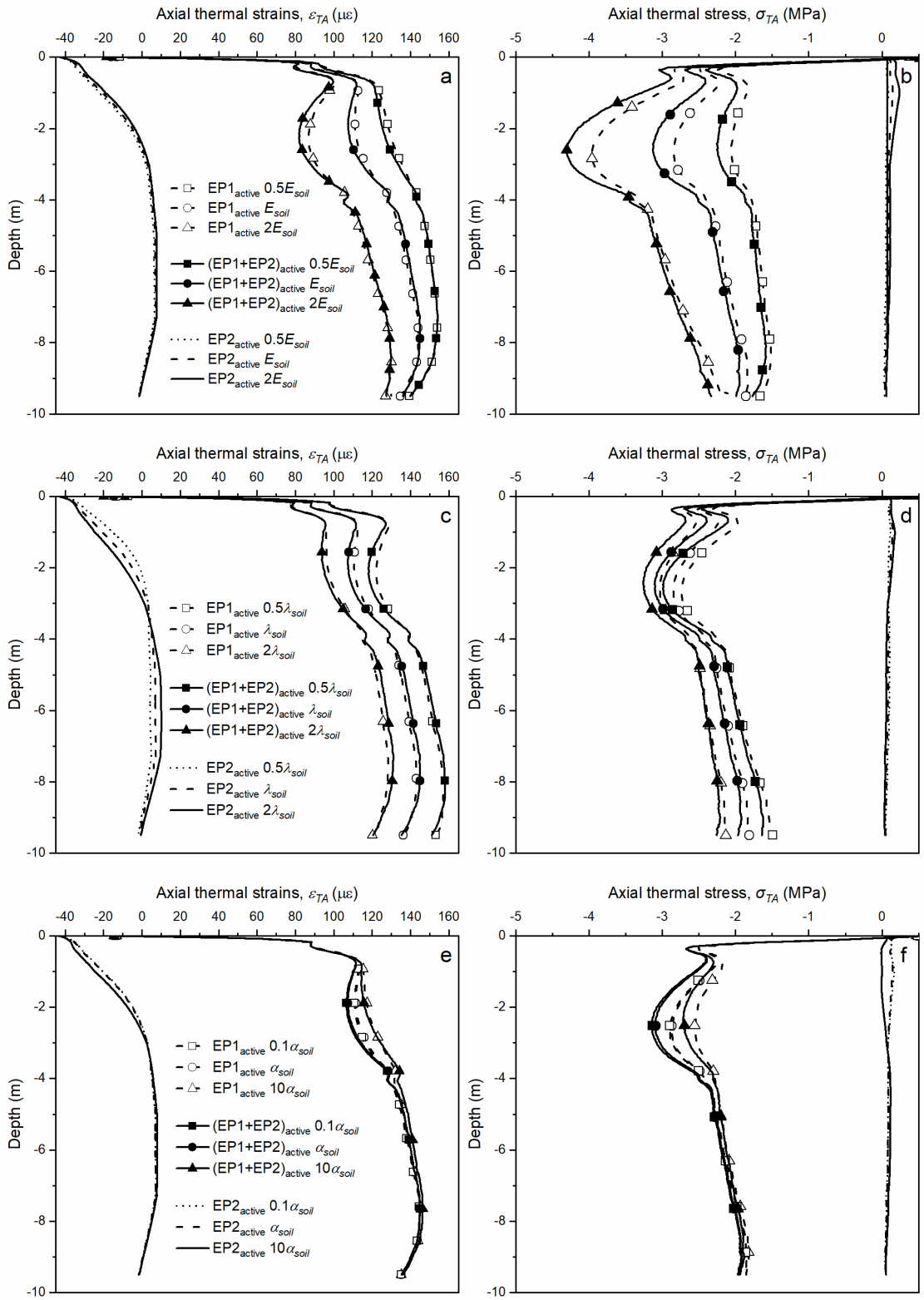

Figure 5.6. Axial thermal responses of EP1 from the parametric evaluation: (a) strains when varying E_{soil}; (b) stresses when varying E_{soil}; (c) strains when varying λ_{soil}; (d) stresses when varying λ_{soil}; (e) strains when varying α_{soil}; (f) stresses when varying α_{soil}.

Increasing α_{soil} to $10\alpha_{soil}$ (corresponding to $\alpha_{soil}/\alpha_{pile}$ of 0.7 and 7 respectively) resulted in a small reduction in axial thermal stresses in EP1 for both $EP1_{active}$ and $(EP1+EP2)_{active}$ tests, mostly for the upper pile section for $10\alpha_{soil}$ ($\alpha_{soil}/\alpha_{pile}$ of 7). This can be related to the increased soil expansion for higher values of α_{soil} which resulted in a lower restriction on EP1. This behaviour is consistent with the observations reported by Bourne-Webb et al. (2016) and Salciarini (2017). Similar to the effects of E_{soil} and λ_{soil}, there were negligible effects of EP2 operation on EP1 in the $EP2_{active}$ test. The values of $\alpha_{soil}/\alpha_{pile}$ used in this study are consistent with those of other studies which have been reported to vary between 0 and 2 (Bodas Freitas et al., 2013), 0.033 and 3.3 (Rotta Loria and Laloui 2017), and 1 to10 (Salciarini et al. 2017).

5.3.3 Pile radial thermal strains and stresses

The effects of varying soil properties on the radial thermal strains and stresses of EP1 for the three test scenarios are shown in Figure 5.7. The magnitudes of the radial thermal stresses in EP1 for all investigated soil parameters were significantly lower than the axial thermal stresses shown in Figure 5.6. The radial thermal strains were more significant and closer to the free thermal expansion of the pile compared to the axial thermal strains reported in Figure 5.6. These confirm the findings of previous studies that radial thermal stresses are insignificant compared to the magnitudes of axial thermal stresses in energy piles (Ozudogru et al. 2015; Gawecka et al. 2017; Faizal et al. 2018, 2019). The highest magnitudes of radial thermal stresses in EP1 for all cases are at a depth of 3 m due to the higher soil rigidity at this depth. Also, E_{soil} had higher impacts on the radial thermal stresses in EP1 compared to λ_{soil} and α_{soil}.

The effect of E_{soil} on the radial thermal strains and stresses of EP1 are shown in Figure 5.7a and 5.7b, respectively. An increase in E_{soil} resulted in an increase in the magnitudes of radial thermal stresses in EP1 in $EP1_{active}$ and $(EP1+EP2)_{active}$ tests due to increased soil rigidity. These observations are consistent with the results reported by Olgun et al. (2014), where the

normal stresses increased from 3.5 to 14 kPa when E_{soil} increased from 25 MPa to 100 MPa. For a given E_{soil}, the radial thermal stresses in EP1 were similar for $EP1_{active}$ and $(EP1+EP2)_{active}$ tests, with minor differences of approximately 5 kPa for $2E_{soil}$.

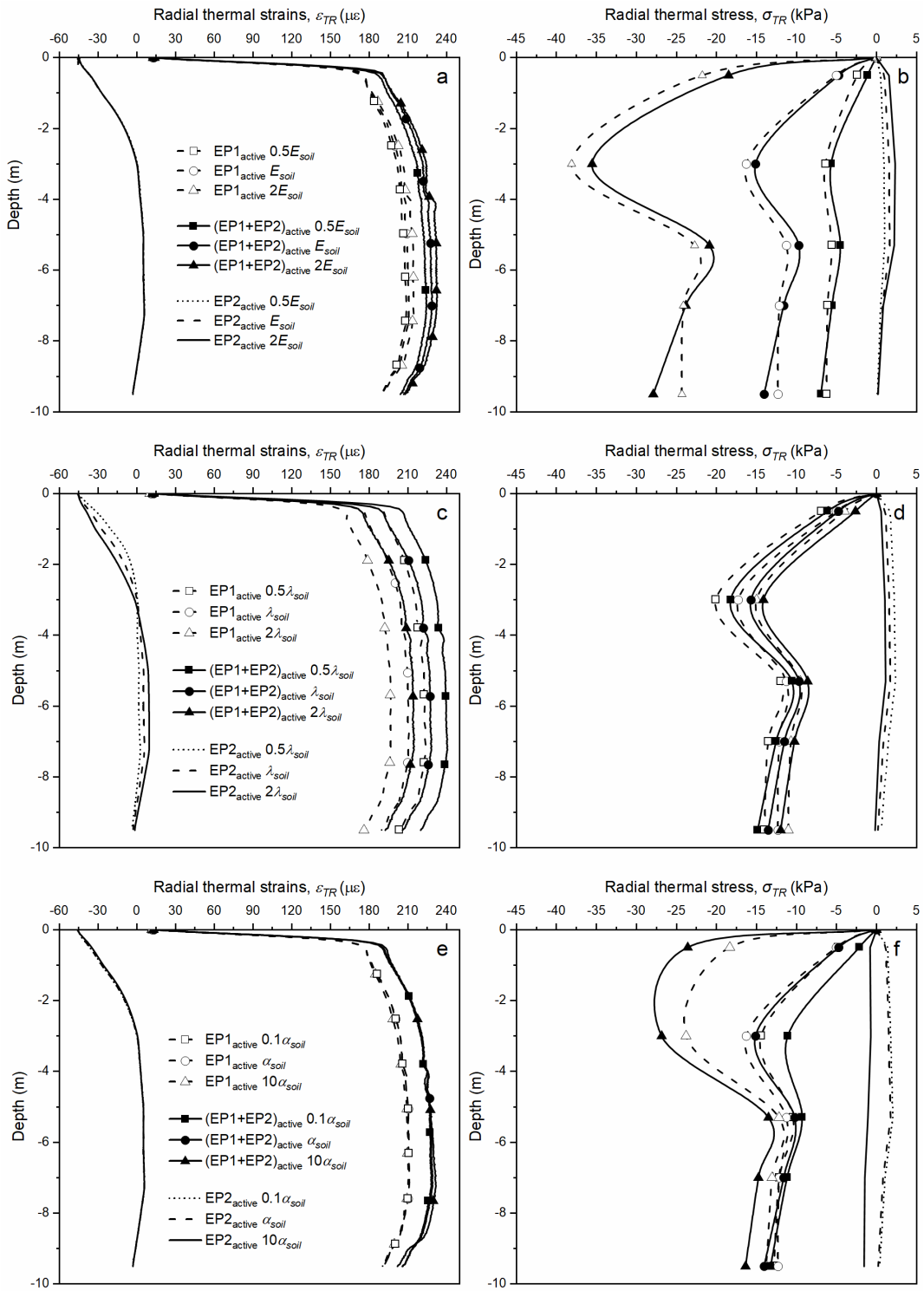

Figure 5.7. Radial thermal responses of EP1 from the parametric evaluation: (a) strains when varying E_{soil}; (b) stresses when varying E_{soil}; (c) strains when varying λ_{soil}; (d) stresses when varying λ_{soil}; (e) strains when varying α_{soil}, (f) stresses when varying α_{soil}.

This confirms the negligible effects of the operation of one energy pile on the other nearby energy pile for the setting investigated in this study. Insignificant stress changes of up to 2.2 kPa were observed in EP1 during the $EP2_{active}$ test. The effects of λ_{soil} on radial thermal strains and stresses of EP1 are shown in Figure 5.7c and 5.7d, respectively. The radial thermal stresses of EP1 slightly reduced when λ_{soil} increased, with a maximum reduction of 4.5 kPa at 3 m depth when λ_{soil} increased from $0.5\lambda_{soil}$ to $2\lambda_{soil}$. No significant differences were observed in radial thermal stresses of EP1 between the $EP1_{active}$ and $(EP1+EP2)_{active}$ tests indicating insignificant thermal effects of the operation of one energy pile on the other energy pile.

Similar to E_{soil}, negligible stress changes of up to 2.2 kPa were observed in EP1 in the $EP2_{active}$ test. The effects of α_{soil} on the radial thermal strains and stresses in EP1 are shown in Figure 5.7c e and 5.7f, respectively. The radial thermal stresses in EP1 increased for both $EP1_{active}$ and $(EP1+EP2)_{active}$ tests with increasing α_{soil}. The radial thermal stresses in EP1 in the $EP1_{actvice}$ test were higher than in the $(EP1+EP2)_{active}$ test for $0.1\alpha_{soil}$ and α_{soil} (corresponding to $\alpha_{soil}/\alpha_{pile}$ of 0.07 and 0.7 respectively). However, for $10\alpha_{soil}$ ($\alpha_{soil}/\alpha_{pile}$ of 7) the opposite behaviour observed is likely due to increased thermal expansion of the soil. A higher volume of soil is subjected to temperature change when both piles are heated together (Rotta Loria and Laloui 2017b). The radial thermal stresses in EP1 during the $EP2_{active}$ test was very low compared to the $EP1_{active}$ and $(EP1+EP2)_{active}$ tests.

5.3.4 Thermal displacements

The effects of varying soil properties on the axial and radial thermal displacements of EP1, for all three test scenarios, is shown in Figure 5.8. The radial thermal displacements were very low with a range of -0.03 mm to 0.01 mm, for all soil properties. The axial thermal displacements at the pile head of EP1 were much higher than radial thermal displacements and ranged between 0.3 mm to 0.5 mm for all soil properties. The radial and axial thermal

displacements of EP1 were, however, up to 0.005% and 0.1% of the pile diameter, respectively, much lower than the generally allowable 10% of the pile diameter failure criteria.

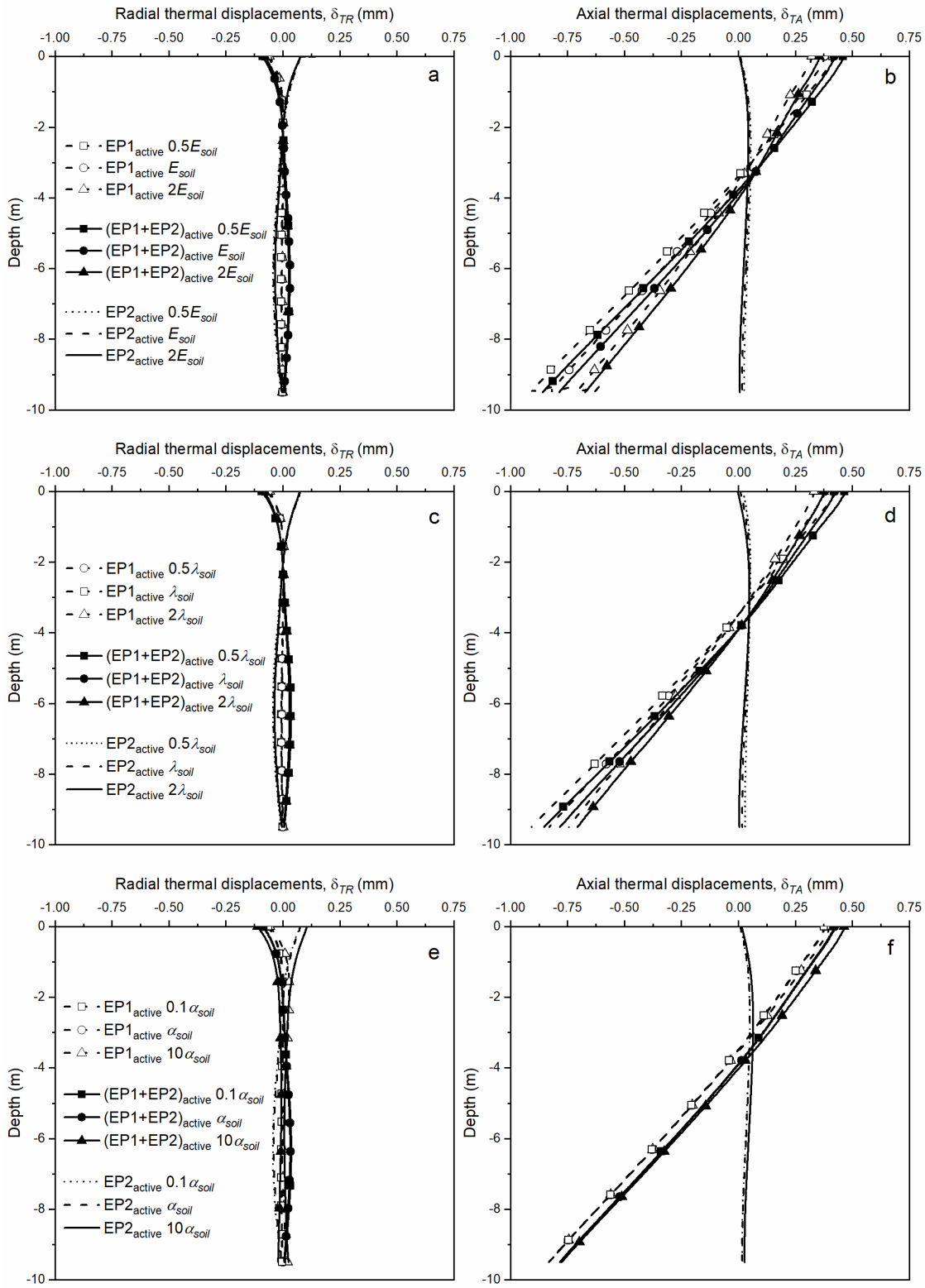

Figure 5.8. Radial (δ_{TR}) and axial (δ_{TA}) thermal displacements of EP1 from the parametric evaluation: (a) δ_{TR} when varying E_{soil}; (b) δ_{TA} when varying E_{soil}; (c) δ_{TR} when varying λ_{soil}; (d) δ_{TA} when varying λ_{soil}; (e) δ_{TR} when varying α_{soil}; (f) δ_{TA} when varying α_{soil}.

Increasing E_{soil} resulted in a slight decrease in axial thermal displacements of EP1 for both $EP1_{active}$ and $(EP1+EP2)_{active}$ tests due to the higher restriction of the surrounding soil (Figure 5.8b). The axial thermal displacements of EP1 also reduced with increasing λ_{soil} for both $EP1_{active}$ and $(EP1+EP2)_{active}$ tests, likely due to increased soil strength near the pile due to temperature changes.

Increasing α_{soil} did not significantly affect the axial thermal displacement of EP1 for both $EP1_{active}$ and $(EP1+EP2)_{active}$ tests. There were no significant differences in axial and radial thermal displacements of EP1 between the $EP1_{active}$ and $(EP1+EP2)_{active}$ tests for all soil properties, confirming the negligible effects of the operation of one energy pile on the other. The axial and radial thermal displacements of EP1 for the $EP2_{active}$ test were insignificant for all soil properties confirming negligible effects of an operating energy pile on a nearby non-thermal pile.

5.4 Chapter summary

In this chapter, three cases were studied to assess the axial and radial thermal responses of one of the energy piles (EP1): (1) heating of the energy pile alone (EP1); (2) heating of both energy piles simultaneously (EP1 + EP2), and (3) heating of the other energy pile (EP2) while the considered energy pile was not heated. The effects of varying soil thermal conductivity, thermal expansion coefficient, and elastic modulus on the thermal response of the considered energy pile were investigated. Higher ground temperature changes were observed between the piles due to thermal interaction through the soil when the two piles were heated together. However, the magnitudes of thermal stresses developed in the considered energy pile for all soil properties were not affected by the operation of the two piles at the same time. This indicates that there were negligible thermal effects of the operation of one energy pile on the other energy pile during dual pile operation for the pile spacing considered in this thesis.

Heating of the second pile only (EP2) also induced insignificant thermal effects on the other non-thermal pile (EP1) for all soil properties. Increasing the thermal conductivity of the soil induced higher ground temperature changes around both energy piles. However, compared to the impact of thermal conductivity and thermal expansion coefficient of the soil, the effect of elastic modulus of the soil was more significant on the thermal stresses and displacements developed in the considered energy pile (EP1) for all heating cases. The results of this chapter will be useful in assessing the thermal interaction among closely spaced energy piles when designing energy piles at different sites with soil properties similar to those reported in this chapter.

6 Cross-sectional thermal responses of an energy pile

6.1 Introduction

The majority of the available studies conducted on energy piles focussed on their thermal response at a single location in the cross-section of the pile (e.g. Faizal et al. 2016, 2018; Mimouni and Laloui 2015; Rotta Loria and Laloui 2017a, 2017b, 2018; Fang et al. 2020). However, recent numerical studies conducted on solitary piles showed that non-uniform temperature and stress variations occurred between the pile's centre and the pile's edge (Abdelaziz and Ozudogru 2016a, 2016b; Caulk et al. 2016; Han and Yu 2020; Liu et al. 2020). These studies were conducted for given inlet fluid temperatures and given set of soil properties; hence the effect of various inlet fluid temperatures and soil properties, and the effect of nearby energy pile on the cross-sectional thermal response of an energy pile was not addressed and still unknown.

This chapter presents the cross-sectional thermal responses of an energy pile (i.e. the third objective of this thesis). The numerical model was first validated against field results and then used to investigate the influence of inlet fluid temperatures, soil properties (soil thermal conductivity, λ_{soil}, thermal expansion coefficient, α_{soil}, and elastic modulus, E_{soil}) and the presence of a nearby energy pile on the temperature and stress distribution in the cross-section of the considered energy pile (EP1).

6.2 Validation of numerical model with experimental results

In this chapter, two heating and two cooling experiments were conducted on a single pile (EP1) and dual piles (EP1 + EP2). The inlet water temperatures and the ambient temperatures for all experiments are described in Figure 6.1 and Table 3.2 in Chapter 3. The fluid temperatures were recorded using Type T thermocouples. The sudden increase in inlet

fluid temperature on day 4 of the dual pile heating experiment, shown in Figure 6.1, was due to switching on an additional heating element to increase the inlet fluid temperature. The inlet fluid temperature trend for the dual pile cooling experiment was affected on Days 8 and 15 due to some heat pump's performance issues. The temperature data for heating and cooling tests for the single and dual pile experiments were obtained from Faizal et al. (2019a) and Moradshahi et al. (2020). These data sets were used to validate the numerical model and investigate the influence of different parameters on the cross-sectional temperatures and axial thermal strains and stresses of EP1.

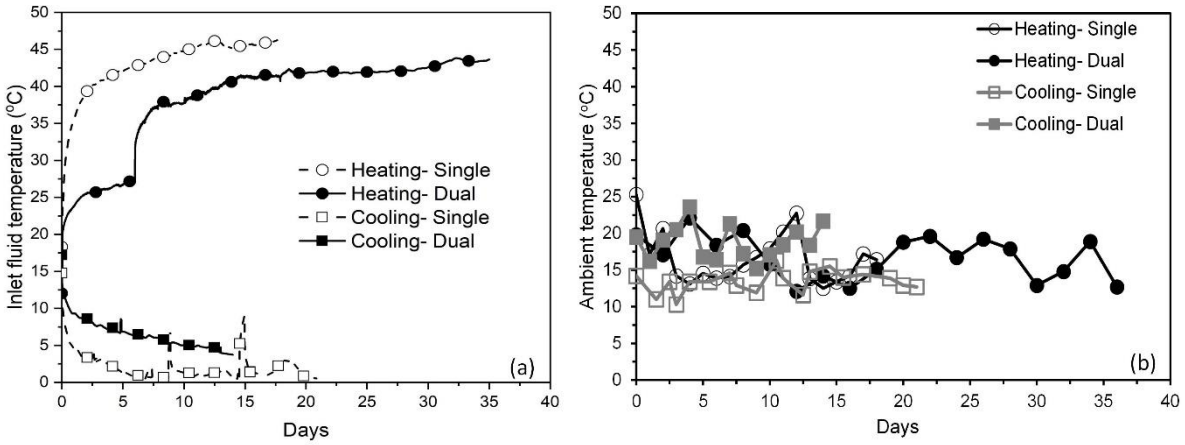

Figure 6.1. Temperatures for single and dual pile heating and cooling experiments (a) fluid temperatures; and (b) ambient.

The distribution of EP1 temperatures and axial thermal strains were obtained from the axial VWSGs located in the planar cross-section of EP1. The locations of these axial VWSGs, shown in Figure 3.2 in Chapter 3, were non-dimensionalised with respect to the radius of EP1. In this regard, the axial VWSG at location V5 (Figure 3.2) corresponds to the centre of EP1, V1 and V2 correspond to the non-dimensional radius of -0.47, and V3 and V4 correspond to the non-dimensional radius of 0.47. The field and numerical results for Day 14 of each experiment along the cross-section of EP1 for the depths of 3.05 m (near the null point) and 7.28 m (representative of EP1 behaviour of lower parts of EP1) are shown in Figure 6.2. There

is a good match between experimental and numerical results, hence giving confidence in using the model for more detailed parametric investigations.

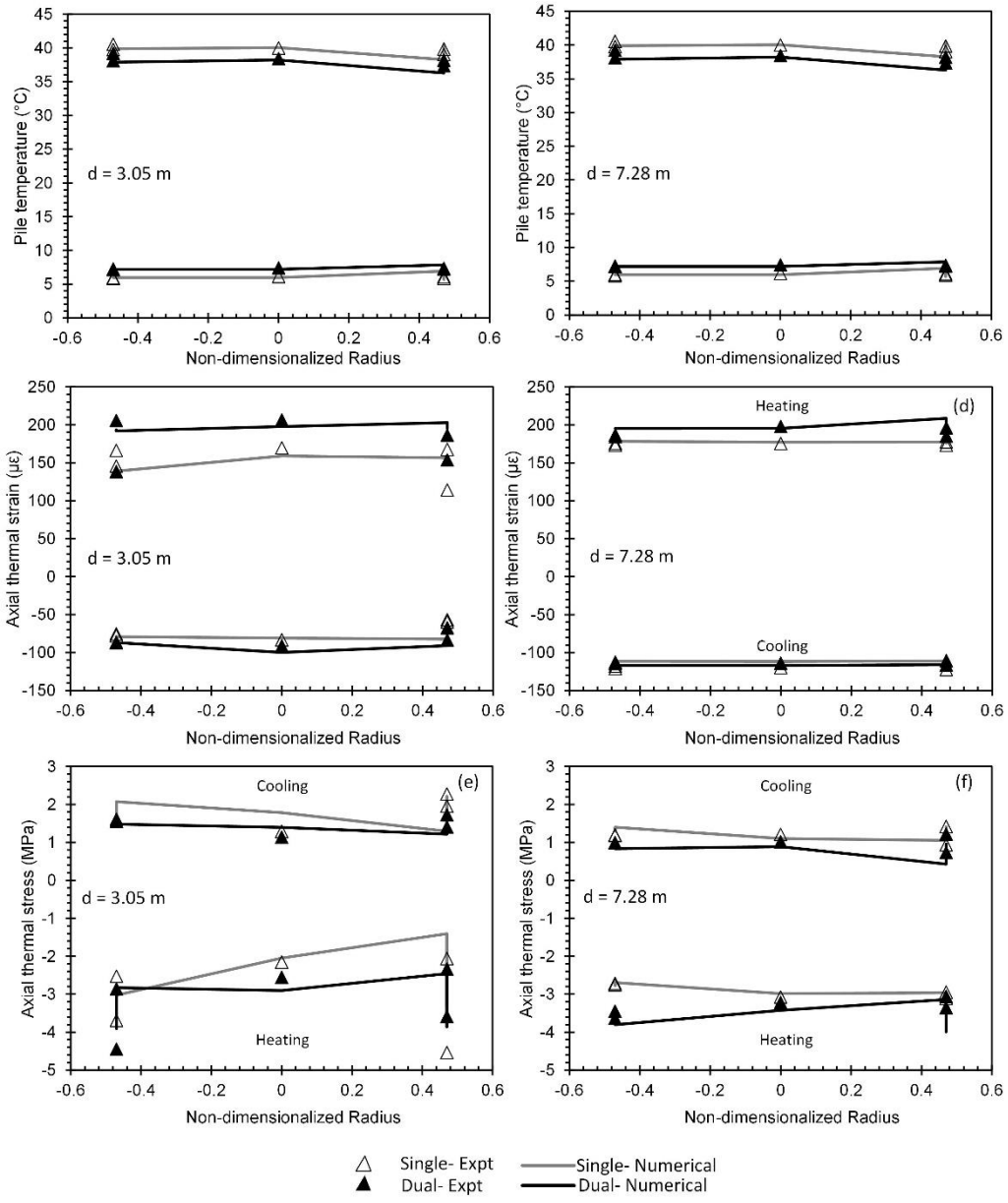

Figure 6.2. Field experimental and numerical cross-sectional distribution of thermal responses for EP1 at the end of Day 14: (a) and (b) temperatures at depths of 3.05 m and 7.28 m, respectively; (c) and (d) axial thermal strains at depths of 3.05 m and 7.28 m, respectively; and (e) and (f) axial thermal stresses at depths of 3.05 m and 7.28 m, respectively.

A good match between experimental and numerical results was also obtained at other depths. The experimental and numerical results show a low range of variations of temperature (up to 1.5^{o}C), strains (up to 26με) and stresses (up to 2 MPa) over the cross-section of EP1 for all experiments (Figure 6.2a and 6.2b). The overall trends and magnitudes of temperatures and

axial thermal strains and stresses were similar in single and dual pile experiments, indicating the negligible effect of the operation of EP2 on the cross-sectional thermal response of EP1.

The experimental and numerical transient ground temperature changes in boreholes 1 and 2 (see Figure 3.2 in Chapter 3) for all four experiments are shown in Figure 6.3. There was a good match between experimental and numerical results. For single heating and cooling experiments, the ground temperature changes in BH1 is greater than that of BH2. However, in dual pile experiments, the ground temperature changes in BH2 are greater than in single pile experiments as a result of EP2 being heated or cooled.

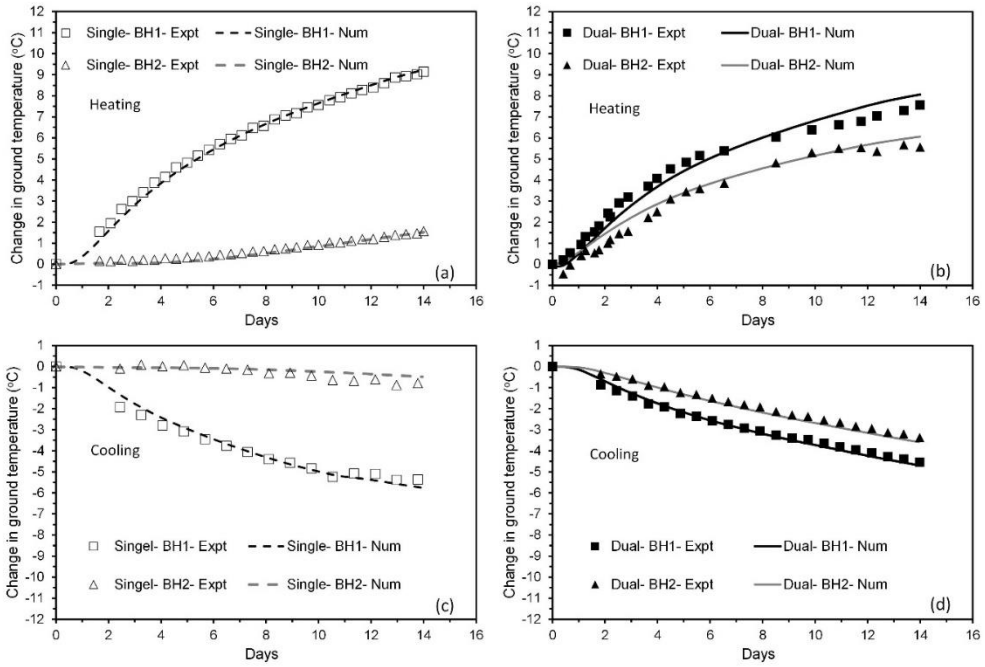

Figure 6.3. Field experimental and numerical change in ground temperatures: (a) for single pile heating operation; (b) for dual pile heating operation; (c) for single pile cooling operation; and (d) for dual pile cooling operation at a depth of 2.5 m.

6.3 Results of parametric evaluation of different fluid temperatures and soil properties

A parametric evaluation was performed using the validated numerical model to investigate the effect of varying fluid temperature and varying λ_{soil}, E_{soil}, and α_{soil} on the cross-sectional thermal response of EP1. For each heating and cooling experiment, two inlet fluid temperatures were studied, as shown in Figure 6.4. The fluid temperatures were varied by ±

10°C intervals for heating and cooling operations (i.e. $|\Delta T_f|$ = 10°C, and 20°C, where ΔT_f is the difference between the inlet fluid temperatures at the end of the experiment and the initial fluid temperature of 20°C which is close to the average ground temperature). The intervals of $|\Delta T_f|$ = 10°C were chosen to perform the parametric analysis on the effect of soil properties on the thermal response of EP1 for both heating and cooling operations. Three different values of each soil parameter were investigated (i.e. $0.5\lambda_{soil}$, λ_{soil}, $2\lambda_{soil}$; $0.5E_{soil}$, E_{soil}, $2E_{soil}$; $0.1\alpha_{soil}$, α_{soil}, 10 α_{soil}). The initial pile and ground temperatures, fluid flow rate and ambient temperatures were kept the same for all the simulations. The two energy piles were also not connected in series and worked separately with the same inlet fluid temperatures (shown in Figure 6.4) and the same fluid flow rate of 11 l/min.

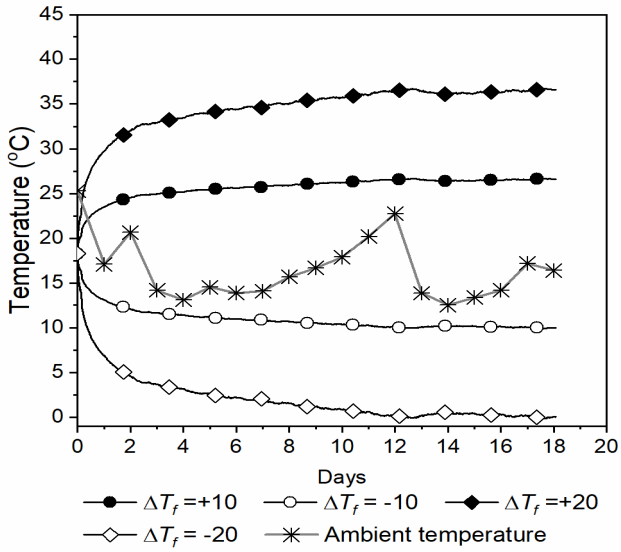

Figure 6.4. Inlet fluid and ambient temperatures for parametric evaluations.

6.3.1 Thermal responses across different diametrical axes

The cross-sectional thermal response of EP1 over the four different axes (i.e. X-axis, Y-axis, D1-axis, and D2-axis, as shown in Figure 3.7 in Chapter 3) at a depth of 2.5 m for $|\Delta T_f|$ = 10°C is shown in Figure 6.5. The depth of 2.5 m had the highest stresses compared to other depths, likely the location of the null point. The magnitudes of temperatures and thermal strains/stresses were symmetrical between heating and cooling for a given axis. Higher values

of temperature, thermal strains and stresses were also observed at the centre of EP1 compared to the edge of EP1 for both single and dual pile tests.

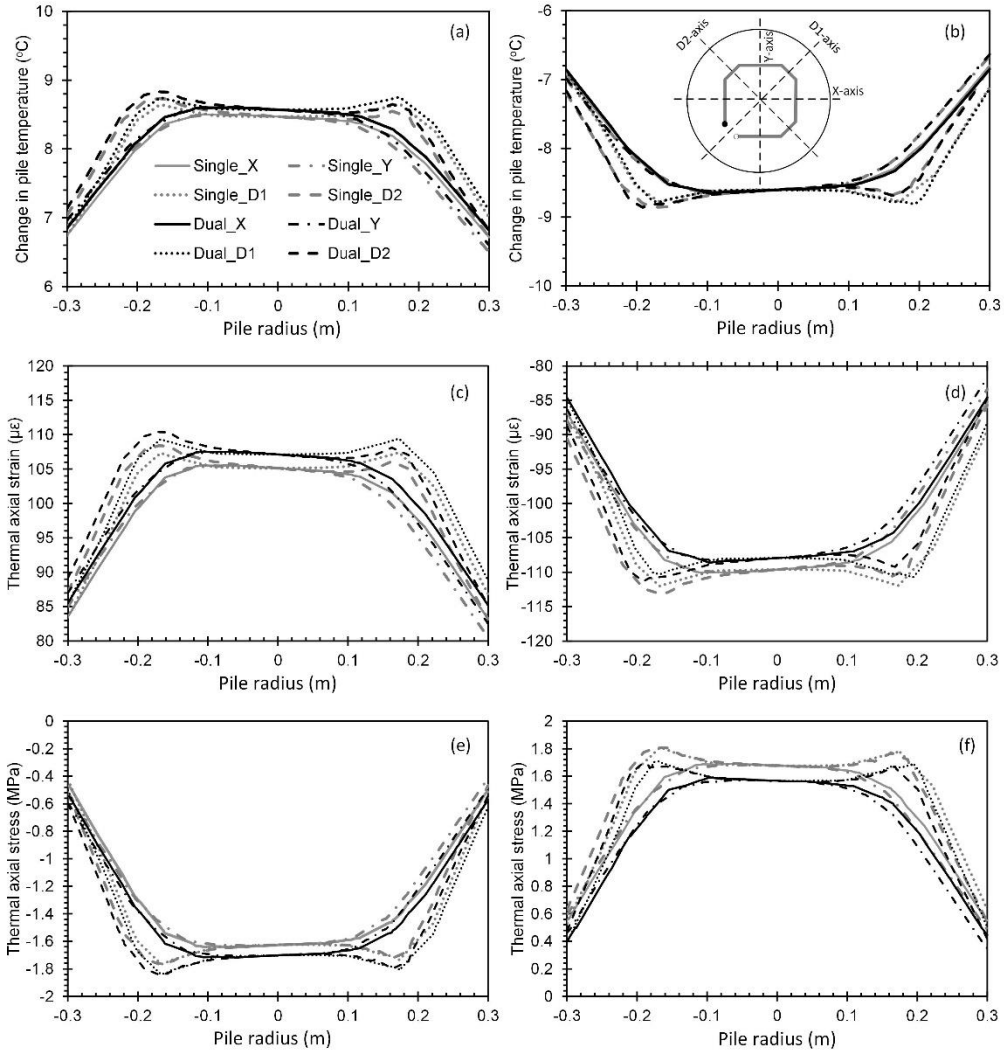

Figure 6.5. Numerical predictions of cross-sectional thermal responses of EP1 over different axes: (a) and (b) change in temperature during heating and cooling, respectively; (c) and (d) axial thermal strains during heating and cooling, respectively; and (e) and (f) axial thermal stresses during heating and cooling.

The change in temperature at the centre and edge of the pile were approximately ± 8.5°C and ± 6.9°C (difference of ~ 1.6°C), respectively, while the stresses were ± 1.7 MPa and ± 0.4 MPa (difference of ~ 1.3MPa), respectively. The pile temperature reduced to the magnitudes of ground temperatures at the pile-soil interface (discussed in the following sections). The strains and stresses varied along the cross-section due to variations in temperature distribution and variations in the pile's thermal expansion/contraction across the

cross-section. The temperatures and strains/stresses are largest with almost constant magnitudes between R = – 0.14 m and R = 0.14 m as this region is enclosed by the evenly distributed thermally active heat exchanger loops. The reduction in temperatures and thermal strains/stresses between R = ± 0.14 m and the pile-soil interface, at R = ± 0.3 m, is due to the difference in temperatures between the heat exchanger loops and the soil.

The differences between the cross-sectional thermal response of EP1 for all different four axes is insignificant with the maximum difference of about 0.3°C, 7$\mu\varepsilon$, and 0.2 MPa for changes in pile temperature, thermal axial strains, and thermal axial stresses, respectively, for all operations. Therefore, the distribution of thermal responses in the cross-section can be considered similar across different diametrical axes of the pile. As there were no significant differences in the different axes' thermal responses, the X-axis in the following sections of the chapter is chosen to investigate the cross-sectional thermal response of EP1 for varying soil parameters.

6.3.2 Fluid temperatures

The effect of varying inlet fluid temperatures on the cross-sectional thermal responses of EP1 at a depth of 2.5 m and adjacent ground temperature changes at the same depth are shown in Figure 6.6. The change in pile and ground temperatures and thermal strains/stresses increased with increasing fluid temperatures. The pile temperatures are largest at the centre of the pile (Figure 6.6a) and reduce to the value of ground temperatures at the pile-soil interface (Figure 6.6b). The two energy piles' operation simultaneously increased/decreased the change in ground temperatures between the two energy piles, compared to single pile operation for heating/cooling operation (Figure 6.6b). The ground temperature changes were greater during dual pile tests due to thermal interference between the soil volumes influenced by each energy pile. The difference between the magnitude of temperature and axial thermal stresses between the centre and edge of EP1 increased from 1.6℃ to 3.1℃ and from 1.3 MPa to 2.1 MPa

respectively, with increasing fluid temperature from $|\Delta T_f|$ of 10°C to 20°C. Liu et al. (2020) and Abdelaziz and Ozudogru (2016b) also reported differences of 1.5 MPa and 2 MPa, respectively, between the centre and the edge of the energy pile.

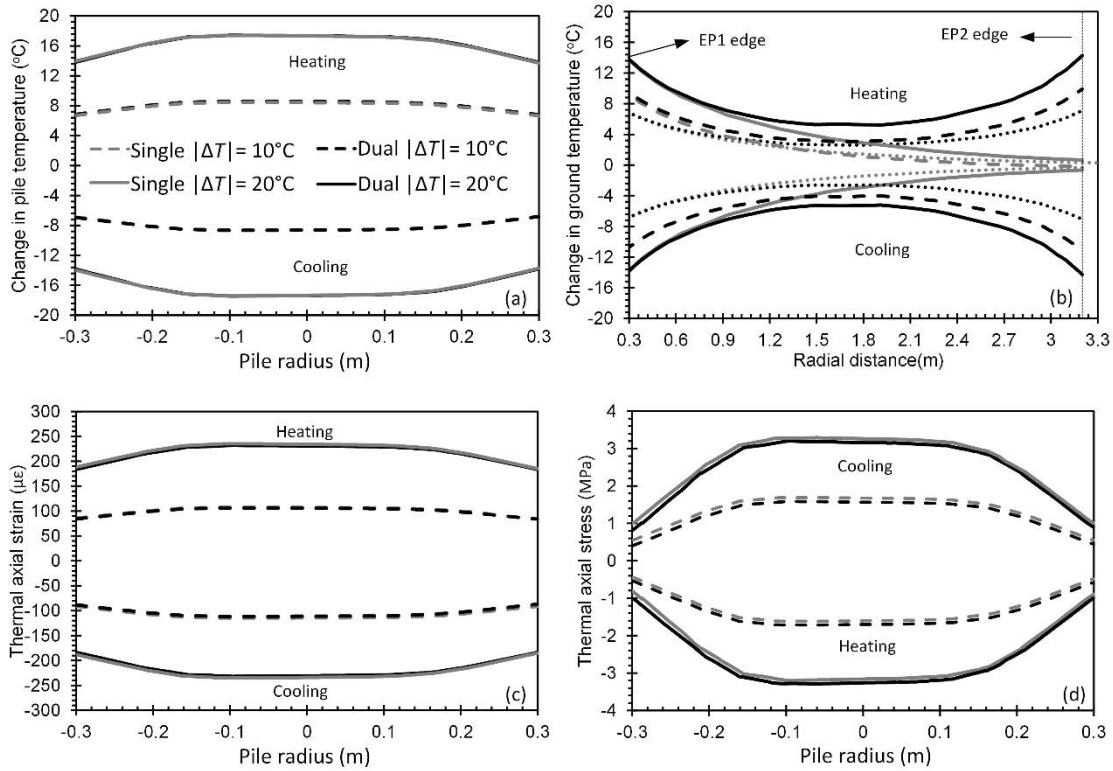

Figure 6.6. Numerical predictions of the effect of fluid temperature changes on the cross-sectional thermal responses of EP1 and ground temperatures: (a) change in temperature; (b) change in radial distribution of ground temperatures; (c) thermal axial strains; and (d) thermal axial stresses in EP1.

Larger fluid temperatures during the operation of the GSHP will therefore induce higher differential temperatures and stresses in the cross-section of the piles. Even though the ground temperatures between the two energy piles were affected by the operation of EP2 in dual pile operation, the temperatures and thermal strains/strains developed in EP1 were similar for both single and dual pile operations. The negligible effects of EP2 on EP1 likely occurred due to minor changes in ground temperatures near the edge of EP1 (up to 0.3 m away from EP1 edge) for both single and dual pile operations. This indicates that the operation of EP2 did not have significant effects on the cross-sectional distribution of temperatures and thermal stresses of EP1. This can be related to the fact that a pile-cap does not connect the piles and that the piles

are not close enough to cause any effects on the thermal responses of EP1 as a result of EP2 operation.

6.3.3 Soil thermal conductivity

The effect of soil thermal conductivity, λ_{soil}, on the cross-sectional thermal responses of EP1 and adjacent ground temperature changes at a depth of 2.5 m, for $|\Delta T_f| = 10$°C, is shown in Figure 6.7. Symmetrical thermal responses were observed for heating and cooling operations for all λ_{soil} values. Higher λ_{soil} resulted in lower EP1 temperature changes. Higher λ_{soil} resulted in faster heat propagation in the soil, which resulted in lower thermal confinement around EP1, hence the pile temperatures were low. For a given λ_{soil}, the changes in ground temperature near EP1 is similar for both single and dual pile operations indicating that variation of λ_{soil} did not affect the temperature changes near EP1 edge for the pile spacing of this study. However, the overlapping of the ground temperatures indicates that thermal interaction occurred in the soil between the two piles between R = 0.6 m and 2.7 m for dual pile tests.

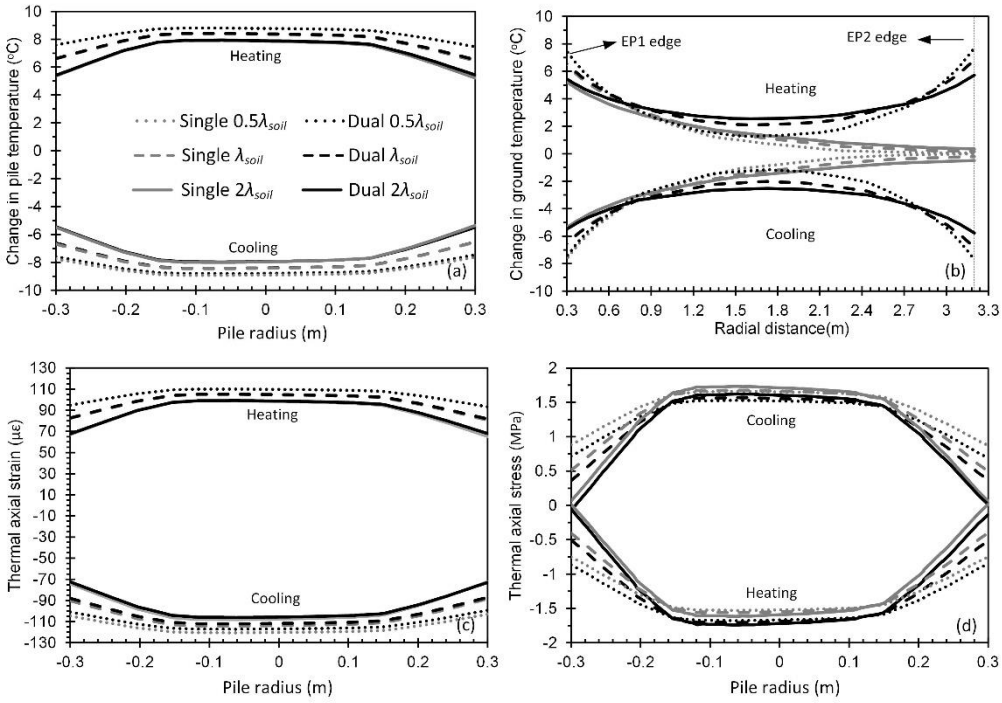

Figure 6.7. Numerical predictions of the effect of soil thermal conductivity, λ_{soil}, on the cross-sectional thermal responses of EP1 and ground temperatures: (a) change in temperature; (b) change in radial distribution of ground temperatures; (c) thermal axial strains; and (d) thermal axial stresses.

The stress variations at the centre of EP1 were insignificant compared to those at the edge of EP1 when λ_{soil} increased from $0.5\lambda_{soil}$ to $2\lambda_{soil}$. This can be related to the fact that the centre of EP1 is more influenced by the heat-exchanger loops, whereas the edges of EP1 is more affected by ground temperature changes at the pile-soil interface. As a result, the difference between thermal stresses at the centre and edge of EP1 increased from 0.8 MPa to 1.65 MPa when λ_{soil} increased from $0.5\lambda_{soil}$ to $2\lambda_{soil}$. The effect of operating EP2 in dual pile operation on EP1 temperature distribution, axial thermal strains and stresses was insignificant for all values of λ_{soil}, which indicates that thermal interaction between the two energy piles is negligible in the current study.

6.3.4 Soil elastic modulus

The effect of soil elastic modulus, E_{soil}, on the cross-sectional thermal responses of EP1 and adjacent ground temperature changes at a depth of 2.5 m, for $|\Delta T_f|$=10°C, is shown in Figure 6.8.

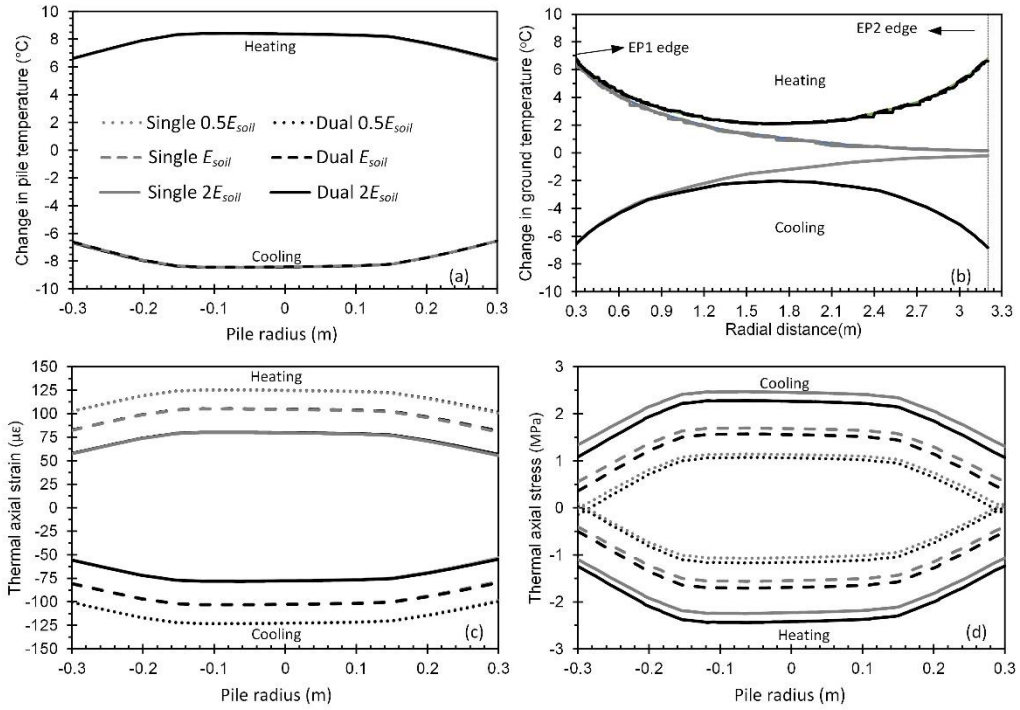

Figure 6.8. Numerical predictions of the effect of soil elastic modulus, E_{soil}, on the cross-sectional thermal responses of EP1 and ground temperatures: (a) change in temperature; (b) change in radial distribution of ground temperatures; (c) thermal axial strains; and (d) thermal axial stresses.

The thermal responses were symmetrical for heating and cooling. The pile and ground temperatures were not affected by varying E_{soil} (Figure 6.8a and 6.8b). The thermal stresses increased (and hence decrease in thermal strains) with increasing $E_{soil,}$ which can be attributed to increased soil restriction on thermal expansion/contraction of EP1. Khosravi et al. (2016) also reported an increase in pile thermal stresses with increasing E_{soil}. The distribution of temperatures and thermal stresses and strains were similar over the cross-section of EP1 for both single and dual pile operation indicating that operation of EP2 in dual pile operation did not have significant effects on EP1 thermal responses for different values of E_{soil}. An increase of 1.5 MPa of thermal stresses was observed when E_{soil} increased from $0.5E_{soil}$ to $2E_{soil}$. However, the difference between the thermal stresses between the centre and edge of EP1 remained approximately 1 MPa for any given E_{soil} for single and dual piles' heating and cooling operations.

6.3.5 Soil thermal expansion coefficient

Figure 6.9 shows the effect of soil's thermal expansion coefficient, α_{soil}, on the cross-sectional thermal responses of EP1 and adjacent ground temperature changes at a depth of 2.5 m, for $|\Delta T_f|$ = 10°C. Similar to E_{soil} and λ_{soil}, the thermal responses of EP1 for heating and cooling operations were symmetrical for both single and dual pile operations. Variations of α_{soil} did not affect the pile and ground temperature changes (Figure 6.9a and 6.9b).

The range of thermal stresses for various magnitudes of α_{soil} was lower than that for E_{soil}. Similar to what was observed for λ_{soil} and E_{soil}, the distribution of thermal stresses in EP1 was similar for both single and dual pile operations, hence the operation of EP2 did not affect the thermal responses of EP1 for the pile spacing investigated in this study. The differences in thermal stresses between the centre and edge of EP1 were about 1 MPa for all values of $\alpha_{soil,}$ for both heating and cooling operations of single and dual piles. A reduction of thermal stresses resulted for higher values of α_{soil} (i.e., 10 α_{soil} which corresponds to a ratio of $\alpha_{soil}/\alpha_{pile}$ of 7)

which can be attributed to greater soil expansion which resulted in lower soil restriction on EP1. Similar behaviour of thermal stresses was observed by Bourne-Webb et al. (2016) and Salciarini (2017) along the depth of an energy pile.

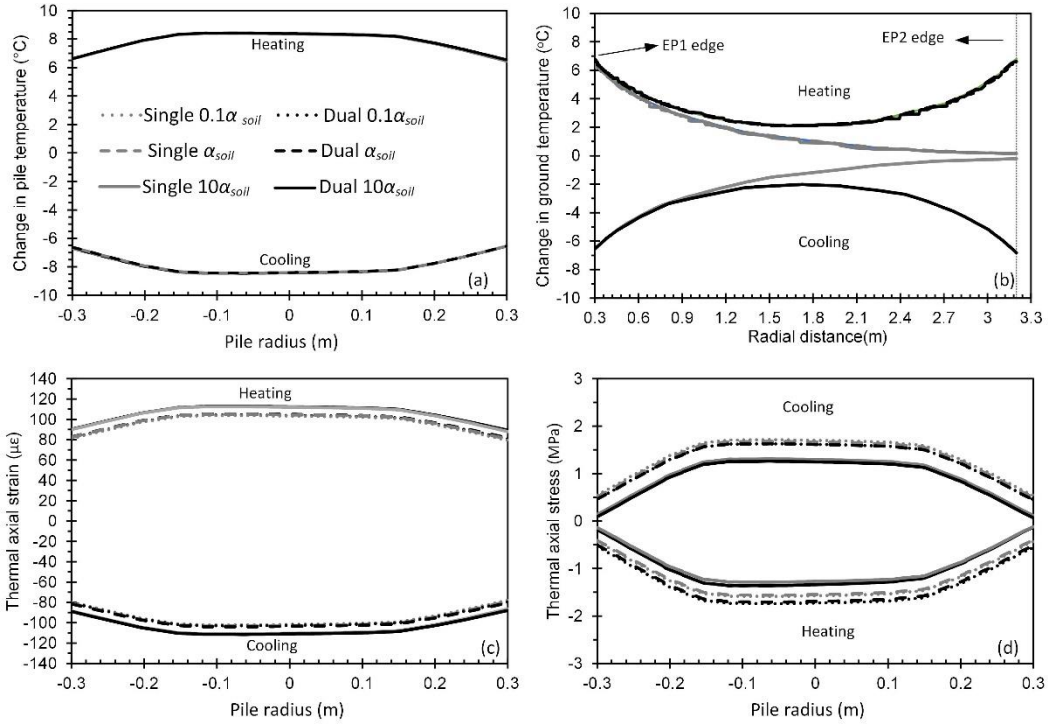

Figure 6.9. Numerical predictions of the effect of soil thermal expansion coefficient, α_{soil}, on the cross-sectional thermal responses of EP1 and ground temperatures: (a) change in temperature; (b) change in radial distribution of ground temperatures; (c) thermal axial strains; and (d) thermal axial stresses.

6.4 Chapter summary

This chapter investigated the cross-sectional thermal response of one of the two energy piles (EP1) when operated alone and when operated together with another pile (EP2). The effects of varying inlet fluid temperatures, soil thermal conductivity, thermal expansion coefficient, and elastic modulus on the cross-sectional thermal response of the considered energy pile (EP1) were investigated. The temperatures and axial thermal stresses were found to increase with the inlet fluid temperature. Symmetrical responses were observed over the cross-section of the considered energy pile during heating and cooling. The temperatures and thermal axial stresses were largest at the centre of the considered energy pile (EP1) compared

to the pile's edge for all fluid temperatures and soil properties. For all fluid temperatures and soil parameters investigated, the influence of the second energy pile (EP2) on the temperatures and thermal stresses of the considered energy pile (EP1) during dual pile operation was found to be negligible. However, due to thermal interaction, the ground temperature changes between the two energy piles during dual pile operation was larger than those of the operation of a single energy pile for all studied cases.

The effect of soil elastic modulus on the cross-sectional thermal response of the considered energy pile was more significant compared to the soil thermal conductivity and soil thermal expansion. However, the variations of the soil thermal conductivity influenced the ground temperatures. They mostly affected the magnitudes of thermal stresses at the edge of the considered energy pile (EP1) due to variations in pile-soil interface temperatures. This chapter's outcomes show that the differences between the centre and edge of energy piles will differ for different fluid temperatures and soil properties encountered at various sites and should also be accounted for in the energy piles' design.

7 Conclusions and recommendations

7.1 Introduction

The study conducted in this thesis added to the existing knowledge on the impact of temperature and soil properties' role on the thermal interaction between energy piles. This was achieved by conducting field tests on two piles spaced at a centre-to-centre distance of 3.5 m and installed under a six-storey residential building at Monash University (Clayton Campus), Australia. A numerical model was developed and validated with field data to investigate the effect of soil parameters, inlet fluid temperature, and the impact of nearby energy pile on the thermal response of an energy pile. This chapter summarises the key conclusions of the work achieved in this thesis, followed by recommendations for future work.

7.2 Conclusions

7.2.1 Effect of monotonic and cyclic temperature variations on the thermal interaction between two energy piles

This section investigated the axial and radial thermal responses of one of the two energy piles spaced under monotonic and cyclic temperature changes, numerically and experimentally. The ground temperature changes between the energy piles were noticeably affected by the second energy pile's operation, especially for monotonic temperatures with higher inlet fluid temperatures. The influence of the second energy pile on the magnitudes of temperature, axial and radial stresses and strains of the considered energy pile was negligible, indicating that the impact of thermal interaction among the energy piles on the pile thermal responses was insignificant.

Higher values of axial thermal stresses developed in the considered energy pile, during monotonic heating and cooling operations compared to cyclic operations for both single and

dual pile tests, were due to more significant changes in pile temperature. The pile toe displacements of the considered pile were greater than pile head displacements for all tests due to the higher stiffness imposed by the building loads at the pile head. Higher inlet fluid temperatures induced greater thermal displacements, and lower thermal displacements were observed during cyclic operations compared to monotonic operations. The thermal strains followed linear paths during monotonic and cyclic operations for both single and dual piles. The rates of change in thermal strains against change in pile temperatures for the considered energy pile were similar for both single and dual pile operations for any given fluid temperature, indicating negligible effects of thermal interaction between the piles on the pile thermal responses for the conditions investigated in this study. The outcome of this work would be useful for the design of energy piles for a range of different magnitudes of monotonic and cyclic fluid temperatures typically encountered in energy piles.

7.2.2 Effect of nearby piles and soil properties on the thermal response of an energy pile

This section explored the effects of varying soil thermal conductivity, thermal expansion coefficient, and elastic modulus on one of the two energy piles' thermal response. Heating the two piles together increased thermal interaction between the piles due to higher ground temperature changes between the piles caused by thermal overlapping. However, this thermal interaction did not affect the magnitude of thermal stresses developed in the considered energy pile for all soil properties, indicating negligible thermal effects from the operation of one energy pile on the other energy pile during simultaneous heating. Heating only one pile also induced insignificant thermal effects on the other non-thermal pile for all soil properties. This outcome indicates that the operation of energy piles will not induce thermal stresses in nearby non-operating piles in the setting investigated in this chapter. The effect of elastic modulus of the soil was more significant on the thermal stresses and displacements developed

in the considered energy pile compared to the impact of thermal conductivity and thermal expansion coefficient of the soil. However, increasing the thermal conductivity of the soil induced higher ground temperature changes around both energy piles. The numerical simulations confirmed the field results that the magnitudes of radial thermal stresses developed in the energy pile were insignificant compared to the axial thermal stresses for all soil properties. The thermal displacements of the considered energy pile were negligible and significantly lower than 10% of the pile diameter for all studied cases and are not expected to affect the energy piles' structural integrity. This section's outcomes will help assess the thermal interaction among closely spaced energy piles that are not linked by a pile-cap when designing energy piles at different sites with soil properties similar to those reported in this paper. It should be noted that for energy piles spaced closer to each other (i.e., in secant or tangent walls), thermal interaction between the energy piles might be more significant.

7.2.3 Cross-sectional thermal responses of an energy pile

This section investigated the cross-sectional thermal response of one of the two energy piles under monotonic heating and cooling operations. A parametric study was conducted to investigate the effects of varying inlet fluid temperatures, soil thermal conductivity, thermal expansion coefficient, and elastic modulus on the considered energy pile's cross-sectional thermal response. The influence of the second energy pile on the temperatures and thermal stresses of the considered energy pile during dual pile operation was negligible for all fluid temperatures and soil parameters investigated in this study. However, the ground temperatures between the two energy piles during dual pile operation experienced larger changes than the operation of a single energy pile for all studied cases. The temperatures and stresses at the centre of the considered energy pile were larger than at the edge of the pile, for all fluids and soil properties.

The soil elastic modulus effect was more significant on the cross-sectional thermal response of the considered energy pile compared to the soil thermal conductivity and soil thermal expansion. However, the soil thermal conductivity influenced the ground temperatures while the effects of soil elastic modulus and thermal expansion coefficient on ground temperatures were negligible. Variation of soil thermal conductivity mostly affected the magnitudes of thermal stresses at the edge of the considered energy pile due to variations in pile-soil interface temperatures. This section outcomes show that only considering the thermal responses at the centre of energy piles might result in design errors as the temperatures and thermal stresses at the edge of the energy piles are lower than those at the centre of the energy pile. Moreover, the differences between the centre and edge of energy piles will differ for different fluid temperatures and soil properties encountered at different sites and should also be accounted for in energy pile designs.

7.3 Recommendations for future work

The following recommendations are made for future work to improve the current knowledge on the performance and behaviour of energy piles:

- The current study only assessed the thermal response of single and dual-energy piles, experiencing continuous and intermittent cooling with natural ground thermal recovery. It is recommended to conduct further field tests and numerical studies to assess the thermal response of energy piles group subjected to intermittent cooling with forced ground thermal recharging and a greater number of energy piles. It is also essential to assess the interaction between the energy piles through the soil volume between a larger number of energy piles in a group with different pile spacing.
- The energy pile in the current work were installed in dense to very dense sands where the resistance to thermal deformations is relatively high; hence the soil deformation was likely in the elastic range. It is recommended that the thermal response of energy piles

for different types of soils, such as normally and over consolidated clays, be studied as the behaviour of this type of soil could be inelastic.

- This thesis assessed the development of thermal stresses and strains inside the energy piles only. However, the thermally induced deformations of the energy piles led to the development of stresses in the overlying slab and the surrounding soil. Hence, field-scale monitoring of the development of thermal stresses in the soil and the slab is recommended.
- Monitoring soil moisture variations by instrumenting the surrounding soil at different radial locations from the edge of the pile is also recommended to assess the effects of monotonic and intermittent operations on the water content fluctuation of the surrounding soil. Thermally-induced moisture transfer and variations in soil water content might affect the soil-pile interaction and the thermal interaction through the soil volume.
- More instrumentations are recommended over the cross-section of the energy piles, specifically, near the edges of the energy piles, to assess the cross-sectional thermal response of the energy piles. This will help justify the possible non-uniform thermal stresses between the centre and edge of the energy piles' cross-section.
- The numerical study conducted in this thesis was for the soil in a dry condition. However, to capture a more realistic soil volume changes caused by temperature changes, it is recommended to consider an unsaturated condition for the soil volume by including a constitutive unsaturated model for the soil.

References

Abdelaziz S.L. (2013). Deep Energy Foundations: Geotechnical Challenges and Design Considerations. PhD thesis, Virginia Polytechnic Institute and State University, Blacksburg, VA, USA.

Abdelaziz, S. L., and Ozudogru, T. Y. 2016a. Selection of the design temperature change for energy piles. Applied Thermal Engineering, 107, 1036–1045. https://doi.org/10.1016/j.applthermaleng.2016.07.067.

Abdelaziz, S., and Ozudogru, T. Y. 2016b. Non-uniform thermal strains and stresses in energy piles. Environmental Geotechnics, 3(4): 237-252. https://doi.org/10.1680/jenge.15.00032.

Adinolfi, M., Maiorano, R. M. S., Mauro, A., Massarotti, N., and Aversa, S. 2018. On the influence of thermal cycles on the yearly performance of an energy pile. Geomechanics for Energy and the Environment, 16, 32-44. https://doi.org/10.1016/j.gete.2018.03.004.

Akrouch, G., Sánchez, M., and Briaud, J-L. 2014. Thermo-mechanical behavior of energy piles in high plasticity clays. Acta Geotechnica, 9(3): 399-412. https://doi.org/10.1007/s11440-014-0312-5.

Allani, M., Van Lysebetten, G., and Huybrechts, N. 2017. Experimental and numerical study of the thermo-mechanical behaviour of energy piles for Belgian practice. In Advances in laboratory Testing and modelling of soils and Shales (pp. 405-412). Springer, Cham. https://doi.org/10.1007/978-3-319-52773-4_48.

Adam, D., and Markiewicz, R. 2009. Energy from earth-coupled structures, foundations, tunnels and sewers. Géotechnique, 59(3), 229-236. https://doi.org/10.1680/geot.2009.59.3.229.

Amatya, B.L., Soga K., Bourne-Webb P.J. 2012. Thermo-mechanical behaviour of energy piles. Géotechnique, **62**(6):503-519. https://doi.org/10.1680/geot.10.P.116.

Amis, A., and Loveridge, F. A. 2014. Energy piles and other thermal foundations for GSHP–Developments in UK practice and research. Rehva journal, 2014(1): 32-35.

Anongphouth, A., Maghoul, P. and Alfaro, M. 2018. Numerical Modeling of Concrete Energy Piles Using a Coupled Thermo-Hydro-Mechanical Model. In: 71st Canadian Geotechnical Conference, Edmonton, Alberta, Canada.

Australian Sustainable Built Environment Council, ASBEC 2018. Built to perform: An industry led pathway to a zero carbon ready building code. ClimateWorks Australia, Melbourne.

Barry-Macaulay, D., Bouazza, A., Singh, R., Wang, B., and Ranjith, P. 2013. Thermal conductivity of soils and rocks from the Melbourne (Australia) region. Engineering Geology, **164**: 131-138. https://doi.org/10.1016/j.enggeo.2013.06.014.

Batini, N., Rotta Loria, A.F., Conti, P., Testi, D., Grassi, W. and Laloui, L. 2015. Energy and geotechnical behaviour of energy piles for different design solutions. Computers and Geotechnics, **86** (1): 199–213. https://doi.org/10.1016/j.applthermaleng.2015.04.050.

Bodas Freitas, T., Cruz Silva, F., and Bourne-Webb, P.J. 2013. The response of energy foundations under thermo-mechanical loading. In Proceedings of 18th international

conference on soil mechanics and geotechnical engineering, **4**: 3347-3350. Paris, France: Comité Français de Mécanique des Sols et de Géotechnique.

Bouazza, A., Singh, R.M., Wang, B., Barry-Macaulay, D., Haberfield, C., Chapman, G., Baycan, S. and Carden, Y. 2011. Harnessing on site renewable energy through pile foundations. Australian Geomechanics, 46(4), 79-89. http://epubs.surrey.ac.uk/id/eprint/811582.

Bourne-Webb, P.J., B. Amatya, K. Soga, T. Amis, C. Davidson, and P. Payne. 2009. Energy pile test at Lambeth College, London: Geotechnical and thermodynamic aspects of pile response to heat cycles. Géotechnique, **59**(3): 237–248. https://doi.org/10.1680/geot.2009.59.3.237.

Bourne-Webb, P. J., Amatya, B., and Soga, K. 2013. A framework for understanding energy pile behaviour. Geotechnical Engineering, 166(2), 170-177. https://doi.org/10.1680/geng.10.00098.

Bourne-Webb, P.J., Bodas Freitas, T.M., and Freitas Assunção, R. M. 2015. Soil–pile thermal interactions in energy foundations. Géotechnique, **66**(2): 167-171. https://doi.org/10.1680/jgeot.15.T.017.

Bourne-Webb, P. J., and Freitas, T. B. 2020. Thermally-activated piles and pile groups under monotonic and cyclic thermal loading–A review. Renewable Energy, 147, 2572-2581. https://doi.org/10.1016/j.renene.2018.11.025.

Bowles, Joseph E. 1968. Foundation analysis and design. New York: McGraw-Hill.

Brandl, H. 2006. Energy foundations and other thermo-active ground structures. Géotechnique, 56(2), 81-122. https://doi.org/10.1680/geot.2006.56.2.81.

Brandl, H. 2013. Thermo-active ground-source structures for heating and cooling. Procedia Engineering, 57, 9-18. https://doi.org/10.1016/j.proeng.2013.04.005.

Brettmann, T., and Amis, T. 2011. Thermal conductivity evaluation of a pile group using geothermal energy piles. In Geo-Frontiers 2011: Advances in Geotechnical Engineering, 499-508. https://doi.org/10.1061/41165(397)52.

Caulk, R., Ghazanfari, E., and McCartney, J.S. 2016. Parameterization of a calibrated geothermal energy pile model. Geomechanics for Energy and the Environment, **5**: 1-15. https://doi.org/10.1016/j.gete.2015.11.001.

Centre for International Economics (CIE) 2007. Capitalising on the building sector's potential to lessen the costs of a broadbased GHG emissions cuts. Report prepared for ASBEC Climate Change Task Group.

Chen, D., and McCartney, J.S. 2016. Parameters for load transfer analysis of energy piles in uniform non-plastic soils. International Journal of Geomechanics, 17 (7), 04016159-1-17. https://doi.org/10.1061/(ASCE)GM.1943-5622.0000873.

Chen, Y., Xu, J., Li, H., Chen, L., Ng, C. W. W., and Liu, H. 2017. Performance of a prestressed concrete pipe energy pile during heating and cooling. Journal of Performance of Constructed Facilities, 31(3), 06017001-1-7. https://doi.org/10.1061/(ASCE)CF.1943-5509.0000982.

Choi, J.H., and Chen, R.H.L. 2005. Design of continuously reinforced concrete pavements using glass fiber reinforced polymer rebars. Publication No. FHWA-HRT-05-081. Washington, D.C.

Climateworks 2014. Pathways to deep decarbonisation in 2050, how Australia can prosper in a low carbon world, initial project report. Climateworks Australia, Melbourne.

De Moel, M., Bach, P. M., Bouazza, A., Singh, R. M., and Sun, J. L. O. 2010. Technological advances and applications of geothermal energy pile foundations and their feasibility in Australia. Renewable and Sustainable Energy Reviews, 14(9), 2683-2696. https://doi.org/10.1016/j.rser.2010.07.027.

Department of the Environment, Water, Heritage and the Arts, DEWHA 2008. Energy use in the Australian residential sector, 1986 – 2020. Commonwealth of Australia, Canberra.

Engineers Australia (2017). Create. Balmain, NSW Mahlab Media, 3 (11).

Di Donna, A., and Laloui, L. 2015. Numerical analysis of the geotechnical behaviour of energy piles. International journal for numerical and analytical methods in geomechanics, 39(8), 861-888. https://doi.org/10.1002/nag.2341.

Di Donna, A., Rotta Loria, A.F., and Laloui, L. 2016. Numerical study of the response of a group of energy piles under different combinations of thermo-mechanical loads. Computers and Geotechnics, **72**: 126-142. https://doi.org/10.1016/j.compgeo.2015.11.010.

Elzeiny, R., Suleiman, M. T., Xiao, S., Abu Qamar, M. A., and Al-Khawaja, M. 2020. Laboratory-Scale Pull-Out Tests on a Geothermal Energy Pile in Dry Sand Subjected to Heating Cycles. Canadian Geotechnical Journal, (ja). https://doi.org/10.1139/cgj-2019-0143.

Faizal, M., Bouazza, A., and Singh, R. M. 2016. An experimental investigation of the influence of intermittent and continuous operating modes on the thermal behaviour of a full scale geothermal energy pile. Geomechanics for Energy and the Environment, **8**: 8-29. https://doi.org/10.1016/j.gete.2016.08.001.

Faizal, M. 2018. Axial and radial thermal responses of field-scale energy piles. PhD thesis, Monash University, Melbourne, Australia.

Faizal, M., Bouazza, A., Haberfield, C., and McCartney J.S. 2018. Axial and radial thermal responses of a field-scale energy pile under monotonic and cyclic temperature changes. Journal of Geotechnical and Geoenvironmental Engineering, **144**(10): 04018072. https://doi.org/10.1139/cgj-2018-0246.

Faizal, M., Bouazza, A., McCartney, J.S., and Haberfield, C. 2019a. Axial and radial thermal responses of an energy pile under a 6-storey residential building. Canadian Geotechnical Journal, **56**(7): 1019–1033. https://doi.org/10.1061/(ASCE)GT.1943-5606.0001952.

Faizal, M., Bouazza, A., McCartney, J.S. and Haberfield, C. 2019b. Effects of cyclic temperature variations on the thermal response of an energy pile under a residential building. Journal of Geotechnical and Geoenvironmental Engineering **145** (10): 04019066. https://doi.org/10.1061/(ASCE)GT.1943-5606.0002147

Fang, J., Kong, G., Meng, Y., Wang, L., and Yang, Q. 2020. Thermomechanical behavior of energy piles and interactions within energy pile–raft foundations. Journal of

Geotechnical and Geoenvironmental Engineering, 146(9), 04020079. https://doi.org/10.1061/(ASCE)GT.1943-5606.0002333.

Gawecka, K.A., Taborda, D.M.G., Potts, D.M., Cui, W., Zdravković, L., and Kasri, M.S.H. 2017. Numerical modelling of thermo-active piles in London Clay. Proceedings of the Institution of Civil Engineers - Geotechnical Engineering, 170(3): 201-219. https://doi.org/10.1680/jgeen.16.00096.

Ghasemi-Fare, O., and Basu, P. 2013. A practical heat transfer model for geothermal piles. Energy and Buildings, 66, 470-479. https://doi.org/10.1016/j.enbuild.2013.07.048.

Global Alliance for Buildings and Construction, GlobalABC 2018. 2018 Global status report: Towards a zero-emission, efficient and resilient buildings and construction sector. United Nations Environment Programme.

Gnielinski, V. 1975. New equations for heat and mass transfer in the turbulent flow in pipes and channels. NASA STI/recon technical report A, **75**: 8-16.

Goode, J. C. I., and McCartney, J. S. 2015. Centrifuge modeling of end-restraint effects in energy foundations. Journal of Geotechnical and Geoenvironmental Engineering, 141(8), 04015034-1-13. https://doi.org/10.1061/(ASCE)GT.1943-5606.0001333.

Guo, Y., Zhang, G., and Liu, S. 2018. Investigation on the thermal response of full-scale PHC energy pile and ground temperature in multi-layer strata. Applied Thermal Engineering, 143: 836–848. https://doi.org/10.1016/j.applthermaleng.2018.08.005.

Habert, J., M. El Mejahed, and Bernard, J. B. 2016. Lessons learned from mechanical monitoring of a thermoactive pile. Proceedings of the 1st International Conference on Energy Geotechnics, Kiel, Germany, pp. 29-31.

Haaland, S.E. 1983. Simple and explicit formulas for the friction factor in turbulent pipe flow. Journal of Fluids Engineering, **105**(1): 89-90.

Hamada, Y., Saitoh, H., Nakamura, M., Kubota, H., and Ochifuji, K. 2007. Field performance of an energy pile system for space heating. Energy and Buildings, **39**(5): 517-524. https://doi.org/10.1016/j.enbuild.2006.09.006.

Han, C., and Yu, X. B. 2020. Analyses of the thermo-hydro-mechanical responses of energy pile subjected to non-isothermal heat exchange condition. Renewable Energy. https://doi.org/10.1016/j.renene.2020.04.118.

International Energy Agency (IEA) 2013. Transition to Sustainable Buildings, IEA, Paris https://www.iea.org/reports/transition-to-sustainable-buildings.

Jensen-Page, L., Narsilio, G. A., Bidarmaghz, A., and Johnston, I. W. 2018. Investigation of the effect of seasonal variation in ground temperature on thermal response tests. Renewable Energy, 125, 609-619. https://doi.org/10.1016/j.renene.2017.12.095.

Jeong, S., Lim, H., Lee, J.K., and Kim, J. 2014. Thermally induced mechanical response of energy piles in axially loaded pile groups. Applied Thermal Engineering, 71(1): 608-615. https://doi.org/10.1016/j.applthermaleng.2014.07.007.

Johnston, I. W., Narsilio, G., Colls, S., Kivi, A. V., Payne, D., Wearing-Smith, M., and Noonan, G. 2014. Direct geothermal energy demonstration projects for Victoria, Australia. Proceedings of New Zealand Geothermal Workshop 2012, Auckland, New Zealand.

Kalantidou, A., Tang, A. M., Pereira, J.M., and Hassen, G. 2012. Preliminary study on the mechanical behaviour of heat exchanger pile in physical model. Géotechnique, 62(11), 1047-1051. https://doi.org/10.1680/geot.11.T.013.

Khan, M. and Wang, J. 2014. "Study on energy foundation design in South Louisiana". In Proceedings Geo-Congress 2014, 3799 – 3806. https://doi.org/10.1061/9780784413272.368.

Khosravi, A., Moradshahi, A., McCartney, J.S., and Kabiri, M. 2016. Numerical analysis of energy piles under different boundary conditions and thermal loading cycles. E3S Web Conference, **9**: 05005. EDP Sciences.

Kong, G., Wu, D., Liu, H., Laloui, L., Cheng, X., and Zhu, X. 2019. Performance of a geothermal energy deicing system for bridge deck using a pile heat exchanger. International Journal of Energy Research, 43(1), 596-603. https://doi.org/10.1002/er.4266.

Laloui, L., Nuth, M., and Vulliet, L. 2006. Experimental and numerical investigations of the behaviour of a heat exchanger pile. International Journal for Numerical and Analytical Methods in Geomechanics, **30**(8): 763-781. https://doi.org/10.1002/nag.499.

Laloui, L., and Di Donna, A. 2011. Understanding the behavior of energy geo-structures.

In Proceedings of the Institution of Civil Engineers. 184-191. https://doi.org/10.1680/cien.2011.164.4.184.

Liu, R. Y. W., Taborda, D. M. G., Gawecka, K. A., Cui, W., and Potts, D. M. 2019. Computational study on the effects of boundary conditions on the modelled thermally induced axial stresses in thermo-active piles. In Proceedings of the XVII ECSMGE-2019.

Liu, R. Y. W., Sailer, E., Taborda, D. M., Potts, D. M., and Zdravković, L. 2020. A practical method for calculating thermally-induced stresses in pile foundations used as heat exchangers. Computers and Geotechnics, 126, 103743. https://doi.org/10.1016/j.compgeo.2020.103743.

Lu, Q., Narsilio, A., Aditya, G. R. and Johnston, I. W. 2017. Economic analysis of vertical ground source heat pump systems in Melbourne. Energy, 125 (Apr): 107 – 117. https://doi.org/10.1016/j.energy.2017.02.082.

Lu, Q. and Narsilio, G. 2019. Cost effectiveness of energy piles in residential dwellings in Australia. Current Trends in Civil and Structural Engineering, 3 (3). DOI: 10.33552/CTCSE.2019.03.000564.

Lv, Z., Kong, G., Liu, H., and Ng, C. W. 2020. Effects of soil type on axial and radial thermal responses of field-scale energy piles. Journal of Geotechnical and Geoenvironmental Engineering, 146(10), 06020018. https://doi.org/10.1061/(ASCE)GT.1943-5606.0002367.

Lysebetten G.V., Allani, M., Huybrechts, N. 2017. Real-scale test campaign on energy piles for Belgian practice and numerical modelling of their behaviour. In: Proceedings of the 19th International Conference on Soil Mechanics and Geotechnical Engineering, Seoul, South Korea, 3475-3478.

Makasis, N., Narsilio, G. A., and Bidarmaghz, A. 2018. A machine learning approach to energy pile design. Computers and Geotechnics, 97, 189-203. https://doi.org/10.1016/j.compgeo.2018.01.011.

McCartney, J.S. and Rosenberg, J. E. 2011. Impact of heat exchange on side shear in thermo-active foundations. Geo-Frontiers 2011, Texas, United States, 488-498. https://doi.org/10.1061/41165(397)51.

McCartney, J.S. and Murphy, K.D. 2012. Strain distributions in full-scale energy foundations. DFI Journal - The Journal of the Deep Foundations Institute, **6**(2): 26-38. https://doi.org/10.1179/dfi.2012.008.

McCartney, J. S., Murphy, K. D., and Henry, K. S. 2015. Response of an energy foundation to temperature fluctuations. In IFCEE 2015, (pp. 1691-1700).

McCartney, J. S., and Murphy, K. D. 2017. Investigation of potential dragdown/uplift effects on energy piles. Geomechanics for Energy and the Environment, 10, 21-28. https://doi.org/10.1016/j.gete.2017.03.001.

Mimouni, T. 2014. Thermomechanical characterization of energy geostructures with emphasis on energy piles. PhD thesis, École Polytechnique Fédérale de Lausanne, Lausanne, Switzerland.

Mimouni, T., Dupray, F., and Laloui, L. 2014. Estimating the geothermal potential of heat-exchanger anchors on a cut-and-cover tunnel. Geothermics, 51, 380-387. https://doi.org/10.1016/j.geothermics.2014.02.007.

Mimouni, T., and Laloui, L. 2015. Behaviour of a group of energy piles. Canadian Geotechnical Journal, 52(12): 1913-1929. https://doi.org/10.1139/cgj-2014-0403.

Mitchell, J.K. and Soga, K. 2005. Fundamentals of soil behavior, 3rd edition. Wiley, New Jersey.

Moradshahi, A., Khosravi, A., McCartney, J. S., and Bouazza, A. 2020a. Axial load transfer analyses of energy piles at a rock site. Geotechnical and Geological Engineering, **38**: 4711–4733. https://doi.org/10.1007/s10706-020-01322-5.

Moradshahi, A., Faizal, M., Bouazza, A., and McCartney, J. S. 2020b. Effect of nearby piles and soil properties on the thermal behaviour of a field-scale energy pile. Canadian Geotechnical Journal. **0**(ja): . https://doi.org/10.1139/cgj-2020-0353

Murphy, K.D., and McCartney, J.S. 2015. Seasonal response of energy foundations during building operation. Geotechnical and Geological Engineering, 33(2): 343-356. https://doi.org/10.1007/s10706-014-9802-3.

Murphy, K.D., McCartney, J.S., and Henry, K. S. 2015. Evaluation of thermo-mechanical and thermal behavior of full-scale energy foundations. Acta Geotechnica, **10**(2): 179-195. https://doi.org/10.1007/s11440-013-0298-4.

Ng, C. W. W., Shi, C., Gunawan, A., and Laloui, L. 2014a. Centrifuge modelling of energy piles subjected to heating and cooling cycles in clay. Géotechnique Letters, 4(4), 310-316. https://doi.org/10.1680/geolett.14.00063.

Ng, C. W. W., Shi, C., Gunawan, A., Laloui, L., and Liu, H. L. 2014b. Centrifuge modelling of heating effects on energy pile performance in saturated sand. Canadian Geotechnical Journal, 52(8), 1045-1057. https://doi.org/10.1139/cgj-2014-0301.

Ng, C. W. W., Gunawan, A., Shi, C., Ma, Q. J., and Liu, H. L. 2016. Centrifuge modelling of displacement and replacement energy piles constructed in saturated sand: a comparative study. Géotechnique Letters, 6(1), 34-38. https://doi.org/10.1680/jgele.15.00119.

Ng, C. W. W., and Ma, Q. J. 2019. Energy pile group subjected to non-symmetrical cyclic thermal loading in centrifuge. Géotechnique Letters, **9**(3), 173-177. https://doi.org/10.1680/jgele.18.00161

Olgun, C. G. 2013. Energy piles: background and geotechnical engineering concepts. In Proceedings of the 16th Annual George F. Sowers Symposium, Atlanta, GA, USA (Vol. 7).

Olgun, C., Ozudogru, T., and Arson. 2014. Thermo-mechanical radial expansion of heat exchanger piles and possible effects on contact pressures at pile–soil interface. Géotechnique Letters, **4**(3): 170-178. https://doi.org/10.1680/geolett.14.00018.

Olgun, C. G., Ozudogru, T. Y., Abdelaziz, S. L., and Senol, A. 2015. Long-term performance of heat exchanger piles. Acta Geotechnica, 10(5), 553-569. https://doi.org/10.1007/s11440-014-0334-z.

Ouyang, Y., Soga, K., and Leung, Y. F. 2011. Numerical back-analysis of energy pile test at Lambeth College, London. In Geo-Frontiers 2011: Advances in Geotechnical Engineering (pp. 440-449). https://doi.org/10.1061/41165(397)46.

Ozudogru, T.Y., Olgun, C.G., and Arson, C.F. 2015. Analysis of friction induced thermo-mechanical stresses on a heat exchanger pile in isothermal soil. Geotechnical and Geological Engineering, **33**(2): 357-371. https://doi.org/10.1007/s10706-014-9821-0.

Pahud, D., and Hubbuch, M. 2007. Measured thermal performances of the energy pile system of the Dock Midfield at Zürich Airport. Proceedings Eurpoean Geothermal Congress 2007, Unterhaching, Germany, 1-7.

Pasten, C., and Santamarina, J. C. 2014. Thermally induced long-term displacement of thermoactive piles. Journal of Geotechnical and Geoenvironmental Engineering, 140(5), 06014003. https://doi.org/10.1061/(ASCE)GT.1943-5606.0001092.

Peck, R. B., Hanson, Walter E., and Thornburn, Thomas H. 1974. Foundation engineering (2nd ed.). Wiley.

Peng, H. F., Kong, G. Q., Liu, H. L., Abuel-Naga, H., and Hao, Y. H. 2018. Thermo-mechanical behaviour of floating energy pile groups in sand. Journal of Zhejiang University-SCIENCE A, 19(8), 638-649. https://doi.org/10.1631/jzus.A1700460.

Poulos, H.G., Mattes, N.S. 1985. Settlement and load distribution analysis of pile groups. In: Golden Jubilee of the International Society for Soil Mechanics and Foundation Engineering: Commemorative Volume. Institution of Engineers, Barton, Australia, p.155-165.

Ravera, E., Sutman, M. and Laloui, L. 2019. Analysis of the interaction factor method for energy pile groups with slab. Computers and Geotechnics, p.103294. https://doi.org/10.1016/j.compgeo.2019.103294.

Ravera, E., Sutman, M., and Laloui, L. 2020. Load Transfer Method for Energy Piles in a Group with Pile–Soil–Slab–Pile Interaction. Journal of Geotechnical and

Geoenvironmental Engineering, 146(6), 04020042. https://doi.org/10.1061/(ASCE)GT.1943-5606.0002258.

Rosenberg, J.E. 2010. Centrifuge Modeling of Soil Structure Interaction in Thermo-Active Foundation. M.S. Thesis. University of Colorado Boulder.

Rotta Loria, A.F. and Laloui, L. 2016. The interaction factor method for energy pile groups. Computers and Geotechnics, **80**: 121-137. https://doi.org/10.1016/j.compgeo.2016.07.002.

Rotta Loria, A.F. and Laloui, L. 2017a. Displacement interaction among energy piles bearing on stiff soil strata. Computers and Geotechnics, 90, 144-154. https://doi.org/10.1016/j.compgeo.2017.06.008.

Rotta Loria, A.F. and Laloui, L. 2017b. The equivalent pier method for energy pile groups. Géotechnique, 67(8): 691–702. https://doi.org/10.1680/jgeot.16.P.139.

Rotta Loria, A.F. and Laloui, L. 2017c. Thermally induced group effects among energy piles. Géotechnique, 67(5): 374-393. https://doi.org/10.1680/jgeot.16.P.039.

Rotta Loria, A. F. and Laloui, L. 2018. Group action effects caused by various operating energy piles. Géotechnique, **68**(9): 834-841. https://doi.org/10.1680/jgeot.17.P.213.

Rui, Y., and Soga, K. 2019. Thermo-hydro-mechanical coupling analysis of a thermal pile. Proceedings of the Institution of Civil Engineers-Geotechnical Engineering, 172(2), 155-173.

Rotta Loria, A. F. Oltra, J. V. C., and Laloui, L. 2020. Equivalent pier analysis of full-scale pile groups subjected to mechanical and thermal loads. Computers and Geotechnics, 120, 103410. https://doi.org/10.1016/j.compgeo.2019.103410.

Salciarini, D., Ronchi, F., Cattoni, E., and Tamagnini, C. 2015. Thermo-mechanical effects induced by energy piles operation in a small piled raft. International Journal of Geomechanics, **15**(2): 04014042. https://doi.org/10.1061/(ASCE)GM.1943-5622.0000375.

Salciarini, D., Ronchi, F., and Tamagnini, C. 2017. Thermo-hydro-mechanical response of a large piled raft equipped with energy piles: a parametric study. Acta Geotechnica, **12**(4): 703-728. https://doi.org/10.1007/s11440-017-0551-3.

Saggu, R. and Chakraborty, T. 2015. Cyclic thermo-mechanical analysis of energy piles in sand. Geotechnical and Geological Engineering, 33(2), 321-342. 10.1007/s10706-014-9798-8.

Saggu, R., and Chakraborty, T. 2016. Thermo-mechanical response of geothermal energy pile groups in sand. International Journal of Geomechanics, **16**(4): 04015100. https://doi.org/10.1061/(ASCE)GM.1943-5622.0000567.

Sani, A.K., Singh, R.M., Tsuha, C.de H.C., and Cavarretta, I. 2019. Pipe–pipe thermal interaction in a geothermal energy pile. Geothermics, **81**: 209–223. https://doi.org/10.1016/j.geothermics.2019.05.004.

Singh, R. M. and Bouazza, A. 2013. Thermal conductivity of geosynthetics. Geotextiles and Geomembranes, 39, 1-8.

Singh, R. M., Bouazza, A., and Wang, B. 2015. Near-field ground thermal response to heating of a geothermal energy pile: Observations from a field test. Soils and Foundations, 55(6), 1412-1426.

Stewart, M. A., and McCartney, J. S. 2014. Centrifuge modeling of soil-structure interaction in energy foundations. Journal of Geotechnical and Geoenvironmental Engineering, 140(4), 04013044-1-11. https://doi.org/10.1061/(ASCE)GT.1943-5606.0001061.

Sung, C., Park, S., Lee, S., Oh, K., and Choi, H. 2018. Thermo-mechanical behavior of cast-in-place energy piles. Energy, 161: 920-938. https://doi.org/10.1016/j.energy.2018.07.079.

Suryatriyastuti, M.E., Mroueh, H., and Burlon, S. 2012. Understanding the temperature-induced mechanical behaviour of energy pile foundations. Renewable and Sustainable Energy Reviews, **16**(5): 3344-3354. https://doi.org/10.1016/j.rser.2012.02.062.

Suryatriyastuti, M. E., Mroueh, H., and Burlon, S. 2014. A load transfer approach for studying the cyclic behavior of thermo-active piles. Computers and Geotechnics, 55, 378-391. https://doi.org/10.1016/j.compgeo.2013.09.021.

Suryatriyastuti, M.E., Burlon, S., and Mroueh, H. 2016. On the understanding of cyclic interaction mechanisms in an energy pile group. International Journal for Numerical and Analytical Methods in Geomechanics, **40**(1): 3-24. https://doi.org/10.1002/nag.2382.

Sutman, M., Olgun, C. G., and Brettmann, T. 2015. Full-scale field testing of energy piles. In IFCEE 2015, (pp. 1638-1647).

Sutman, M., Olgun, G., Laloui, L., and Brettmann, T. 2017. Effect of end-restraint conditions on energy pile behavior. Geotechnical Frontiers 2017, Florida, USA, 165-174. https://doi.org/10.1061/9780784480472.017.

Sutman, M., Brettmann, T. and Olgun, C.G., 2019. Full-scale in-situ tests on energy piles: Head and base-restraining effects on the structural behaviour of three energy piles. Geomechanics for Energy and the Environment, **18**: 56-68. https://doi.org/10.1016/j.gete.2018.08.002.

Wang, B., Bouazza, A., Singh, R.M., Haberfield, C., Barry-Macaulay, D., and Baycan, S., 2015. Posttemperature effects on shaft capacity of a full-scale geothermal energy pile. Journal of Geotechnical and Geoenvironmental Engineering, **141**(4): 04014125. https://doi.org/10.1061/(ASCE)GT.1943-5606.0001266.

Wang, W., Regueiro, R. A., and McCartney, J. S. 2015. Coupled axisymmetric thermo-poro-mechanical finite element analysis of energy foundation centrifuge experiments in partially saturated silt. Geotechnical and Geological Engineering, 33(2), 373-388. 10.1007/s10706-014-9801-4.

Wang, C., Liu, H., Kong, G., Ng, C. W. W., and Wu, D. 2016. Model tests of energy piles with and without a vertical load. Environmental Geotechnics, 3(4), 203-213. https://doi.org/10.1680/jenge.15.00020.

Wang, B. 2017. Behaviour of pile foundations subjected to thermal loading. Master of Engineering Thesis, Monash University, Melbourne, Australia.

Wu, D., Liu, H.L., Kong, G.Q., Ng, C.W.W., and Cheng, X.H. 2018. Displacement response of an energy pile in saturated clay. Proceedings of the Institution of Civil Engineers-Geotechnical Engineering, **171**(4): 285-294. https://doi.org/10.1680/jgeen.17.00152.

Wu, D., Liu, H., Kong, G., and Li, C. 2019. Thermo-mechanical behavior of energy pile under different climatic conditions. Acta Geotechnica, 14(5), 1495-1508. https://doi.org/10.1007/s11440-018-0731-9.

Wu, D., Liu, H., Kong, G., and Ng, C.W.W. 2020. Interactions of an energy pile with several traditional piles in a row. Journal of Geotechnical and Geoenvironmental Engineering, **146**(4). https://doi.org/10.1061/(ASCE)GT.1943-5606.0002224.

Yang, W., Zhang, L., Zhang, H., Wang, F., and Li, X. 2020. Numerical investigations of the effects of different factors on the displacement of energy pile under the thermo-mechanical loads. Case Studies in Thermal Engineering, 100711. https://doi.org/10.1016/j.csite.2020.100711.

Yavari, N., Tang, A. M., Pereira, J. M., and Hassen, G. 2014. Experimental study on the mechanical behaviour of a heat exchanger pile using physical modelling. Acta Geotechnica, **9**(3), 385-398. https://doi.org/10.1007/s11440-014-0310-7.

Yavari, N., Tang, A. M., Pereira, J.-M., and Hassen, G. 2016a. Effect of temperature on the shear strength of soils and the soil–structure interface. Canadian Geotechnical Journal, 53(7), 1186-1194. https://doi.org/10.1139/cgj-2015-0355.

Yavari, N., Tang, A. M., Pereira, J. M., and Hassen, G. 2016b. Mechanical behaviour of a small-scale energy pile in saturated clay. Géotechnique, 66(11), 878-887. https://doi.org/10.1680/jgeot.15.T.026.

You, S., Cheng, X., Guo, H., and Yao, Z. 2014. In-situ experimental study of heat exchange capacity of CFG pile geothermal exchangers. Energy and Buildings, **79**: 23-31. https://doi.org/10.1016/j.enbuild.2014.04.021.

You, S., Cheng, X., Guo, H., and Yao, Z. 2016. Experimental study on structural response of CFG energy piles. Applied Thermal Engineering, 96, 640-651. https://doi.org/10.1016/j.applthermaleng.2015.11.127.